Structuring oil by protein building blocks

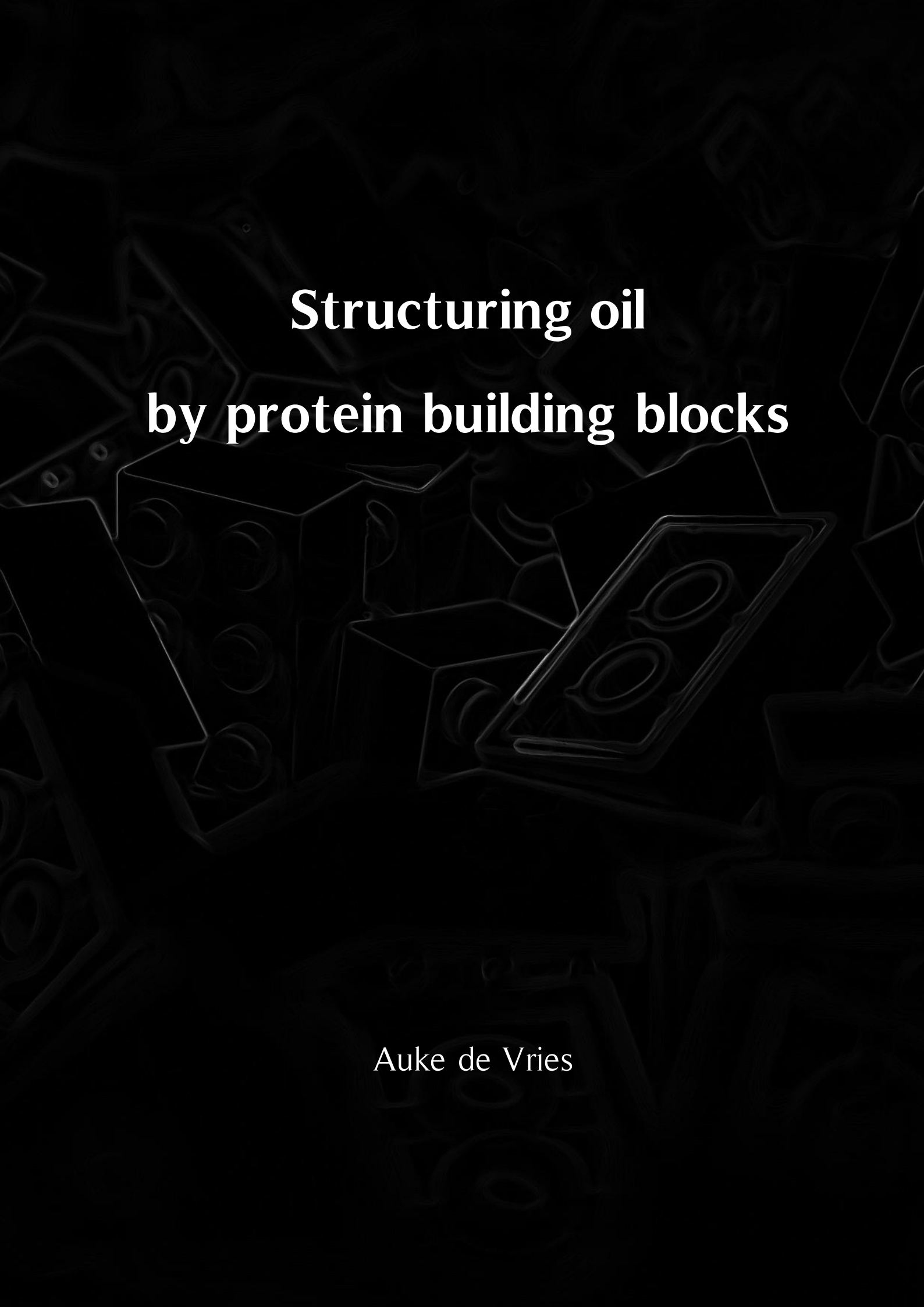

Auke de Vries

Structuring oil by protein building blocks

Auke de Vries

Thesis committee

Promotor

Prof. dr. E. van der Linden

Professor of Physics and Physical Chemistry of Foods

Wageningen University & Research

Co-promotor

Dr. E. Scholten

Associate Professor, Physics and Physical Chemistry of Foods

Wageningen University & Research

Other members

Prof. dr. Ir. A.J. van der Goot, Wageningen University & Research, The Netherlands

Prof. dr. D. Rousseau, Ryerson University, Canada

Prof. dr.-ing. E. Flöter, Technical University of Berlin, Germany

Dr. M. Davidovich-Pinhas, Technion ITT, Israel

This research was conducted under the auspices of the Graduate School VLAG (Advanced studies in Food Technology, Agrobiotechnology, Nutrition and Health Sciences).

Structuring oil by protein building blocks

Auke de Vries

Thesis

submitted in fulfilment of the requirements for the degree of doctor
at Wageningen University & Research
by the authority of the Rector Magnificus
Prof. Dr A.P.J. Mol
in the presence of the
Thesis Committee appointed by the Academic Board
to be defended in public
on Wednesday, 8th March 2017 at 1:30 p.m. in the Aula.

Auke de Vries

Structuring oil by protein building blocks
175 pages

PhD thesis, Wageningen University & Research, Wageningen, NL (2017)
With references, with summary in English

ISBN: 978-94-6343-076-0
DOI: 10.18174/403635

Voor D,D,D, & F

Table of contents

Chapter 1 **1**
General introduction

Chapter 2 **15**
Protein oleogels from protein hydrogels via
a stepwise solvent exchange route

Chapter 3 **39**
Protein oleogels from heat-set whey protein aggregates

Chapter 4 **61**
The effect of oil type on network formation by protein
aggregates into oleogels

Chapter 5 **83**
Tuning the rheological properties of protein-based oleogels
by water addition and heat treatment

Chapter 6 **107**
Controlling agglomeration of protein aggregates for structure
formation in liquid oil: a sticky business

Chapter 7 **135**
General discussion

Summary **161**

Chapter 1

General Introduction

Introduction

Food researchers and the food industry are confronted with the conundrum of how to produce safe, affordable, and nutritious foods in a sustainable manner while the world population is increasing. This leads to many challenges and an increasing need for flexibility in the use of ingredients for food production. For example, the use of plant-derived ingredients and local sourcing has received an increased attention. Many foods are multicomponent systems and a large variety of ingredients is available to alter the structure of foods. An increased knowledge on their functionality provides major benefits for the development of novel foods. For aqueous phases, a large flexibility in the choice of ingredients exists, as many proteins and polysaccharides can be used to provide structure to semi-solid foods, such as cheeses, desserts, tofu, etc. The flexibility of structuring agents for lipid-based liquid phases in food products, on the other hand, is rather limited. To increase the solid-like character of lipid phases mainly saturated and *trans* fatty acids are used. Therefore, solid fats like butter, shortening, or lard have a high content of saturated fats, while liquid oils have a low content of saturated fats.

The composition of the fatty acid profile in the human diet has long been recognized to affect human health, with the prevalence of cardiovascular diseases (CVD) in particular. As is now well established, saturated, and in particular *trans* fatty acids are associated with an increase of LDL cholesterol in the blood at the expense of HDL cholesterol, which increases the risk of developing CVD [1, 2]. The main source of these *trans* fatty acids in foods is hydrogenated fat and it may come as no surprise that legislative actions have been taken to limit or even ban the use of these fats in food products. While the exact relation between the fatty acid profile in the diet and human health is still under debate [3], substituting saturated fats by unsaturated fats is advised to reduce the risk of developing CVD [1, 4].

Solid fats

Although the replacement of saturated fats (solid fats) for unsaturated fats (oils) would lead to food products that fit better within a healthy diet and would increase formulation flexibility, this is not a straightforward exercise. Owing to its solid character at room temperature, saturated fats contribute to a large extent to the stability and texture of many food products. The solid-like character of many meat products, the crunchiness of cookies, the ‘snap’ of chocolate, and the texture of cream fillings are examples of fat solidity playing an important role. A simple replacement by liquid oil would in many occasions lead to an inferior product due to a loss of texture, such as crunchiness and firmness, and oil loss. The solidity of solid fats stems from a high

quantity of crystalline triacylglycerides (TAGs). The basis of a TAG molecule is a tri-ester of fatty acids with a glycerol molecule. TAGs with a large degree of saturated or *trans* fatty acids have the ability to assemble into crystalline lamellae upon lowering the temperature [5]. These lamellae assemble further into nano-sized crystalline platelets. These platelets, in turn, form the basic building blocks of a three-dimensional network, capable of entrapping the liquid oil. The final hardness and melting temperature of the solid fat can be tuned by altering the amount of solid TAGs, fatty acid composition, and processing conditions [6]. This provides a great versatility in the final properties of the solid fat. Typically, the total saturated and/or *trans* fatty acid content required in shortenings is more than 25% [7]. Without this substantial amount of saturated fatty acids, however, a space spanning crystal network is not formed and the oil stays in a liquid form.

Oleogels

Given the important functional properties, but deleterious health effects of solid fats, an alternative way could be to identify structuring agents for liquid oil other than saturated fatty acids. Hereby the solid-like character of traditional solid fats should then be achieved without altering the fatty acid profile of the liquid oil. This alternative way of oil structuring is called 'oleogelation' and it has gained much attention in the past decade [8, 9]. Gelation of organic liquids in a general term is called 'organogelation', and when the gelled liquid is an edible oil, usually the term 'oleogelation' is used. Organogelation is a topic that has been studied for many different purposes like oil spills [10], art cleaning [11], electronics [12], and drug delivery [13, 14]. Over the years, a large number of organogelators have been identified, such as amino acid derivatives, steroid-based compounds, organometallic compounds, and anthryl derivatives [15, 16]. In most of these cases, however, the gelator molecule is of synthetic nature and therefore not applicable to foods. For food purposes, even though oleogelation is a relatively new field of study, already several gelator molecules that are capable of providing a solid-like character to liquid oil have been identified [8, 9, 17, 18]. Usually, a relatively small amount (< 10%) of gelator molecules is necessary to create a network that is able to entrap the liquid oil and form a solid-like material.

By way of classification of the gelator molecules, a differentiation is made according to their size; either as being a large polymeric organogelator or a low molecular weight organogelator (LMOG), as depicted in Figure 1.1. Within the class of LMOGs the differentiation is made between molecules that self-assemble into fibers, tubules or inverse micelles, or assemble further into larger hierarchical crystal structures [13]. Polymeric oil structuring oleogelators can be divided according to the type of network structure they provide: a fine-stranded, entangled polymer gel or a particle gel by interconnected colloidal particles as the dispersed phase.

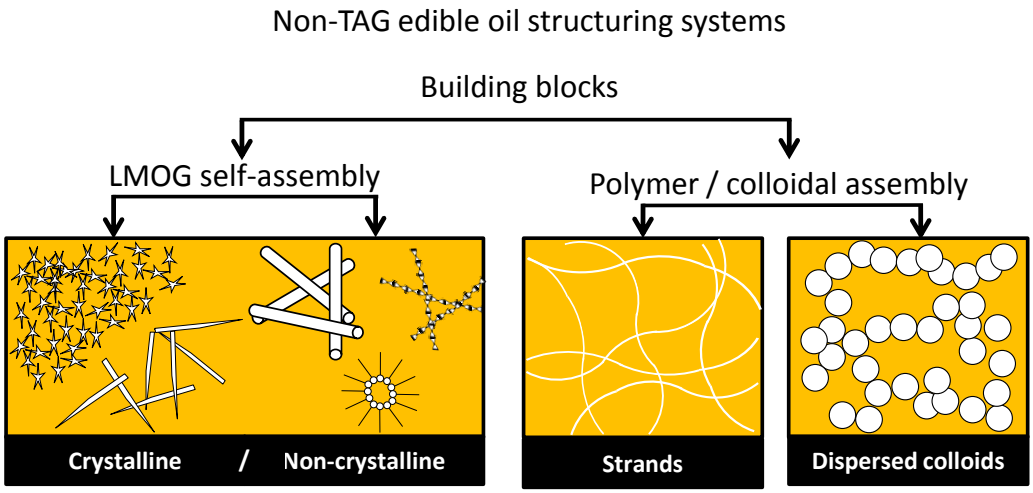

Figure 1.1. Classification of non-TAG oil structuring based on the molecular size of the building block and gelation mechanism.

Oleogels from LMOG's

The most studied oleogels are formed by LMOGs, and a number of gelators have been identified as an alternative oil structuring agent. In this paragraph, well known examples will be discussed. In general, most of these molecules are of amphiphilic nature, and their gelation relies on their ability to self-assemble into various supramolecular assemblies, resulting in the formation of a space-spanning network.

LMOG oleogels based on single structuring components

Next to triacylglycerides, also monoacylglycerides (MAGs) have been studied for their oil-gelling capability. Typically, these glycerol esters contain C:16 or C:18 saturated fatty acids (monopalmitin and monostearin, respectively) and gels are made by dissolving the MAGs in oil at elevated temperature, followed by a cooling step to allow for crystallization. The crystals consist of lamellar bilayer platelets formed by hydrogen bonding [19]. By changing the MAG concentration, the cooling rate, or by applying shear during cooling, the gelling properties can be tuned [20].

Natural waxes are perhaps among the most studied alternative non-TAG oil structuring agents. Waxes are available in different varieties, such as rice bran, sunflower, candelilla, carnauba, or bees wax and consist of mixtures of wax esters of saturated fatty acids, free fatty acids, alcohols, hydrocarbons, and resins. Wax-based oleogels are formed upon cooling, where needle-like crystals ranging from 10 – 25 μm are formed due to the assembly of the large fatty acid chains [21]. Given the high aspect ratio of the crystals, waxes are highly efficient gelators to form a network and gels

can already be formed with concentrations as low as 1% w/w [22]. Due to the low gelling concentration, their large availability, and the thermo-reversible nature of the oleogels [21], this class is a highly promising alternative for solid TAG oil structuring.

Ceramides, a class of polar lipids found in cell membranes, are also proposed as alternative oil structuring agents. Ceramides consist of a sphingosine, a fatty acid, and may contain a phosphocholine or sugar residue. This gives a large diversity of various types, which differ in chain length or type of substituted sugar group. Oleogels are formed by crystallization at a ceramide concentration of ~5 wt%. Its crystal shape as well as the rheological properties depends on the purity of the compound and the length of the fatty acid chain [23].

Another class of efficient oil structuring agents are hydroxylated fatty acids, such as 12-hydroxystearic acid. Upon dissolution in oil and subsequent cooling, one-dimensional growth of such molecules leads to self-assembled fibrillar structures due to specific interactions between the hydroxyl groups on the molecules. Gels can be formed with concentrations as low as 1% w/w [24]. The formed fibrillar strands, however, show temperature dependent changes upon storage that are related to changes in the microstructure [25].

LMOG oleogels based on two-component structuring systems

Besides single-component systems, also two-component oleogel systems have been investigated. Combinations of two gelator molecules can promote synergistic effects when it comes to forming a network structure. For instance, by using a combination of fatty acids (C_nCOOH, with n = 16 – 20) and fatty alcohols (C_nOH, with n = 16 – 22), gel strength of the mixtures outperformed that of the single components [26]. Oleogels can also be prepared using a combination of an unsaturated fatty acid (oleic acid) and sodium oleate [27]. It was shown that the gel strength depended on the ratio of the two structuring components, which determines the self-assembly into either reverse micellar or lamellar phases. Moreover, due to enhanced hydrogen bonding, addition of a small amount of water increased the gel strength [27].

Another example of a two components system is a mixture of sorbitan tri-stearate and lecithin [28]. Both single components were not able to gelate oil, but mixtures between a ratio of 40:60 and 60:40 showed crystal formation, and thermo-reversible gels were formed at 6% w/w. Combining lecithin with tocopherol also led to the formation of a network [29]. In this case, a total concentration of 25 wt% was needed to form reverse micellar structures, capable of forming supramolecular assemblies [29].

Yet another well-studied example of oil gelation is by using a mixture of γ-oryzanol and β-sitosterol, which are capable of forming hollow tubular structures that aggregate into a network [30]. It was shown that the presence of water inhibited tubule formation by forming monohydrate crystals [31]. Furthermore, the tubule formation was shown to be affected by the polarity of the oil [32].

Polymeric oleogels

Although in the LMOG category many examples can be found, only a few polymers have been shown to have the ability to structure oil. Many polymers are hydrophilic in nature, which makes the dispersibility in oil difficult.

Direct dissolution method

The most extensively studied polymer for oleogel formation is the cellulose derivative ethylcellulose (EC). To increase the hydrophobicity of cellulose, polar hydroxyl groups on the glucose monomers are replaced by a more hydrophobic ethyl group through chemical modification. The degree of polymerisation and substitution can be altered, leading to a variety of EC polymers. EC oleogels are prepared by heating the oil above the glass transition temperature of EC (~ 140 °C) and upon subsequent cooling, the polymer chains entangle into a network. It was shown that using EC of different molecular weight, altering the cooling rate or polymer concentration, affected the final gel properties [33]. Moreover, the addition of different types of surfactants [34] and different oil types [35, 36] altered the dispersibility of the polymers and the interactions between them, leading to different properties of the final EC-based oleogels.

Another example of a polymer with the ability to structure oil is chitin. Due to its fairly hydrophobic nature, this crustacean-derived biopolymer is capable of forming gels in its crude form. The dispersibility of the chitin can be enhanced by hydrolysing chitin into nano-crystals, improving the gelling ability [37]. In other work, the oil dispersibility of hydrolysed chitin 'whiskers' was enhanced by attaching surfactants. Upon dispersing the chitin at elevated temperatures, thermo-reversible gels were obtained [38].

Indirect dispersion methods

Besides direct dispersion of the polymers into oil, also indirect methods can be used to incorporate polymers into oil. By following a foam- or emulsion-templated route, different polymers can be

used to form oleogels. In a first step, polymers like proteins or polysaccharides are added to form an oil-in-water emulsion or an aqueous foam, in which the polymers adsorb at the interface. The procedure is then followed by a freeze drying step to remove the continuous aqueous phase. Drying such an emulsion leads to the formation of a fine polyhedral network of the protein films that is able to entrap a very high amount of oil (~ 99%) [39]. In other work, to prepare a dried emulsion, a combination of gelatin and xanthan or methyl cellulose and xanthan have been used to stabilize the oil-water interface. Upon subsequent shearing, the dried emulsions could be converted into oleogels [40, 41]. The foam-templated approach was shown to work for hydroxyl propyl methylcellulose (HPMC). Upon drying the aqueous foam, and subsequent dispersing the dried product into liquid oil, the polymer sheets were able to bind liquid oil, forming self-standing oleogels [42].

Examples of oleogel functionality

Although the field of oil structuring is still relatively young, applications of oleogels in food systems have already been studied for several products. Ethylcellulose oleogels have been used to replace beef fat in Frankfurter-style sausages. When pure canola oil was used, a reduction in the average oil droplet size was observed compared to the globule size of beef fat. This reduction in droplet size resulted in much harder and more chewy samples. When the oil was structured with ethylcellulose, the 'fat' globules were much larger and similar to the size of the beef fat globules. As a result, the sausages with the oleogel sample were similar in textural properties to the sausage prepared with beef fat.

Sunflower- and beeswax oleogels have been studied for their potential as baking shortening in cookies. Here, sensory evaluation shows a good acceptance of the oleogel-based cookies [43]. Using the wax oleogels as breakfast margarine replacement on a slice of bread, sensory analysis showed that although the differences between the products were generally small, the waxy taste and gritty mouthfeel was higher for the wax-based oleogels compared to the margarine samples [44]. In a study on ice creams, rice bran wax oleogels were used as a replacement for milk fat. The ice cream prepared with the oleogel were compared to ice cream prepared either with high oleic sunflower oil or milk fat. Compared to oil, the ice cream with oleogel showed improved properties, such as higher air incorporation. However, the stability of the ice cream prepared with oleogel was lower compared to the ice cream prepared with milk fat [45]. Using the aforementioned foam-templated approach, hydroxyl propyl methylcellulose (HPMC) oleogels were prepared to replace icing shortening in different percentages for cookie cream preparation. HPMC was able to stabilize the liquid oil and at 50 and 75% fat replacement, similar physical

characteristics could be achieved [46]. In other work, shellac-based oleogel emulsions were shown to have promising properties in chocolate paste, spreads, and cakes [47].

Even though much research still needs to be performed to link molecular interactions in the oleogel to macroscopic properties of the final food product, as well as an evaluation of the sensorial and nutritional aspects, based on the developments in recent years, the potential for edible oleogels as solid fat replacement is promising.

A novel candidate for a non-TAG oil structuring agent

Obviously, in order to develop an oleogel that forms a suitable replacement for saturated fats, the requirements for the structuring agent go beyond merely providing a solid appearance to an otherwise liquid oil. A few, but crucial requirements have been identified [9]. For an oil gelator to be suitable, it must be food grade, economically viable, readily and widely available as a common food ingredient, efficient in terms of having a low gelling concentration, and it should have a high versatility in terms of tuning the rheological properties of the oleogel. Furthermore, the oleogel should tolerate water, shear, should be resistant to thermal degradation, should have an acceptable taste and should provide similar physical and rheological properties as the solid fat it is intended to replace. To make matters more complex, the resulting 'solid fat alternative' would be scrutinized by critical consumers. As with any successful innovation, consumers must accept the innovated product for having a clear benefit over the original product. Although many oil gelators have been identified, most of these lack one or more of the requirements mentioned above. Therefore, there is still a need to investigate other potential oil gelators.

A well-known food ingredient that meets all of the requirements, making it a possible oil gelator with a high potential for commercialization, is protein. Moreover, proteins have good nutritional value, have no regulatory issues for their use and would contribute to 'clean labelling'. Although proteins could be of high potential as a novel oil gelator, it has not been investigated whether they are suitable to structure liquid oil. Given their hydrophilic nature and insolubility in oil, proteins are not the most obvious choice to prepare oleogels with. When proven possible, however, it could provide ample opportunities for diversification since it is known that the gelation properties in water can be tailored to a large extent by, for example, changing processing conditions and protein composition. In this thesis, we investigate the potential of proteins as a novel structuring agent for oil.

Protein functionality

Proteins are commonly used for their structuring ability of aqueous phases. For the current thesis, whey proteins were used since they are a well characterized protein source and readily available in highly purified form. Gelation of whey proteins is most commonly achieved by heating an aqueous protein solution above its gelation concentration. Upon heating, the protein molecules unfold, exposing the hydrophobic parts normally buried within the protein centre [48]. This unfolding leads to protein aggregation via hydrophobic interactions and disulphide interaction [49-51]. Depending on the overall attractive and repulsive interactions, as affected by the pH or ionic strength, different types of networks can be formed. At conditions where the electrostatic repulsion is high, i.e. at conditions where the pH is either below or above the isoelectric point (pI) of the protein, and the ionic strength is low, 'fine-stranded' gels are formed. In the opposite case, where the pH is close to the pI, or at higher ionic strength, the gels become opaque and 'particulate' [52]. Besides this heat-induced gelation, also cold-set gelation can be used to form protein gels. In this method, first small aggregates are formed by heat treatment, stabilized against aggregation by repulsive electrostatic interaction. Then, after cooling, gelation is induced by removing the repulsive electrostatic barrier via the addition of salt or reducing the pH [53, 54].

Besides their functionality as gelling agents, proteins and protein aggregates are also used as emulsifiers to stabilize emulsions and foams [55, 56]. This thesis is concerned with extending the already impressive versatile functionality of proteins by using them as a direct structuring agent in oil continuous systems to form edible oleogels. Using proteins as a base for a novel type of oil gelator is challenging since due to their hydrophilic nature, proteins do not readily dissolve in oil. Therefore, an alternative route had to be developed to be able to use proteins as functional building blocks for network formation in an oil continuous phase. The aim of this thesis was to design effective routes to structure oil using protein building blocks and understand the mechanical aspects of the resulting oleogels.

Outline of the thesis

Figure 1.2 shows the general outline of this thesis, and gives an overview of the different aspects important for protein-based oleogelation. In Chapter 2, the aim was to develop a method to obtain protein oleogels based on pre-set hydrogel templates. The oil binding capacity of the oleogels was studied for different hydrogel matrices. Additionally, the protein oleogels were investigated for their rheological properties and were compared to those of the preceding hydrogels. In Chapter 3, submicron aggregates were prepared to allow for enhanced control over the resulting network

properties. In this chapter, we aimed to understand the network formation of protein aggregates and compared the behaviour of the protein oleogels to protein hydrogels of fractal nature. In Chapter 4, the aim was to gain insight in the interactions between protein aggregates in oil by changing the type of oil with respect to oil polarity and chemical composition. Next, in Chapter 5, interactions between protein aggregates were studied with respect to water addition and heat treatment. In Chapter 6, the underlying mechanism to use proteins as oil gelator was studied. Here, different routes to obtain protein oleogels were examined. Moreover, it was aimed to enhance the knowledge for further development in designing an effective route to transfer protein building blocks from the aqueous to the oil phase. Chapter 7 discusses the results across the different chapters by linking interactions between protein aggregates in oil and water on a molecular scale to properties like gel strength of the networks formed on a macroscopic scale. Possible alternative routes are discussed as well as an outlook for further development of protein-based oil structuring.

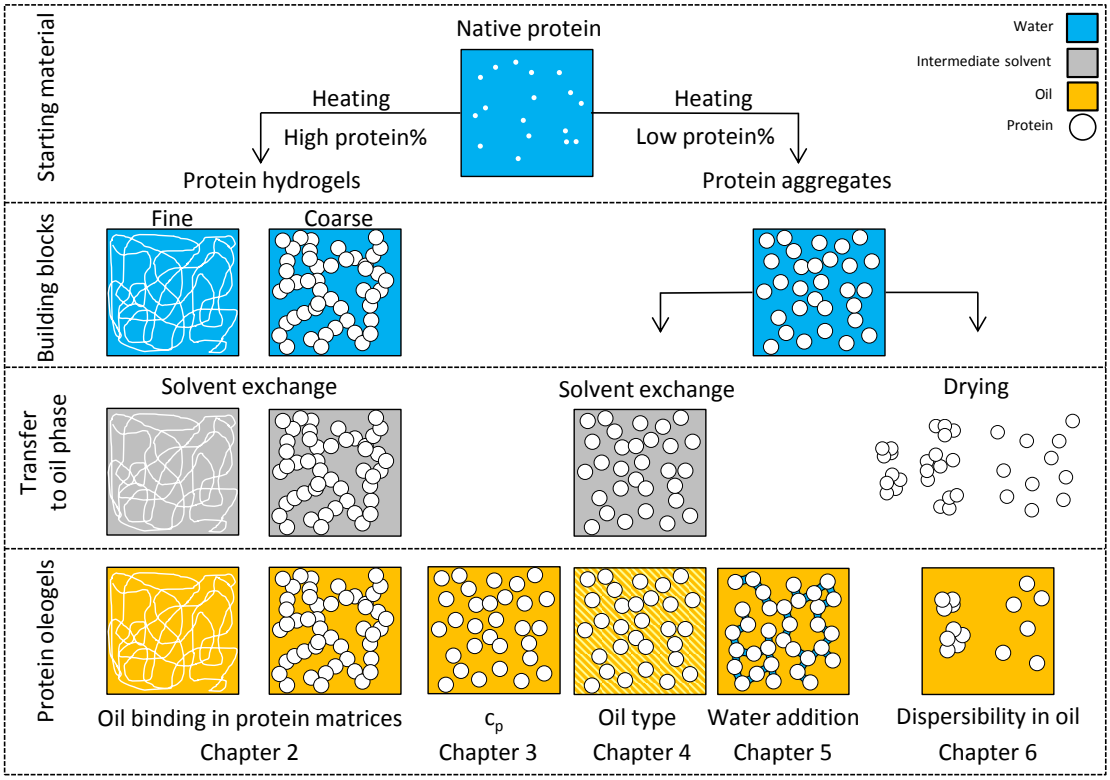

Figure 1.2. Outline of the thesis.

References

1. Hu, F.B. and W.C. Willett, *Optimal diets for prevention of coronary heart disease.* Journal of the American Medical Association, 2002. **288**(20): p. 2569-2578.
2. Mensink, R.P. and M.B. Katan, *Effect of dietary trans fatty acids on high-density and low-density lipoprotein cholesterol levels in healthy subjects.* New England Journal of Medicine, 1990. **323**(7): p. 439-445.
3. Mensink, R.P., et al., *The Increasing Use of Interesterified Lipids in the Food Supply and Their Effects on Health Parameters.* Adv Nutr, 2016. **7**(4): p. 719-29.
4. Mensink, R.P., et al., *Effects of dietary fatty acids and carbohydrates on the ratio of serum total to HDL cholesterol and on serum lipids and apolipoproteins: A meta-analysis of 60 controlled trials.* American Journal of Clinical Nutrition, 2003. **77**(5): p. 1146-1155.
5. Sato, K., *Crystallization behaviour of fats and lipids — a review.* Chemical Engineering Science, 2001. **56**(7): p. 2255-2265.
6. Marangoni, A.G., et al., *Structure and functionality of edible fats.* Soft Matter, 2012. **8**(5): p. 1275-1300.
7. Macias-Rodriguez, B. and A.G. Marangoni, *Rheological characterization of triglyceride shortenings.* Rheologica Acta, 2016. **55**(9): p. 767-779.
8. Patel, A.R. and K. Dewettinck, *Edible oil structuring: an overview and recent updates.* Food & Function, 2016. **7**(1): p. 20-29.
9. Marangoni, A., *Organogels: An Alternative Edible Oil-Structuring Method.* Journal of the American Oil Chemists' Society, 2012. **89**(5): p. 749-780.
10. Basak, S., J. Nanda, and A. Banerjee, *A new aromatic amino acid based organogel for oil spill recovery.* Journal of Materials Chemistry, 2012. **22**(23): p. 11658-11664.
11. Baglioni, P., et al., *Organogel formulations for the cleaning of easel paintings.* Applied Physics a-Materials Science & Processing, 2015. **121**(3): p. 857-868.
12. Babu, S.S., S. Prasanthkumar, and A. Ajayaghosh, *Self-Assembled Gelators for Organic Electronics.* Angewandte Chemie-International Edition, 2012. **51**(8): p. 1766-1776.
13. Vintiloiu, A. and J.C. Leroux, *Organogels and their use in drug delivery - A review.* Journal of controlled release, 2008. **125**(3): p. 179-192.
14. Sagiri, S.S., et al., *Organogels as Matrices for Controlled Drug Delivery: A Review on the Current State.* Soft Materials, 2013. **12**(1): p. 47-72.
15. Brosse, N., D. Barth, and B. Jamart-Grégoire, *A family of strong low-molecular-weight organogelators based on aminoacid derivatives.* Tetrahedron Letters, 2004. **45**(52): p. 9521-9524.
16. Terech, P. and R.G. Weiss, *Low molecular mass gelators of organic liquids and the properties of their gels.* Chemical Reviews, 1997. **97**(8): p. 3133-3159.
17. Rogers, M.A., *Novel structuring strategies for unsaturated fats – Meeting the zero-trans, zero-saturated fat challenge: A review.* Food Research International, 2009. **42**(7): p. 747-753.

18. Rogers, M.A., A.J. Wright, and A.G. Marangoni, *Oil organogels: the fat of the future?* Soft Matter, 2009. **5**(8): p. 1594-1596.
19. Chen, C.H. and E.M. Terentjev, *Aging and metastability of monoglycerides in hydrophobic solutions.* Langmuir, 2009. **25**(12): p. 6717-24.
20. Ojijo, N.K.O., et al., *Effects of monoglyceride content, cooling rate and shear on the rheological properties of olive oil/monoglyceride gel networks.* Journal of the Science of Food and Agriculture, 2004. **84**(12): p. 1585-1593.
21. Toro-Vazquez, J.F., et al., *Thermal and textural properties of organogels developed by candelilla wax in safflower oil.* Journal of the American Oil Chemists Society, 2007. **84**(11): p. 989-1000.
22. Blake, A.I., E.D. Co, and A.G. Marangoni, *Structure and physical properties of plant wax crystal networks and their relationship to oil binding capacity.* JAOCS, Journal of the American Oil Chemists' Society, 2014. **91**(6): p. 885-903.
23. Rogers, M.A., A.J. Wright, and A.G. Marangoni, *Ceramide Oleogels*, in *Edible Oleogels*. 2011, AOCS Press. p. 221-234.
24. Rogers, M.A., A.J. Wright, and A.G. Marangoni, *Nanostructuring fiber morphology and solvent inclusions in 12-hydroxystearic acid / canola oil organogels.* Current Opinion in Colloid and Interface Science, 2009. **14**(1): p. 33-42.
25. Rogers, M.A., A.J. Wright, and A.G. Marangoni, *Crystalline stability of self-assembled fibrillar networks of 12-hydroxystearic acid in edible oils.* Food Research International, 2008. **41**(10): p. 1026-1034.
26. Gandolfo, F.G., A. Bot, and E. Flöter, *Structuring of Edible Oils by Long-Chain FA, Fatty Alcohols, and Their Mixtures.* Journal of the American Oil Chemists' Society, 2004. **81**(1): p. 1-6.
27. Nikiforidis, C.V., E.P. Gilbert, and E. Scholten, *Organogel formation via supramolecular assembly of oleic acid and sodium oleate.* RSC Advances, 2015. **5**(59): p. 47466-47475.
28. Pernetti, M., et al., *Structuring edible oil with lecithin and sorbitan tri-stearate.* Food Hydrocolloids, 2007. **21**(5-6): p. 855-861.
29. Nikiforidis, C.V. and E. Scholten, *Self-assemblies of lecithin and α-tocopherol as gelators of lipid material.* RSC Advances, 2014. **4**(5): p. 2466-2473.
30. Bot, A. and W.G.M. Agterof, *Structuring of edible oils by mixtures of γ-oryzanol with β-sitosterol or related phytosterols.* Journal of the American Oil Chemists' Society, 2006. **83**(6): p. 513-521.
31. Sawalha, H., et al., *Organogel-emulsions with mixtures of β-sitosterol and γ-oryzanol: Influence of water activity and type of oil phase on gelling capability.* Journal of Agricultural and Food Chemistry, 2012. **60**(13): p. 3462-3470.
32. Sawalha, H., et al., *The influence of the type of oil phase on the self-assembly process of γ-oryzanol + β-sitosterol tubules in organogel systems.* European Journal of Lipid Science and Technology, 2013. **115**(3): p. 295-300.

33. Gravelle, A.J., et al., *Towards the development of a predictive model of the formulation-dependent mechanical behaviour of edible oil-based ethylcellulose oleogels.* Journal of Food Engineering, 2014. **143**: p. 114-122.
34. Davidovich-Pinhas, M., S. Barbut, and A.G. Marangoni, *The role of surfactants on ethylcellulose oleogel structure and mechanical properties.* Carbohydrate Polymers, 2015. **127**: p. 355-362.
35. Gravelle, A.J., et al., *Influence of solvent quality on the mechanical strength of ethylcellulose oleogels.* Carbohydr Polym, 2016. **135**: p. 169-79.
36. Laredo, T., S. Barbut, and A.G. Marangoni, *Molecular interactions of polymer oleogelation.* Soft Matter, 2011. **7**(6): p. 2734-2743.
37. Nikiforidis, C.V. and E. Scholten, *Polymer organogelation with chitin and chitin nanocrystals.* RSC Advances, 2015. **5**(47): p. 37789-37799.
38. Huang, Y., et al., *Hydrophobic modification of chitin whisker and its potential application in structuring oil.* Langmuir, 2015. **31**(5): p. 1641-1648.
39. Romoscanu, A.I. and R. Mezzenga, *Emulsion-templated fully reversible protein-in-oil gels.* Langmuir, 2006. **22**(18): p. 7812-7818.
40. Patel, A.R., et al., *Biopolymer-based structuring of liquid oil into soft solids and oleogels using water-continuous emulsions as templates.* Langmuir, 2015. **31**(7): p. 2065-2073.
41. Patel, A.R., et al., *Edible oleogels based on water soluble food polymers: Preparation, characterization and potential application.* Food and Function, 2014. **5**(11): p. 2833-2841.
42. Patel, A.R., et al., *A foam-templated approach for fabricating organogels using a water-soluble polymer.* RSC Advances, 2013. **3**(45): p. 22900-22903.
43. Yilmaz, E. and M. Ogutcu, *The texture, sensory properties and stability of cookies prepared with wax oleogels.* Food Funct, 2015. **6**(4): p. 1194-204.
44. Yılmaz, E. and M. Öğütcü, *Oleogels as spreadable fat and butter alternatives: sensory description and consumer perception.* RSC Adv., 2015. **5**(62): p. 50259-50267.
45. Zulim Botega, D.C., et al., *The potential application of rice bran wax oleogel to replace solid fat and enhance unsaturated fat content in ice cream.* J Food Sci, 2013. **78**(9): p. C1334-C1339.
46. Tanti, R., S. Barbut, and A.G. Marangoni, *Hydroxypropyl methylcellulose and methylcellulose structured oil as a replacement for shortening in sandwich cookie creams.* Food Hydrocolloids, 2016. **61**: p. 329-337.
47. Patel, A.R., et al., *Edible applications of shellac oleogels: Spreads, chocolate paste and cakes.* Food and Function, 2014. **5**(4): p. 645-652.
48. Gosal, W.S. and S.B. Ross-Murphy, *Globular protein gelation.* Current Opinion in Colloid & Interface Science, 2000. **5**(3-4): p. 188-194.
49. Havea, P., A.J. Carr, and L.K. Creamer, *The roles of disulphide and non-covalent bonding in the functional properties of heat-induced whey protein gels.* Journal of Dairy Research, 2004. **71**(3): p. 330-339.

50. Hines, M.E. and E.A. Foegeding, *Interactions of alpha-lactalbumin and bovine serum-albumin with beta-lactoglobulin in thermally induced gelation.* Journal of Agricultural and Food Chemistry, 1993. **41**(3): p. 341-346.

51. Roefs, S. and K.G. Dekruif, *A model for the denaturation and aggregation of beta-lactoglobulin.* European Journal of Biochemistry, 1994. **226**(3): p. 883-889.

52. Langton, M. and A.-M. Hermansson, *Fine-stranded and particulate gels of β-lactoglobulin and whey protein at varying pH.* Food Hydrocolloids, 1992. **5**(6): p. 523-539.

53. Alting, A.C., et al., *Cold-set globular protein gels: Interactions, structure and rheology as a function of protein concentration.* Journal of Agricultural and Food Chemistry, 2003. **51**(10): p. 3150-3156.

54. Ako, K., T. Nicolai, and D. Durand, *Salt-induced gelation of globular protein aggregates: Structure and kinetics.* Biomacromolecules, 2010. **11**(4): p. 864-871.

55. Nicolai, T., M. Britten, and C. Schmitt, *beta-Lactoglobulin and WPI aggregates: Formation, structure and applications.* Food Hydrocolloids, 2011. **25**(8): p. 1945-1962.

56. Schmitt, C., et al., *Whey protein soluble aggregates from heating with NaCl: Physicochemical, interfacial, and foaming properties.* Langmuir, 2007. **23**(8): p. 4155-4166.

Chapter 2

Protein oleogels from protein hydrogels via a stepwise solvent exchange route

This chapter is based on: de Vries, A., Hendriks, J., van der Linden, E., Scholten, E., *Protein Oleogels from Protein Hydrogels via a Stepwise Solvent Exchange Route*, Langmuir 31, 2015, p. 13850-13859.

Introduction

An organogel or oleogel can be defined as an organic liquid with a low polarity entrapped into a three-dimensional network. In recent years, its development has gained much attention from colloid and material scientists and oleogels have applications in the field of pharmaceuticals as drug delivery systems [1, 2], (bio)lubricant technology [3], and as fat replacement in food products [4-6]. Given the great potential of oleogels in different fields, it is of importance to identify sustainable, cost effective and food-safe oleogelators. Therefore, in addition to chemically synthesised molecules, many biocompatible oleogelators have been identified and characterised and can be classified as either low molecular weight oleogelators (LMOGs) or biopolymeric oleogelators. The most common gelators are of low molecular weight and networks are created via their self-assembly. The resulting network morphology can consist of a variety of supramolecular assemblies, such as interconnected crystals, (inverse) micelles, tubules or fibrils. Examples of such LMOGs are waxes [7, 8], 12-hydroxystearic acid [9, 10], fatty acids or alcohols [11, 12], phytosterols [13], lecithins [14, 15], and oligopeptides [16].

Oleogels based on biopolymers are rather scarce, since biopolymers are mostly hydrophilic in nature and thus exhibit poor solubility in nonpolar solvents. One well-known exemption is the cellulose derivative ethylcellulose. Ethylcellulose is insoluble in water, but soluble in liquid oil at high temperatures. Upon cooling, the cellulose chains entangle and form a network [17, 18]. In order to use hydrophilic biopolymers as oil structurants, modifications or surfactants are often necessary. In a recent study, the polysaccharide chitin was modified into hydrophobic “whiskers” [19]. The increased hydrophobicity of the chitin increased the dispersibility in liquid oil and showed a thickening effect at low temperatures. Other researchers have shown that the addition of a surfactant enhanced the dispersibility of both crude chitin and chitin nanocrystals in vegetable oil and thereby creating chitin-based oleogels [20].

Another way to overcome the poor dispersibility of biopolymers in liquid oils, is based on an emulsion-templated approach. In this case, the process relies on the adsorption of proteins or other polymers on an oil-water interface (with or without chemical crosslinking) followed by a subsequent evaporation of the water phase as first studied by Romoscanu [21]. The resulting high internal phase emulsions obtained can have an oil content above 99 wt%. In this case, the aqueous phase is still the continuous phase and the obtained elastic solid can be reversed into a liquid upon rehydration. Other work, using a similar approach, has shown that upon drying and subsequent shearing a gelatin-xanthan or methylcellulose-xanthan stabilised emulsion, an oleogel can be formed [22, 23]. Due to the involved shearing of the dried emulsion, however, it may be difficult

to control the particle shape and size, and thereby the properties of the final oleogel. Although not extensively studied, the design of biopolymer-based oleogels could have many promising features, since many biopolymers are usually inexpensive, readily available, and food-grade.

We choose to investigate the potential of proteins as novel oleogelators where oil is the continuous phase. Gelation of water by proteins into hydrogels is well known. Common examples are milk-derived proteins [24], gelatin [25], egg proteins [26], and many plant-based proteins [27-29]. Proteins have an amphiphilic nature, hence their use as emulsifiers [30]. Despite their partial affinity for apolar solvents, proteins have a predominantly hydrophilic character and are poorly dispersible in oil. To enhance the applicability of proteins as an oleogelator, we have created protein-based oleogels by using a solvent exchange procedure. First, a heat-set protein hydrogel is created in the aqueous phase, followed by an exchange of the internal aqueous phase for a liquid oil via an intermediate solvent. The process of solvent exchange is common practice to produce aerogels, where the water inside a hydrogel is replaced by acetone or an alcohol, which is subsequently removed by supercritical CO_2. An example is the preparation of porous protein aerogels for the use as drug delivery systems [31]. Next to aerogels, a solvent exchange procedure was also applied to (micro)hydrogels to incorporate hydrophobic nanoparticles [32] and to transfer enzymes in hydrogels to organic media [33, 34]. These studies have shown that it is possible to exchange the internal water inside a polymeric hydrogel at least partially for an apolar solvent.

Using a stepwise solvent exchange procedure, we were able to create a protein oleogel from a hydrogel template without affecting the gel network noticeably. We have chosen to use whey proteins as they are widely used in different fields of research, relatively cheap and bio-compatible. Whey protein hydrogels can show various morphologies, from fine-stranded to coarse networks, depending on the hydrogel preparation conditions. In this chapter, the oil holding capacity and the mechanical properties of whey protein oleogels after a solvent exchange procedure was examined as a function of the microstructure of the preceding hydrogels.

Materials and methods

Materials

Whey protein isolate (WPI, BiPro) was obtained from Davisco Foods International (Le Sueur, MN, USA). The protein concentration was 93.2% w/w (N x 6.38) and was used as received. Acetone (AR grade) was supplied by Actu-All Chemicals (Oss, the Netherlands). Tetrahydrofuran (THF, HPLC-grade) was obtained from Chem-Lab (Zeldegem, Belgium) and hexane (HPLC grade) and sodium chloride (NaCl) were obtained from Sigma Aldrich. Sunflower oil (Vandermoortele NV, Breda, the Netherlands) was bought at a local supermarket and was used without further purification. Demineralized water was used throughout the experiments.

Methods

Preparation of protein hydrogels

WPI powder (20% w/w) was added to demineralized water under stirring at room temperature for 2 h to make a protein stock solution. Afterwards, the stock solution was stored overnight in a refrigerator at 4 °C to assure complete hydration of the proteins. To prepare the hydrogels, the stock solution was diluted to the right concentration and brought to the appropriate ionic strength by adding 1 M NaCl solution. Gels were prepared with 0 – 200 mM NaCl at a fixed protein concentration of 15% w/w WPI and with 10 – 16% w/w WPI at a fixed ionic strength of 50 mM NaCl. The pH of all samples was 7.0 (± 0.1) and adjusted when necessary using 1 M NaOH or HCl.

Hydrogels for the solvent exchange and water holding capacity experiments were prepared by heat denaturation of the proteins in cylindrical containers (l = 40 mm, d = 12 mm) using a temperature controlled water bath at 85 °C for 30 min. Afterwards, the gels were allowed to cool down to room temperature for 1 h and were stored overnight at 4 °C. The next day, gels were cut in cylindrical pieces (l = 5 mm, d = 5 mm) using a gel cutter. Hydrogels for the compression tests were made via the same procedure using larger (l = 50 mm, d = 20 mm) cylindrical containers.

Solvent exchange

To exchange the water inside the protein hydrogel matrices for sunflower oil, cylindrical gel pieces (l = 5 mm, d = 5 mm) were placed into mesh metal baskets. In a glass flask containing the solvent, the baskets were immersed for 8 - 12 h per solvent at room temperature under continuous stirring of the solvent. Different solvent exchange procedures were examined varying in the amount of exchange steps and solvent conditions. An overview is outlined in Table 2.1. The intermediate

solvents were either acetone or THF, as both solvents are miscible with both water and sunflower oil. As a standard, procedure 1 was used, unless stated otherwise. In all procedures, the gels were immersed twice in fresh 100% v/v intermediate solvent to assure water removal. Similarly, the gels were immersed twice in fresh sunflower oil, to remove the intermediate solvent. The volume of solvent was in excess to the volume of the gels (200 : 1). Time between transferring the gel from one solvent to the next was kept to a minimum to prevent evaporation. After the final solvent exchange step with oil, the resulting oleogels were taken out of their container, carefully blotted dry with tissue paper and their final weight was recorded. The oil holding capacity (Q_{oil}) was defined as:

$$Q_{oil} = \frac{W_o}{W_i} \qquad (2.1)$$

where W_o represents the weight of the final oleogel and W_i the weight of the initial hydrogel before the solvent exchange procedure. Q_{oil} values reported are the average of two measurements.

Table 2.1. Applied solvent exchange methods. The consecutively used solvents per method are indicated with tick marks. As intermediate solvent either acetone or THF was used.

Method	% (v/v) Intermediate solvent in water					% (v/v) Oil in intermediate solvent			
	0%	30%	50%	70%	100%	30%	50%	70%	100%
1		✓	✓	✓	✓ (2x)	✓	✓	✓	✓ (2x)
2					✓ (2x)				✓ (2x)
3	✓				✓ (2x)				✓ (2x)
4			✓		✓ (2x)		✓		✓ (2x)
5	✓		✓		✓ (2x)		✓		✓ (2x)

Water holding capacity

To gain information on the water holding capacity of the protein hydrogels in aqueous media, we performed a swelling experiment. To this end, cylindrical WPI hydrogels (d = 5 mm, l = 5 mm) were immersed into demineralized water using mesh metal baskets under continuous stirring. At regular time intervals, the gels were taken out of their container, carefully blotted dry with tissue paper and the weight was recorded on an analytical scale. Their swelling ratio (Q_w) was followed over time and was defined as:

$$Q_w = \frac{W_t}{W_i} \qquad (2.2)$$

where W_t represents the weight of the hydrogel at a certain time t and W_i is the initial weight of the hydrogel before immersion in water. After approximately 6 h, no weight change was measured and maximum water holding was assumed. The ratio at this equilibrium condition is denoted as Q_{wEq} and used as a measure of the water holding capacity of the initial protein gel in aqueous environments.

Composition of oleogels

Protein content. Protein content was determined using Dumas. Samples were loaded into a Flash EA 1112 N/protein analyser (Thermo Scientific, Waltham, US) and the protein content was determined from the nitrogen concentration using a conversion factor of N x 6.38.

Oil content. Oil content was determined using a hexane extraction procedure. To this end, the oleogels were sliced into small pieces using a razor and weighed. Hexane was added in excess volume and left to extract the oil from the protein network for 24 h. This extraction procedure was repeated twice with fresh hexane. Afterwards, the de-oiled sample was collected and dried at room temperature under air flow until constant weight was reached. The dry sample was weighed again to calculate the oil content indirectly from the weight loss.

Water content. Water content in the oleogels was determined by dry matter determination. Aluminium cups (ø = 5 cm) were heated to 105 °C in an oven (Venticell, BMT Med. Technology, Brno, Czech Republic) to remove any water contamination. Afterwards, approximately 0.5 – 0.8 g of oleogel sample was added to the cup, and its weight was recorded before and after drying for 3 h at 105 °C.

Compression tests

To determine the mechanical properties of the hydrogels, uniaxial compression tests were performed with a texture analyser (TA.XT plus, Stable Micro Systems Ltd., Godalming, UK) equipped with a 50 kg load cell. The measurements were performed with cylindrical hydrogels (l = 20 mm, d = 20 mm) by compressing the samples with an aluminium probe (d = 10 cm) at a speed of 1 mm/s until a compression strain of 90% of its original height. Prior to the measurements, the top and bottom of the gel was coated with a thin layer of mineral oil to prevent sticking of the sample to the probe. The true stress (σ_t) accounts for the change in cross-sectional area, assuming the sample maintains its cylindrical shape during compression and was calculated as:

$$\sigma_t = \frac{F}{A} \qquad (2.3)$$

where A is the actual cross-sectional area of the sample and F is the force (N) measured during compression. The true strain, or Hencky strain (ε_H) was calculated as:

$$\varepsilon_H = ln\left(\frac{L_i}{L_i - \Delta L}\right) \qquad (2.4)$$

where L_i is the initial height of the sample and ΔL is the decrease in gel height upon compression. The Young's modulus was obtained from the slope in the linear visco-elastic region of the stress – strain curve ($0.04 < \varepsilon_H < 0.08$). The fracture point was determined as the point where a sudden drop in the curve was observed and the corresponding stress and strain at fracture were recorded. Throughout this manuscript, instead of Young's modulus, the term modulus will be used. The mechanical properties of the oleogels were determined using the same procedure as described for the hydrogels. Oleogel samples obtained after the solvent exchange procedure were used without further modification. It was assumed the solvent exchange procedure did not change the surface area and height (l = 5 mm, d = 5 mm) of the oleogel samples.

Scanning Electron Microscopy

The microstructure of the oleogels was analysed using Cryo Scanning Electron Microscopy (Cryo-SEM). Oleogels were cut in approximately 2 mm thick slabs with a razor blade. For partial extraction of the oil, the slabs were immersed in pure hexane for 3 minutes at room temperature. Hereafter, the excess of the hexane was allowed to evaporate from the surface and samples were attached, cut face upwards, on a brass Leica sample holder with carbon glue (Leit-C, Neubauer Chemikalien, Germany). The holder was fitted into the cryo-sample loading system (VCT 100, Leica, Vienna, Austria) and simultaneously frozen in liquid nitrogen. The frozen holder was transferred to the cryo-preparation system (MED 020/VCT 100, Leica, Vienna, Austria) onto the sample stage at -93 °C. For removal of frost contamination on the sample surface, the samples were freeze dried for 5 - 7 min at -93 °C at 1.3×10^{-6} bar. After sputter coating a layer of 10 nm tungsten at the same temperature, the sample holder was transferred into the field emission scanning electron microscope (Magellan 400, FEI, Eindhoven, The Netherlands) onto the sample stage at -120 °C. Analysis was performed at a working distance of 3 - 4.5 mm, with SE detection at 2 kV and 6.3 pA. Digital images were optimized with Photoshop CS5.

Results and discussion

Appearance, composition and microstructure of WPI oleogels

To obtain a variety of whey protein (WPI) oleogels, different WPI hydrogels were prepared with varying microstructure. The hydrogels were prepared at pH 7 by applying heat treatment to allow aggregation of the proteins and the microstructure of the protein network was varied using different ionic strength. WPI, with β-lactoglobulin as its main constituent, has an isoelectric point (pI) of around 5.2 and the net negative charge density of the protein molecules at pH 7 was sufficiently high to obtain fine stranded, transparent gels at low ionic strength. At higher ionic strength, coarser and turbid gels are obtained as seen in Figure 2.1 as the upper pictures. In protein hydrogels, the formation of a coarser network is a common phenomenon at higher ionic strength [35-37]. After the solvent exchange procedure using acetone as an intermediate solvent, WPI gel matrices were still intact and Figure 2.1 shows the appearance of the oleogels obtained (lower pictures). Although the turbidity of the oleogels is similar to that of the hydrogel, the colour had changed from transparent or white to yellow, indicating an effective water removal and oil diffusion into the protein structure. Storing the oleogels for several weeks at room temperature resulted in only minimal oil leakage, indicating that the oil was tightly entrapped inside the protein matrix. Another important observation is that the fine stranded hydrogels prepared at 0 mM NaCl increased in volume after the solvent exchange, whereas at higher ionic strength the volume of the oleogel remains more comparable to the preceding hydrogel.

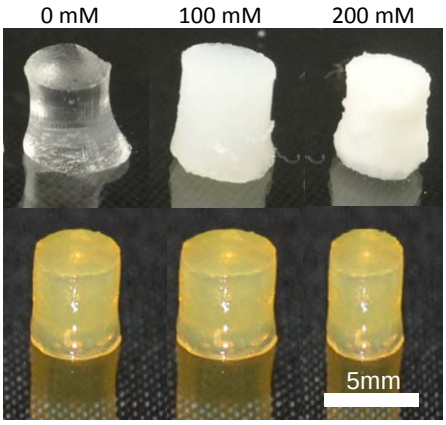

Figure 2.1. Appearance of WPI hydrogels (upper pictures) and oleogels (lower pictures) after the solvent exchange. The composition of the hydrogels was 15% WPI with 0 mM, 100 mM, and 200 mM NaCl.

To confirm the oil diffusion into the protein network and that the water inside the protein gel was replaced by oil, the composition of the formed oleogels was determined and the results are shown in Table 2.2. Water contents were low in all gels (< 1%), indicating the solvent exchange procedure effectively removed most water from the initial gel structure and oil was effectively incorporated. Depending on the type of hydrogel, from fine-stranded to coarse, the oil content decreased from 91% to 79% w/w and the protein concentration increased from 5.3% to 15.8% w/w. The measured protein concentration in the fine-stranded oleogel (0 mM NaCl), corrected for the change in weight before and after the solvent exchange, contained 22% w/w less protein. Apparently, not all protein material was incorporated into the oleogel network and was able to diffuse into the bulk solvent during the solvent exchange. The loss of protein material decreased to 16% w/w as the ionic strength increased to 200 mM. This decrease may be attributed to the lower electrostatic repulsion between the protein molecules during heat set gelation, incorporating more protein into the gel network.

Table 2.2. Composition of WPI oleogels formed from different hydrogels by solvent exchange procedure using acetone as intermediate solvent. Values indicate averages, and values in parentheses indicate standard deviations of duplicate measurements.

Hydrogel type	Composition oleogels		
	Oil% w/w	Protein% w/w	Water% w/w
15% WPI 0mM	91.10 (0.02)	5.33 (0.26)	0.32 (0.08)
15% WPI 50mM	86.35 (0.20)	9.65 (0.10)	0.52 (0.06)
15% WPI 100mM	82.67 (0.11)	12.87 (0.97)	0.68 (0.19)
15% WPI 200mM	79.70 (0.03)	15.82 (0.59)	0.84 (0.06)

To evaluate the distribution of oil in the WPI oleogels, the diffusion of a hydrophobic colorant (Nile Red) was followed in the oleogels and hydrogels. Figure 2.2 shows cross sections of hydrogels and oleogels after they were immersed in sunflower oil containing Nile Red for 4 h and 24 h. On the surface of the hydrogel some adsorption of Nile Red was observed, but no diffusion inside the hydrogel matrix was seen. In contrast, the colorant was able to diffuse into and spread throughout the oleogel structure. The unhindered diffusion of the hydrophobic colorant indicates that the oil is homogeneously distributed throughout the gel, where the oil is entrapped by the WPI network.

In order to determine whether microstructural changes of the protein network took place during the solvent exchange procedure, the microstructure of the different oleogels was visualized with cryo-SEM (Figure 2.3). As can be seen, the microstructure of the gel prepared at low ionic strength has a smooth appearance and the structural elements (i.e. the protein aggregates) are small (< 100 nm). This is consistent with the transparent appearance of the gel. As the ionic strength increases, a coarser microstructure with larger structural elements and larger mesh sizes is observed. Larger mesh sizes and a coarser appearance is typical in protein hydrogels when ionic strength increases [37, 38]. It is important to note that neither voids nor evidence of 'oil pools' were observed in the microstructure, showing that the protein network was undamaged after the solvent exchange.

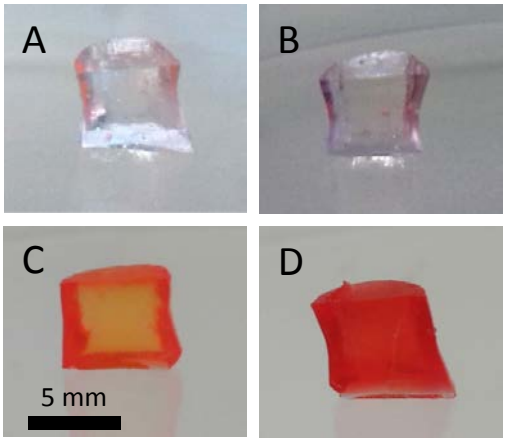

Figure 2.2. Diffusion of hydrophobic dye (0.05% Nile Red) into a 15% WPI hydrogel after 4h (A) and 24h (B) and the resulting oleogel after 4h (C) and 24h (D). Diffusing medium was sunflower oil.

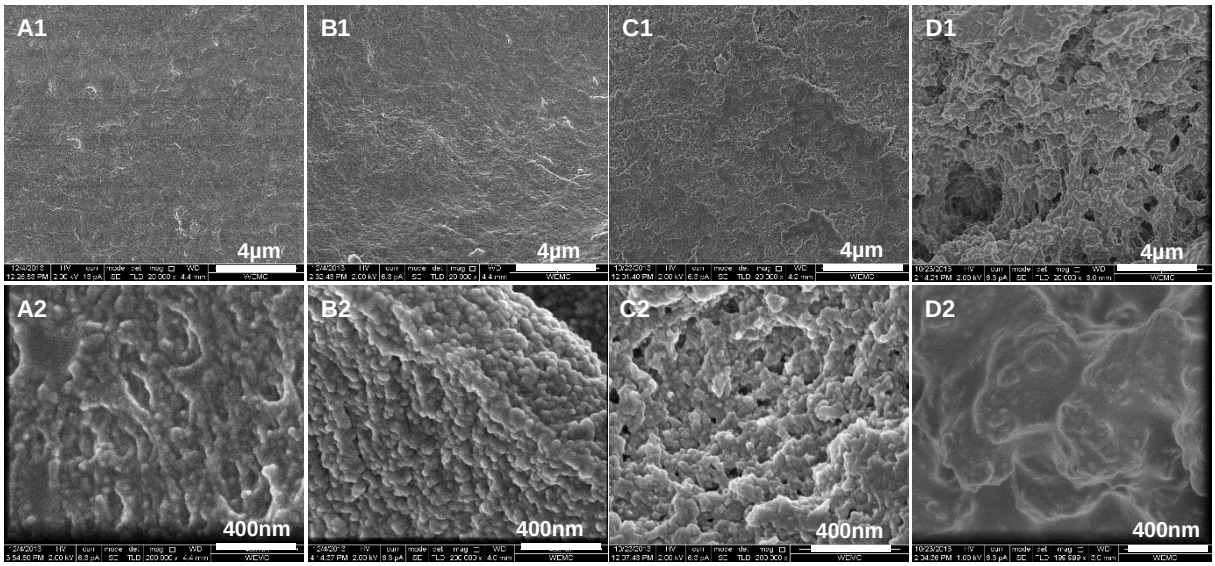

Figure 2.3. Microstructure of WPI oleogels as observed by cryo-SEM. Starting material was 15% WPI hydrogel with (A) 0 mM, (B) 50 mM, (C) 100 mM and (D) 200 mM NaCl. Numbers 1 and 2 represent different magnifications of the same sample.

The results show that by applying a solvent exchange procedure, the aqueous phase inside the protein hydrogel can be successfully replaced by oil, resulting in oleogels with a homogeneous structure of fine-stranded or coarse nature. As the microstructure of the oleogels can be set by controlling the conditions of the preceding hydrogels, the oil holding capacity was studied further for different gel microstructures.

Oil holding capacity as affected by microstructure and protein concentration

A change in volume between the hydrogels and formed oleogels after the solvent exchange procedure was observed, and this change depended on the coarseness of the gel matrix. To analyze this phenomenon further, we examined the effect of different microstructure and protein concentration during hydrogel formation on the weight ratio (Q_{oil}) between the initial hydrogel and the formed oleogel after the solvent exchange. Here, we used the standard solvent exchange procedure, starting with 30 vol% intermediate solvent, and we assume that all water has been replaced by oil.

Ionic strength and protein concentration during hydrogel preparation were varied from 0 – 200 mM and 10 – 16% w/w, respectively, to change the properties of the protein network. Besides changing the gel matrix, two different intermediate solvents were used; acetone and THF. In Figure 2.4, Q_{oil} values are plotted for the different types of hydrogels. Q_{oil} values larger than 1

mean that, compared to the initial hydrogel, the resulting oleogel increased in weight during the solvent exchange procedure, whereas a $Q_{oil} < 1$ indicates shrinkage. Figure 2.4A shows the effect of the network type by changing the ionic strength during hydrogel preparation. In the case acetone was used as the intermediate solvent, an increase in ionic strength from 0 to 200 mM resulted in a decrease in Q_{oil} from 2.13 to 0.85, indicating that the fine-stranded gel had roughly doubled in weight, whereas the coarse gel shrunk. Given the fact that oil has a lower density than water, the changes in volume are even larger. Increasing protein concentration from 10 to 16% w/w at a fixed ionic strength (50 mM) decreased Q_{oil} from 1.71 to 1.18, as seen in Figure 2.4B. Using THF as an intermediate solvent generated lower Q_{oil} values for all gel matrices compared to acetone. Similar to when acetone was used as an intermediate solvent, the effects of microstructure and protein concentration are still observed, but the differences are less noticeable. A decrease in Q_{oil} was observed from 0.85 to 0.65 with increasing ionic strength and from 0.97 to 0.75 with increasing protein concentration. In contrast to acetone, however, all of the gels had a Q_{oil} value lower than 1. The large difference in Q_{oil} values as a result of variations in the gel matrix, and as a result of interchanging acetone and THF indicate that, besides the type of gel matrix, also the intermediate solvent has an effect on the oil holding capacity.

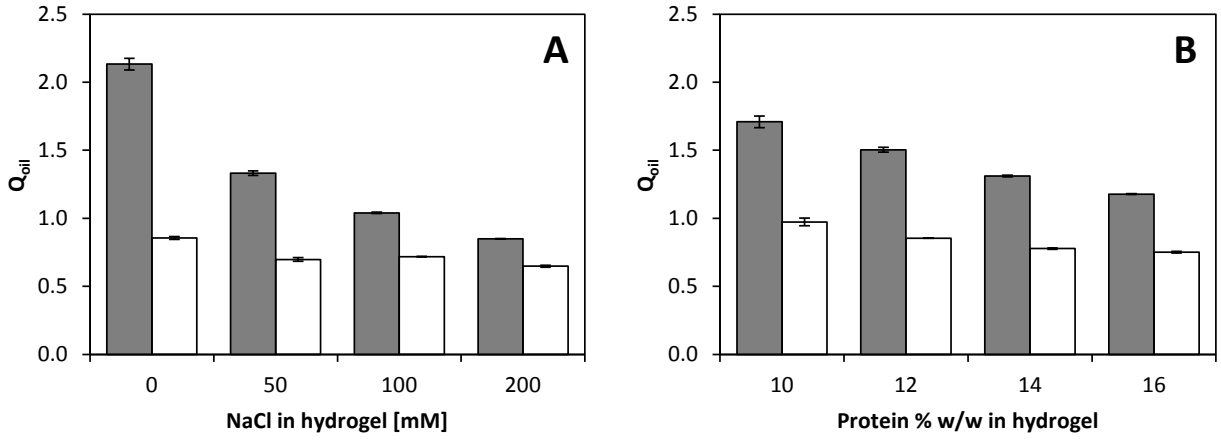

Figure 2.4. Q_{oil} of oleogels after solvent exchange for WPI hydrogels at different NaCl and protein concentration using acetone (grey bars) or THF (white bars) as an intermediate solvent. A) hydrogels were prepared at 15% w/w WPI, B) hydrogels were prepared at 50 mM NaCl.

In general, it is well known that protein hydrogels take up considerable amounts of solvent and swell extensively when immersed in a good solvent. However, apolar solvents, such as oil, are not considered as good solvents for proteins. To compare the effect of different solvents, the water holding capacity in a good solvent (water) was determined and compared to the oil holding capacity. To this end, the initial hydrogels were immersed in excess demineralized water, taken out

periodically and their weight was recorded. After 6 h, no change in weight was observed and the final water holding capacity (Q_{wEq}) was noted. It was observed that upon increasing ionic strength during hydrogel preparation, the amount of water uptake was reduced. Similarly, when the protein concentration was increased, maximum water holding was reduced. The reduced swelling is a result of a more dense network and such a change in swelling has also been shown in other studies where the network of whey protein hydrogels was changed by varying protein concentration and pH during gelation [39, 40].

Figure 2.5A combines the Q_{oil} and Q_{wEq} values of the gels as affected by NaCl and protein concentration into one curve. A fairly good relation can be obtained between Q_{oil} and Q_{wEq} using acetone or THF as an intermediate solvent. Overall, those hydrogels that showed high water holding capacity could also incorporate more oil. Q_{oil} values, however, are lower compared to Q_{wEq} values, indicating all gel matrices had a higher water holding capacity than oil holding capacity. Similarly, Gawlitza and co-workers also noted a decrease in hydrodynamic radius (indicating shrinkage) of Poly-*N*-isopropylacryamide microgels when the inner water phase was exchanged for isopropanol [33].

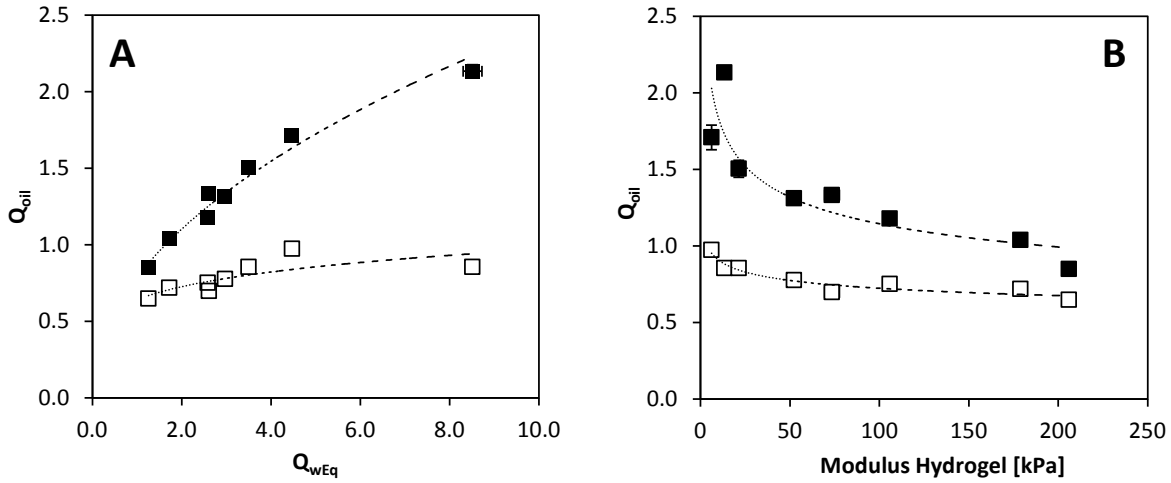

Figure 2.5. A) Relation between Q_{oil} and Q_{wEq} values of the different hydrogels. B) Relation between Q_{oil} and the modulus of the hydrogels. For both figures, variation in protein or NaCl concentration are summarized into one curve. Either acetone (filled symbols) or THF (open symbols) was used as intermediate solvent for the solvent exchange procedure. Dotted lines were added to guide the eye.

Besides the solvent quality, swelling of a (hydro)gel is dependent on the mechanical properties of the network. For polymer gels, this is often changed by the amount of crosslinks in the gel network [41]. For protein gels, the amount of crosslinks is difficult to determine, but can be related

to the gel stiffness (modulus). In our case, the modulus of protein hydrogels can be varied by changing the microstructure and protein concentration and it was found that the modulus increased as a result of increasing coarseness and increasing protein concentration, as will be discussed in more detail below. In general, an increase in coarseness (and protein concentration) leads to a denser network, and therefore leads to less swelling as was already observed in Figure 2.4. The Q_{oil} values of all gels were plotted against the measured modulus of the preceding hydrogels as affected by NaCl or protein concentration, and can be seen as one curve in Figure 2.5B. Hydrogels with a lower modulus showed higher Q_{oil} values, i.e. the oil holding capacity seems to be related to the gel stiffness. The results show that for different microstructure or network density, both swelling capacity and the gel modulus of the hydrogel are good indicators for the oil holding capacity of the successively formed oleogel.

Oil holding capacity by applying different solvent exchange procedures

The type of intermediate solvent used during the solvent exchange procedure had an effect on the oil holding capacity of the protein matrix. This shows that the conditions during the solvent exchange procedure affects the final properties of the oleogel. To investigate variations in the procedure further, we examined the oil holding capacity using five different solvent exchange procedures. These procedures varied in number of steps and the starting solvent as outlined in Table 2.1. As the initial hydrogel, we have used a 15% w/w WPI gel containing 0 mM NaCl since this gel gave the highest $Q_{oil,}$ and therefore the largest differences can be observed. The appearance of the resulting oleogels and the accompanying Q_{oil} values as a result of the different solvent exchange procedures, using both acetone and THF as intermediate solvent, are shown in Figure 2.6.

Starting with 30% v/v intermediate solvent and keeping the steps relatively small (method 1), using acetone as an intermediate solvent, gave a Q_{oil} of 2.13. When the binary mixtures of water-intermediate solvent and intermediate solvent-oil were omitted (method 2) and only pure acetone and oil were used, Q_{oil} was reduced quite extensively to 0.50. Pre-swelling the WPI hydrogels in water (method 3) increased the oil holding capacity to Q_{oil} = 1.68, but not to the same values as obtained by method 1 (Q_{oil} = 2.13). In the case the first solvent was a 50 vol% binary solvent (method 4) Q_{oil} was found to be 1.72, slightly higher values then for method 3. When the starting solvent was of high quality (100% water, method 5) and mixtures of acetone with water or oil were used, even higher Q_{oil} values of 3.23 were measured. For all methods studied, Q_{oil} values using THF as an intermediate solvent were considerably lower (~ 60 - 70%) compared to using acetone as an intermediate solvent.

The appearance of the resulting oleogels are quite different as a result of the chosen solvent exchange procedure. Even though the final solvent (sunflower oil) was the same in all cases, the route towards this point proves to be important for the oil holding capacity. When the hydrogels were placed into pure acetone or THF, the gel matrix almost completely collapsed. Pre-swelling the hydrogels in water, followed by immersing in pure THF, also led to shrinkage and collapse of the gel. Including more steps in the solvent exchange procedure, by using mixtures of solvents, greatly improves Q_{oil}, as seen in Figure 2.6. From these results it can be concluded that the amount of oil bound in a protein gel matrix and its structural integrity is affected by the properties of the intermediate solvent, the starting solvent and the composition of the binary solvents during the solvent exchange procedure.

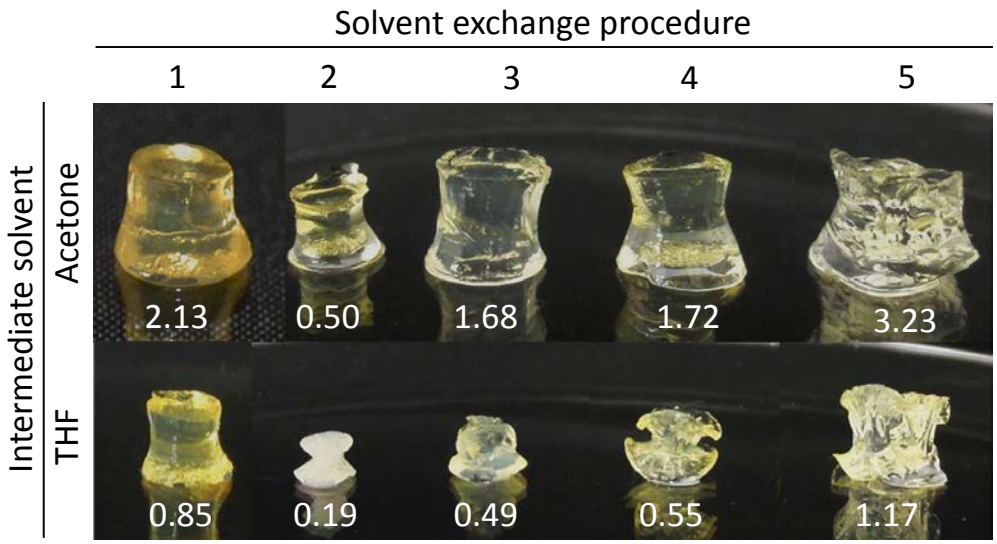

Figure 2.6. Appearance of WPI oleogels after five different methods of solvent exchange (as outlined in Table 2.1) using either acetone or THF as intermediate solvent. Starting hydrogel material was 15% w/w WPI, 0 mM NaCl. Values under the gels represent Q_{oil} values.

Large deformation properties of oleogels

After the solvent exchange procedure, the resulting oleogels have a similar appearance as their preceding hydrogels (i.e. fine-stranded vs coarse) but their internal solvent has changed. The change in solvent quality might change the interactions within the protein strands and the interactions between the strands that form the gel network, and the strength of the gel changes. Therefore, the stress – strain curves of the formed oleogels were compared to those of the preceding hydrogels. Here, we used the standard solvent exchange procedure with acetone as intermediate solvent (method 1), as this gave the most stable oleogels.

An example of a stress – strain curve for a 15%, 0 mM WPI hydrogel and that of the resulting oleogel is given in Figure 2.7A. The hydrogel shows a typical curve where, at higher strains, the stress diverges from linearity, a phenomenon known as strain hardening, until ultimately fracture occurs. The oleogel sample showed a strikingly different stress – strain curve. At low strain, the slope is much steeper compared to the hydrogel and fracture occurs at lower strain values. The modulus, fracture stress, and fracture strain for the hydrogels at different ionic strengths and the formed oleogels from these hydrogels are summarized in Figure 2.7B, C and D respectively. For the hydrogels, as a result of increasing ionic strength and therefore increase in coarseness, the modulus increased up to 100 mM NaCl, and then levelled off at 200 mM NaCl. In a similar way, the fracture stress increased with NaCl concentration, and levelled off at 200 mM. The fracture strain decreases with NaCl concentration, indicating the gel structure becomes more brittle as the coarseness of the gel microstructure is higher. Comparing the mechanical properties of the different hydrogels to the oleogels, we observe a larger modulus, a higher fracture stress and lower fracture strain for the oleogels. The effect of increasing coarseness is shown by an increase in modulus and fracture stress. Fracture strain, however, did not show a dependency on gel coarseness.

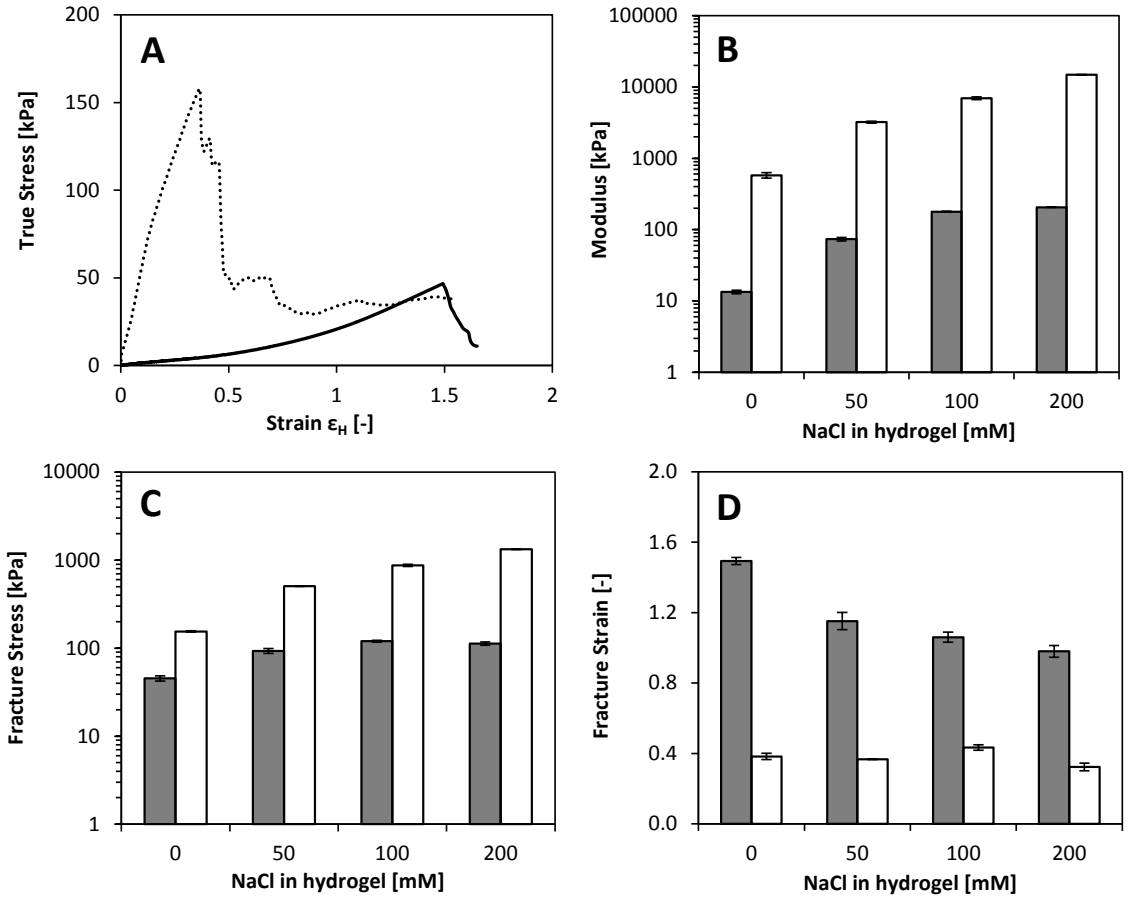

Figure 2.7. Large deformation properties of WPI hydrogels and oleogels after the solvent exchange procedure using acetone as intermediate solvent. A) Stress-strain curve for a representative 15% 0 mM NaCl hydrogel (solid line) and the resulting oleogel after the solvent exchange (dotted line). B-D) Modulus, fracture stress and fracture strain of hydrogels (grey bars) prepared at 15% WPI with different NaCl concentrations and the resulting oleogels (white bars) after the solvent exchange. Error bars represent standard deviation of duplicate measurements.

A similar trend as discussed for the effect of NaCl on large deformation mechanical properties is observed when comparing the WPI hydrogels at increasing protein concentration with those of the accompanying oleogels (Figure 2.8). For the hydrogels, at increasing protein concentration, an increase in modulus and fracture stress was observed whereas the strain at fracture decreased slightly. The higher protein concentration resulted in a denser network and therefore a stiffer and stronger gel. The mechanical properties of the oleogels showed a much larger modulus and fracture stress and lower strain at fracture compared to the hydrogels. With an increase in the density of the gel network, we observed an increase in modulus and fracture stress. The fracture strain, however, seems to be independent on network density.

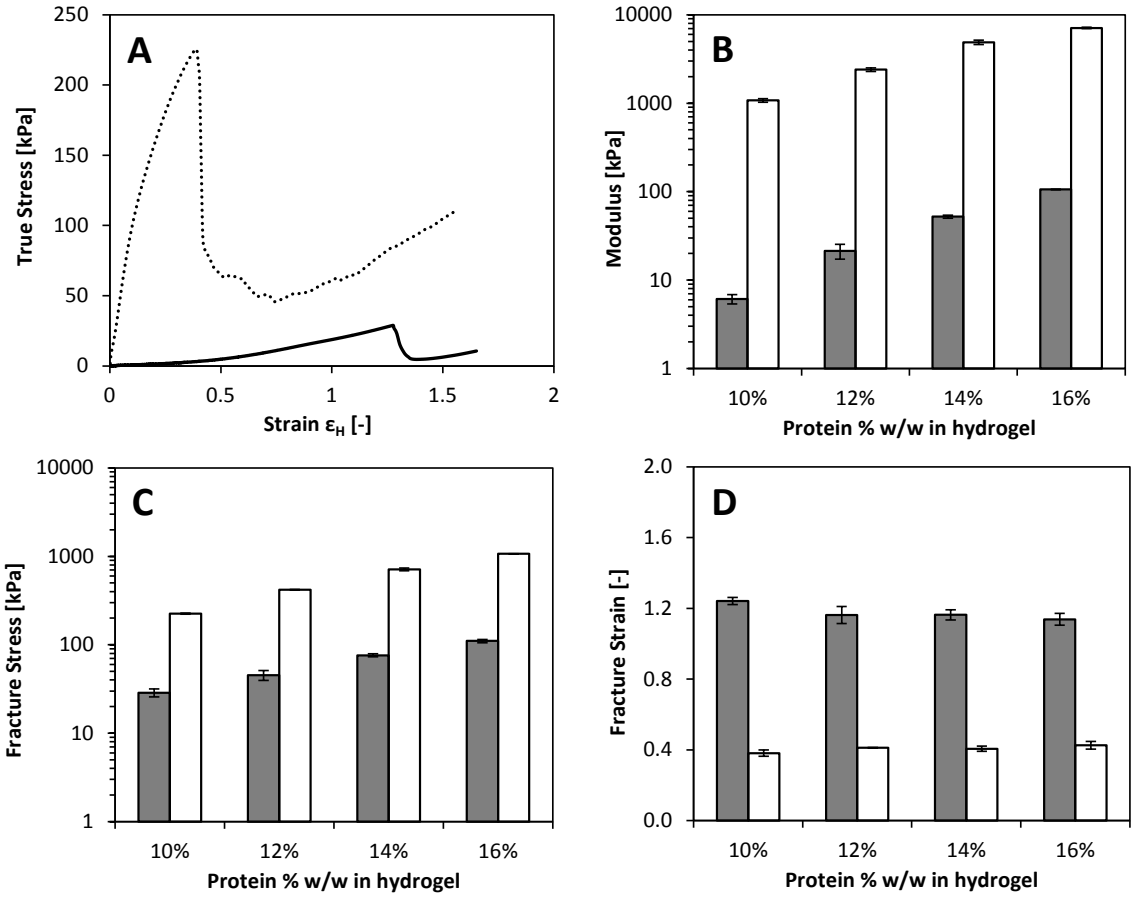

Figure 2.8. Large deformation properties of WPI hydrogels and oleogels after the solvent exchange procedure using acetone as intermediate solvent. A) Stress-strain curve for a representative 10% 50 mM NaCl hydrogel (solid line) and the resulting oleogel after the solvent exchange (dotted line). B-D) Modulus, fracture stress and fracture strain of hydrogels (grey bars) prepared at 50 mM NaCl with different protein concentrations and the resulting oleogels (white bars) after the solvent exchange. Error bars represent standard deviation of duplicate measurements.

The results indicate that the oleogels are much stiffer and stronger than hydrogels, but also more brittle. The difference is obvious as the modulus increased by approximately two orders of magnitude and fracture stress and fracture strain changes considerably. This vast difference can most likely be explained by considering the decrease in solvent quality. As a result of the decrease in solvent quality, the strength of the protein – protein interactions become larger at an expense of protein – solvent interactions, which have become more unfavorable. As a result, the strength of the interactions between the structural elements of the protein network are increased extensively, leading to a stronger network. Other researchers employed an emulsion-templated approach to produce protein-based oleogels. In this case, the oil is enclosed within polyhedral cells of protein bilayers and the researchers show that the rheological behavior is governed by the interfacial properties of these cells and, as a result, the moduli of the final oleogels depend on the size of the initial droplets in the emulsion [21]. Their reported values of the moduli (roughly 2 – 50 kPa),

however, are at least one order of magnitude lower than the moduli of the protein oleogels presented here. The difference may be found in the used protein concentration, which was much lower (< 1%) in their emulsion-templated gels, and therefore lower density of the protein network structure.

Although the changes in the mechanical properties between the preceding hydrogels and the oleogels are obvious, care must be taken when comparing the two systems. The solvent exchange procedure resulted in oleogels that have slightly different dimensions and in some cases diverge from a perfect cylinder, as seen in Figure 2.1. The stress and strain, however, were not recalculated for the change in volume and surface area, and therefore the values for the oleogels may be slightly over- or underestimated. Recalculating the change in surface area of the oleogel that has changed most significantly (prepared from a 15% w/w, 0 mM NaCl hydrogel), the estimated increase in surface area of ~70% decreased the modulus from ~570 kPa to ~470 kPa, which is still substantially different from the hydrogel with a modulus of 13 kPa. Therefore, even when corrected for the changes in surface area after the solvent exchange, the resulting stress – strain curve did not affect the general trends displayed in Figure 2.7 and Figure 2.8.

General discussion

Although hydrophilic polymers like proteins are mostly used for their ability to bind large amounts of water by forming hydrogels, we have shown that a protein gel matrix is capable of holding considerable amounts of oil by applying a solvent exchange procedure. The mechanism for the exchange of solvents within the gel network relies on diffusion, where exchanging solvents flow in opposite direction due to the difference in solvent composition between the external and internal liquid phase. The amount of oil in the final oleogel depends on the gel microstructure, the polarity of intermediate solvent and the number of steps during the solvent exchange.

Generally, when a polymer gel is placed in a solvent, its volumetric change can be described by the swelling theory of Flory [42]. Swelling can be regarded as a consequence of the tendency of the polymer to dissolve in the solvent, counteracted by the elastic retractive force of the network. However, the use of these theories is limited for our kind of protein gels, since their morphology is more akin to a "string of beads" rather than a true polymeric gel. Swelling theories take into account the density of the crosslinks as an important parameter, which is poorly defined in protein gels. Moreover, the use of binary liquid mixtures adds to the complexity of the various interactions between the components [43]. For our protein gels, the gel microstructure was modified from fine-

stranded to coarse by increasing the ionic strength or by changing the protein concentration. As a result, the modulus of the hydrogel increases, which provides the retractive force and counteracts swelling. Besides the increase in modulus, also salts may have a great effect on the swelling ratio of the gels as they influence the quality of the solvent, osmotic pressure and interactions between the proteins. Nevertheless, we assume that during the solvent exchange all the salts are washed out, which is confirmed by a good correlation between the oil holding capacity of the various WPI oleogels and the water holding capacity and modulus of the preceding hydrogels. Therefore, a determining factor for final oil holding capacity of the gel matrix following a solvent exchange procedure, is likely to be related to its swelling ability in the first aqueous solvent the gel is immersed in.

As the solvent exchange procedure advances, the polarity of the solvent decreases. This results in a shrinkage of the gel as was observed by the lower values for Q_{oil} compared to Q_{wEq}. Enhanced shrinkage was observed when THF was used as an intermediate solvent compared to acetone, and this shows that the choice of intermediate solvent in the exchange process is of importance for the oil holding capacity of the gel matrix. The difference must be partially attributed to the lower dielectric constant of THF ($\varepsilon \sim 7$) compared to acetone ($\varepsilon \sim 20$), i.e., THF is considered more apolar than acetone. Volumetric shrinkage of polyvinyl alcohol gels showed a similar dependency on solvent polarity [44]. In our case, low affinity of the protein for the solvent may increase protein – protein interactions leading to shrinkage of the gel. It was not within scope of the current research to follow volumetric changes of the gel during the solvent exchange, but it is very likely that shrinkage occurs throughout the procedure as the polarity continues to decrease until that of the final solvent.

Besides the polarity of the intermediate solvent, the difference in solvent polarity between the liquid phase inside and outside the gel (i.e. number of steps in the solvent exchange procedure) had a great impact on oil holding capacity. When the polarity of the bulk solvent in which the gel is placed, differs greatly from the composition of the liquid phase inside the gel matrix, a larger concentration gradient is obtained between inside and outside the gel (given the miscibility of all liquid components). The concentration gradient determines the kinetics of the solvent exchange; it determines how fast the oil molecules enter the gel matrix and the intermediate solvent leaves the gel. It is hypothesized that for slow kinetics, the protein network is able to adjust to the new situation by slow rearrangements without a sudden collapse. On the contrary, when the composition of the solvent is changed rapidly, the network does not have time to adjust and the gel network collapses. Similar effects were observed for polyacrylamide gels when they were

immersed in poor solvents [45, 46]. Here, even shell formation and inhomogeneities were observed as a result of a rapid change in solvent composition.

Conclusions

A facile solvent exchange procedure was applied to transform heat-set WPI hydrogels into WPI oleogels. Depending on the conditions used during the solvent exchange procedure and the type of gel matrix, up to 91% oil could be incorporated. Residual water contents were very low (< 1%) and the oil had migrated homogeneously throughout the gel network without compromising its structural integrity. The oil holding capacity depended largely on: 1) the properties of the protein network, 2) the polarity of the intermediate solvent and 3) the kinetics of the solvent exchange procedure. The resulting oleogels were much stiffer and more brittle compared to the hydrogels, as shown by an increase in modulus of approximately two orders of magnitude and a decrease in fracture strain, respectively. The composition, oil holding capacity and the mechanical properties of the oleogels can therefore be tuned by changing the type of protein matrix from a fine-stranded to coarse nature and varying the protein concentration. The possibility of immobilizing high quantities of liquid oil inside a biodegradable gel matrix with tunable mechanical properties could be of interest for colloid and material scientists in various fields and may have novel applications in the food, pharmaceutical or cosmetic industry.

References

1. Sagiri, S.S., et al., *Organogels as Matrices for Controlled Drug Delivery: A Review on the Current State.* Soft Materials, 2013. **12**(1): p. 47-72.
2. Vintiloiu, A. and J.C. Leroux, *Organogels and their use in drug delivery - A review.* Journal of controlled release, 2008. **125**(3): p. 179-192.
3. Sánchez, R., et al., *Use of chitin, chitosan and acylated derivatives as thickener agents of vegetable oils for bio-lubricant applications.* Carbohydrate Polymers, 2011. **85**(3): p. 705-714.
4. Rogers, M.A., A.J. Wright, and A.G. Marangoni, *Oil organogels: the fat of the future?* Soft Matter, 2009. **5**(8): p. 1594-1596.
5. Marangoni, A., *Organogels: An Alternative Edible Oil-Structuring Method.* Journal of the American Oil Chemists' Society, 2012. **89**(5): p. 749-780.
6. Pernetti, M., et al., *Structuring of edible oils by alternatives to crystalline fat.* Current Opinion in Colloid and Interface Science, 2007. **12**(4-5): p. 221-231.
7. Hwang, H.S., et al., *Organogel formation of soybean oil with waxes.* Journal of the American Oil Chemists' Society, 2012. **89**(4): p. 639-647.
8. Toro-Vazquez, J.F., et al., *Physical properties of organogels and water in oil emulsions structured by mixtures of candelilla wax and monoglycerides.* Food Research International, 2013. **54**(2): p. 1360-1368.
9. Rogers, M.A., A.J. Wright, and A.G. Marangoni, *Nanostructuring fiber morphology and solvent inclusions in 12-hydroxystearic acid / canola oil organogels.* Current Opinion in Colloid and Interface Science, 2009. **14**(1): p. 33-42.
10. Tamura, T. and M. Ichikawa, *Effect of lecithin on organogel formation of 12-hydroxystearic acid.* Journal of the American Oil Chemists' Society, 1997. **74**(5): p. 491-495.
11. Schaink, H.M., et al., *Crystal network for edible oil organogels: Possibilities and limitations of the fatty acid and fatty alcohol systems.* Food Research International, 2007. **40**(9): p. 1185-1193.
12. Gandolfo, F.G., A. Bot, and E. Flöter, *Structuring of Edible Oils by Long-Chain FA, Fatty Alcohols, and Their Mixtures.* Journal of the American Oil Chemists' Society, 2004. **81**(1): p. 1-6.
13. Bot, A. and W.G.M. Agterof, *Structuring of edible oils by mixtures of γ-oryzanol with β-sitosterol or related phytosterols.* Journal of the American Oil Chemists' Society, 2006. **83**(6): p. 513-521.
14. Kumar, R. and O.P. Katare, *Lecithin organogels as a potential phospholipid-structured system for topical drug delivery: A review.* AAPS PharmSciTech, 2005. **6**(2): p. E298-E310.
15. Nikiforidis, C.V. and E. Scholten, *Self-assemblies of lecithin and α-tocopherol as gelators of lipid material.* RSC Advances, 2014. **4**(5): p. 2466-2473.
16. Gong, R., et al., *A clickable, highly soluble oligopeptide that easily forms organogels.* Supramolecular Chemistry, 2013. **25**(5): p. 269-275.
17. Laredo, T., S. Barbut, and A.G. Marangoni, *Molecular interactions of polymer oleogelation.* Soft Matter, 2011. **7**(6): p. 2734-2743.

18. Davidovich-Pinhas, M., S. Barbut, and A.G. Marangoni, *The gelation of oil using ethyl cellulose.* Carbohydrate Polymers, 2015. **117**: p. 869-878.
19. Huang, Y., et al., *Hydrophobic modification of chitin whisker and its potential application in structuring oil.* Langmuir, 2015. **31**(5): p. 1641-1648.
20. Nikiforidis, C.V. and E. Scholten, *Polymer organogelation with chitin and chitin nanocrystals.* RSC Advances, 2015. **5**(47): p. 37789-37799.
21. Romoscanu, A.I. and R. Mezzenga, *Emulsion-templated fully reversible protein-in-oil gels.* Langmuir, 2006. **22**(18): p. 7812-7818.
22. Patel, A.R., et al., *Biopolymer-based structuring of liquid oil into soft solids and oleogels using water-continuous emulsions as templates.* Langmuir, 2015. **31**(7): p. 2065-2073.
23. Patel, A.R., et al., *Edible oleogels based on water soluble food polymers: Preparation, characterization and potential application.* Food and Function, 2014. **5**(11): p. 2833-2841.
24. Kinsella, J.E., *Milk proteins: physicochemical and functional properties.* Critical Reviews in Food Science and Nutrition, 1984. **21**(3): p. 197-262.
25. Einerson, N.J., K.R. Stevens, and W.J. Kao, *Synthesis and physicochemical analysis of gelatin-based hydrogels for drug carrier matrices.* Biomaterials, 2003. **24**(3): p. 509-523.
26. Weijers, M., R.W. Visschers, and T. Nicolai, *Light scattering study of heat-induced aggregation and gelation of ovalbumin.* Macromolecules, 2002. **35**(12): p. 4753-4762.
27. Kinsella, J.E., *Functional properties of soy proteins.* Journal of the American Oil Chemists' Society, 1979. **56**(3): p. 242-258.
28. Renkema, J.M.S., J.H.M. Knabben, and T. Van Vliet, *Gel formation by β-conglycinin and glycinin and their mixtures.* Food Hydrocolloids, 2001. **15**(4-6): p. 407-414.
29. Shand, P.J., et al., *Physicochemical and textural properties of heat-induced pea protein isolate gels.* Food Chemistry, 2007. **102**(4): p. 1119-1130.
30. Green, R.J., I. Hopkinson, and R.A.L. Jones, *Unfolding and intermolecular association in globular proteins adsorbed at interfaces.* Langmuir, 1999. **15**(15): p. 5102-5110.
31. Betz, M., et al., *Preparation of novel whey protein-based aerogels as drug carriers for life science applications.* Journal of Supercritical Fluids, 2012. **72**: p. 111-119.
32. Bai, S., et al., *Using Hydrogels to Accommodate Hydrophobic Nanoparticles in Aqueous Media via Solvent Exchange.* Advanced Materials, 2010. **22**(30): p. 3247-+.
33. Gawlitza, K., et al., *Immobilization of water-soluble HRP within poly-N-isopropylacrylamide microgel particles for use in organic media.* Langmuir, 2013. **29**(51): p. 16002-16009.
34. Gawlitza, K., et al., *Immobilization of lipase B within micron-sized poly-N-isopropylacrylamide hydrogel particles by solvent exchange.* Physical Chemistry Chemical Physics, 2012. **14**(27): p. 9594-9600.
35. Doi, E. and N. Kitabatake, *Structure of glycinin and ovalbumin gels.* Food Hydrocolloids, 1989. **3**(4): p. 327-337.

36. Foegeding, E.A., E.L. Bowland, and C.C. Hardin, *Factors that determine the fracture properties and microstructure of globular protein gels.* Food Hydrocolloids, 1995. **9**(4): p. 237-249.

37. Hermansson, A.M. and W. Buchheim, *Characterization of protein gels by scanning and transmission electron microscopy A methodology study of soy protein gels.* Journal of Colloid and Interface Science, 1981. **81**(2): p. 519-530.

38. Urbonaite, V., et al., *Water holding of soy protein gels is set by coarseness, modulated by calcium binding, rather than gel stiffness.* Food Hydrocolloids, 2015. **46**(0): p. 103-111.

39. Gunasekaran, S., L. Xiao, and M.M.O. Eleya, *Whey protein concentrate hydrogels as bioactive carriers.* Journal of Applied Polymer Science, 2006. **99**(5): p. 2470-2476.

40. Betz, M., et al., *Swelling behaviour, charge and mesh size of thermal protein hydrogels as influenced by pH during gelation.* Soft Matter, 2012. **8**(8): p. 2477-2485.

41. Brannon-Peppas, L. and N.A. Peppas, *Equilibrium swelling behavior of ph-sensitive hydrogels.* Chemical Engineering Science, 1991. **46**(3): p. 715-722.

42. Flory, P.J. and J. Rehner Jr, *Statistical mechanics of cross-linked polymer networks II. Swelling.* The Journal of Chemical Physics, 1943. **11**(11): p. 521-526.

43. Favre, E., et al., *Application of Flory-Huggins theory to ternary polymer-solvents equilibria: A case study.* European Polymer Journal, 1996. **32**(3): p. 303-309.

44. Kudo, S., E. Otsuka, and A. Suzuki, *Swelling Behavior of Chemically Cross linked PVA Gels in Mixed Solvents.* Journal of Polymer Science Part B-Polymer Physics, 2010. **48**(18): p. 1978-1986.

45. Dhara, D. and P.R. Chatterji, *Swelling and deswelling pathways in non-ionic poly(N-isopropylacrylamide) hydrogels in presence of additives.* Polymer, 2000. **41**(16): p. 6133-6143.

46. Matsuo, E.S. and T. Tanaka, *Patterns in shrinking gels.* Nature, 1992. **358**(6386): p. 482-485.

Chapter 3

Protein oleogels from heat-set whey protein aggregates

This chapter is based on: de Vries, A., Wesseling A., van der Linden, E., Scholten, E., *Protein oleogels from heat-set whey protein aggregates*, Journal of Colloid and Interface Science 486, 2017, p. 75-83.

Introduction

Gels in which the continuous phase is a nonpolar solvent (so-called organogels, or oleogels in the case of edible oil) is a topic of growing interest. Such organo- or oleogels are studied for various purposes, like drug delivery [1, 2], oil spills [3], electronics [4], and foodstuffs [5, 6]. Gelators for nonpolar liquids can be classified into low molecular weight organogelators (LMOGs) or polymeric organogelators. LMOGs are the most common and within this class, gelation is achieved by crystallization or by self-assembly into fibrous networks. Common types of LMOGs are fatty acids or alcohols [7], waxes [8, 9], phytosterols [10, 11], oligopeptides [12], and lecithins [13]. The gelation of such systems relies on the self-assembly behavior of the molecules into structures of larger length scales, such as micellar or lamellar phases. The rheological behavior of such organo- or oleogels is dominated by the specific interactions between the building blocks.

In contrast to LMOGs, the number of (bio)polymers used as oleogelator is limited. One of the best studied examples is the cellulose derivative ethylcellulose [14]. Insoluble in water, this biopolymer dissolves in liquid oil at elevated temperatures, where, upon lowering the temperature, the polymer chains interconnect to form a network resulting in an oleogel. By using different surfactants, or by using ethylcellulose of different molecular weight, the interactions between the polymer chains can be altered, and hence the rheological properties of the final oleogel can be tuned [15-17]. Another example of a biopolymer with oil gelling capabilities is chitin. It has been shown that oleogels can be made by using chitin either in a crude form, as nanocrystals [18], or when modified into hydrophobic whiskers [19].

Although examples like that of ethylcellulose and chitin as biocompatible oil gelators do exist, there is a need to identify gelators that are affordable, efficient, and food grade. These requirements are especially important when the desired applications are in foodstuffs, as replacement for high melting crystalline hardstocks, and in drug delivery systems for controlled release of hydrophobic compounds. To cover a wide range of possible applications, it is desirable to control the rheological behavior of such organo- and oleogels in terms of properties as gel strength, yield stress, and plasticity. One interesting alternative is the gelation of liquid oil based on proteins, as they are widely available and food grade. However, since proteins are poorly dispersible in nonpolar solvents, their capability of forming a gel network in solvents such as liquid oil is limited. Nevertheless, attempts have been made to use proteins as oleogelators. To overcome the problem of poor dispersibility, Romoscanu and Mezzenga [20] used an emulsion-templated approach. Here, the protein is adsorbed at the oil-water interface and upon subsequent removal of the water, a gel with a high oil content can be achieved. The continuous phase in these systems is

still hydrophilic, and the gel can be easily hydrated and reversed into an oil-in-water emulsion upon addition of water. Using a similar emulsion- or foam-templated approach, Patel and co-workers used a dried foam [21] and a dried oil-in-water emulsion [22], using methylcellulose and a gelatin-xanthan mixture, respectively, followed by a shearing step to create oleogels. In these cases, however, the final structure and particle size might be difficult to tune, limiting specific control over the formed network structure and subsequent rheological properties of the formed gel. Moreover, the choice of structuring agents is limited to surface active components that are able to prevent the coalescence of oil droplets and oil separation during drying.

In Chapter 2, it was shown that heat-set whey protein hydrogels could be used as macroscopic templates to create protein oleogels by applying a solvent exchange procedure. This procedure relies on replacing the water in the interstitial areas of the heat-set protein matrix by an intermediate solvent, followed by liquid oil. The gel matrix was shown to be capable of binding a large amount of oil (>91%) and rheological tests showed that the protein oleogels were much stiffer and much more brittle compared to the preceding hydrogels. Although the solvent exchange procedure proved effective, the preparation method gave limited flexibility to alter the rheological properties of the final protein oleogels. In order to do so, control over network formation at smaller length scales is required. Initial building blocks of colloidal size would be more appropriate, as colloidal interactions are essential to control such network formation.

Preparation of protein aggregates of colloidal size is a topic that has already been studied exhaustively. In general, the gelling mechanism of such aggregates into hydrogels is based on protein denaturation (e.g. by applying heat treatment) followed by network formation of the formed aggregates by reducing the electrostatic repulsion [23-25]. However, it is not known whether protein aggregates are able to create networks in oil, and how the network is organized. In this chapter, we investigate the network formation of protein aggregates of colloidal size in oil and compare this to protein gels obtained in aqueous environments. Understanding the network formation of the colloidal protein aggregates in oil can provide insights to create protein oleogels with a larger diversity of rheological characteristics, such as plastic deformation. To investigate the network formation and the resulting visco-elastic properties, we create submicron whey protein aggregates as initial building blocks in an aqueous medium, and subsequently transfer the aggregates into liquid oil by applying a similar solvent exchange approach as described in Chapter 2. In the current chapter, it will be shown that submicron protein aggregates can be used directly to form a network in liquid oil, similar to their well-known ability to form a network in water.

Materials and methods

Materials

Whey protein isolate (WPI, BiPro) was obtained from Davisco Foods International (Le Sueur, MN, USA). The protein concentration was 93.2% (N x 6.38) and was used as received. Acetone (AR grade) was supplied by Actu-All Chemicals (Oss, the Netherlands). Refined sunflower oil (Vandermoortele NV, Breda, the Netherlands) was bought at a local supermarket and was used without further purification. Demineralized water was used throughout the experiments.

Methods

Preparation of protein aggregates

To prepare a protein stock solution, WPI powder (4% w/w) was dissolved in demineralized water under continuous stirring at room temperature for 2 h. Afterwards, the stock solution was stored overnight at 4 °C to assure complete protein hydration. The next day, the pH of the stock solution was adjusted to 5.7 using a 1 M HCl solution. The resulting solution was heated in 50 mL plastic tubes with screwcaps at 85 °C for 15 minutes using a temperature controlled water bath to induce protein denaturation. After cooling in ice water, a weak protein gel was obtained. This weak gel was easily broken into aggregates by hand shaking and vortexing. The resulting protein dispersion was homogenized by using a rotor stator homogenizer (Ultra Turrax, T25, IKA Werke, Germany) at 13000 rpm for 3 min. The protein aggregates were then collected as a pellet by centrifuging at 4000 g (Hermle Z383K, Hermle Labortechnik GmbH, Wehingen, Germany) for 20 minutes at 20 °C. After collection, the pellet was re-dispersed and centrifuged twice with demineralized water to remove remaining soluble protein material.

Preparation of the protein oleogels

To prepare the protein oleogels, the WPI aggregates were transferred to the oil phase using a solvent exchange procedure. In this procedure, the polarity of the solvent was changed gradually to remove the surrounding water from the WPI aggregates and replace the continuous phase for oil. In short, 15 g of aqueous pellet, containing the WPI aggregates, was re-dispersed in 150 mL acetone, and mixed thoroughly using rotor stator homogenization. Afterwards, the sample was centrifuged at 4000 g for 20 min at 20 °C. Excess acetone was removed by decanting and the pellet, containing the protein aggregates, was collected. The pellet was then re-dispersed in the proceeding solvents. The procedure of re-dispersing and centrifugation was repeated once more using acetone to assure water removal, and twice using sunflower oil. The obtained pellet of WPI

aggregates in oil was diluted in a ratio of 1:10 with sunflower oil and left overnight under continuous stirring to allow for evaporation of the remaining acetone. The next day, the suspension was centrifuged at 4000 g for 20 min at 20 °C to increase the concentration of the protein aggregates and induce gel formation.

To show the necessity of the solvent exchange procedure, protein aggregates were also dispersed in oil after freeze-drying. In this case, the pellet obtained after the initial heat treatment in aqueous conditions, was frozen at -20 °C for 16 h, followed by freeze-drying (Christ alpha 2-4 LD plus, Martin Christ Gefriertrocknungsanlagen GmbH, Osterode am Harz, Germany) for 24 h to obtain a dried powder of protein aggregates. The powder was dispersed into sunflower oil using rotor stator homogenization (13000 rpm, 3 min) and additional stirring on a magnetic stirrer plate for 30 min at room temperature. Afterwards, the sample was centrifuged at 3904 g for 20 min to increase the protein concentration, and the oil dispersion containing the WPI aggregates was collected.

Composition of the oleogel

Protein concentration. The nitrogen content was determined using Dumas (Dumas Flash EA 1112 Series, N Analyser, Thermo Scientific). After weighing, the samples were dried overnight in an oven at 60 °C before analysis. To calculate the protein content, a nitrogen conversion factor of 6.38 was used. Two separately prepared batches of oleogel were prepared and analysed in triplicate to obtain an averaged value and standard deviation.

Water concentration. Water content in the oleogel was determined in duplicate by dry matter determination. Aluminium cups (ø = 5 cm) were first heated to 105 °C in an oven (Venticell, BMT Medical Technology, Brno, Czech Republic) to remove any water contamination. Afterwards, approximately 1 g of oleogel sample was added to the cup, and its weight was recorded before and after drying for 4 h at 105 °C.

Acetone concentration. The amount of residual acetone during evaporation was measured using headspace chromatography. The obtained oleogel pellet, after it was dispersed and centrifuged twice with sunflower oil, was diluted in a ratio of 1:1 (w:w) with fresh oil and the acetone was allowed to evaporate for a maximum of 48 h under continuous stirring at room temperature. After 0, 16, 24, 40 and 48 h, a sample of 10 mL was collected and placed in a 250 mL Schott bottle closed with a screwcap. Parafilm was wrapped around the screwcap to prevent acetone evaporation and uptake of contaminants from the environment. Subsequently, the bottle was wrapped in aluminium foil and stored in the dark in order to prevent lipid oxidation. Samples were collected at least one day (24 h) before the analysis to ensure equilibrated conditions. From the

headspace in the bottle, the acetone concentration was determined using a mass spectrometer (HR PTR/MS, Ionicon, Innsbruck, Austria). A calibration curve was used with known concentrations (0, 0.5, 5, 10, 15, 50 and 100 ppm) of acetone in sunflower oil. These samples were also prepared 24 h before the measurement and stored under the same conditions. The reported amount of acetone in the samples was determined from the signal at m/z 59 and was calculated from duplicate measurements, after subtraction of the signal of the blank (pure sunflower oil).

Particle size analysis

The particle size distribution of WPI aggregates was determined by static light scattering (Mastersizer 2000, Malvern Instruments, Worcestershire, UK) with either sunflower oil or demineralized water as the continuous phase. The refractive index of water was set to 1.33 and for sunflower oil to 1.469. The particle size was determined as an average of three measurements. Particle size was measured either after rotor-stator homogenization (at 13000 rpm) or after sonication for 5, 10 or 15 min using a sonicator (Branson Ultrasonics Corporation, Danbury, CT USA) with a 20 kHz, 12.7 mm probe at power level 2 and 50% duty cycle as output (indicating an amplitude of 24 μm).

Confocal Laser Scanning Microscopy (CLSM)

To visualize the protein suspensions, the WPI aggregates in water or oil were analysed using a confocal laser scanning microscope (Leica tcs sp5, Leica Microsystems, Wetzlar, Germany). A rhodamine B solution (0.2%) in water or ethanol was used to stain the proteins. After staining, the sample was gently mixed by hand and was then placed on the microscope slide.

Rheology

Oscillatory rheology was performed on the oleogels. To investigate the behavior of the protein aggregates under different conditions, the obtained dense pellet containing the WPI aggregates was diluted with sunflower oil to obtain various weight ratios. To this end, the dispersions were homogenized using rotor-stator homogenization (9000 x rpm) for approximately 90 s until the sample appeared homogeneous. Afterwards, samples were degassed using a vacuum pump for 5 min and loaded into a stress-controlled rheometer (AP 301, Anton Paar GmbH, Graz, Austria) using a coaxial cylinder (CC17) setup. Before any measurements were performed, the samples were allowed to equilibrate for 30 min at a frequency of 1 Hz and a strain (γ) of 0.01% (which was within the linear viscoelastic region). Frequency sweeps were performed by increasing the frequency logarithmically from 0.01 to 10 Hz at γ = 0.01%. Amplitude sweeps were performed by

increasing the strain logarithmically from 0.001 to 100% at 1 Hz. All measurements were performed in duplicate from two different batches of oleogel and all samples were prepared individually.

Fractal analysis

Using rheological data, scaling theories are often used to characterize protein gel networks. In these theories, the particle network is considered an assembly of fractal flocs, which themselves consist of primary particles. In literature, different models can be found that describe the interactions between such primary particles in elastic networks. In these models, the elastic constant and the limit of linearity turn out to scale in a power-law fashion as a function of the particle volume fraction [26, 27]. To characterize the network structure of the WPI aggregates in liquid oil, we use the expressions as described by Shih et al. [26]. These authors distinguish two regimes to describe the interactions within a fractal network of flocs: the strong-link and weak-link regime. In the weak-link regime, the interactions between the flocs are weaker than those within the flocs, whereas in the strong-link regime, the interactions between the flocs are stronger than within the flocs. Differences are reflected in the relations between the storage modulus (G') and the limit of linearity (γ_0) versus the volume fraction of the particles. In the strong-link regime one has:

$$G' \sim \varphi^{(d+x)/(d-d_f)} \quad (3.1)$$

$$\gamma_0 \sim \varphi^{-(1+x)/(d-d_f)} \quad (3.2)$$

while in the weak-link regime one has:

$$G' \sim \varphi^{(d-2)/(d-d_f)} \quad (3.3)$$

$$\gamma_0 \sim \varphi^{1/(d-d_f)} \quad (3.4)$$

where d denotes the Euclidean dimension, d_f the fractal dimension of the flocs and x the backbone fractal dimension of the flocs built up by primary particles. G' increases as a function of volume fraction for both regimes, but more slowly in the weak link regime than in the strong link regime. The limit of linearity as a function of increasing volume fraction of the particles differs for both regimes: γ_0 decreases in the strong-link regime and increases in the weak-link regime. This difference allows to experimentally determine whether a gel system is in the strong-link or weak-link regime. The fractal dimension (d_f) was determined using the slope of the log-log plot of G' versus the protein concentration (c_p). Here, we assume the volume fraction (φ) of particles (protein aggregates) to be proportional to c_p. Values for γ_0 were obtained from strain sweep experiments in

a similar fashion as described by Hagiwara et al. [28] as the strain value at which G' decreased more than 5% from its ordinate value.

Results and discussion

Appearance of whey protein aggregates in water and sunflower oil

When whey proteins in water are heated above their denaturation temperature, unfolding of the protein leads to aggregation. The internal structure of the aggregates are stabilized by chemical covalent bonds in the form of disulfide bonds and physical interactions like hydrophobic interactions. As shown by Schmitt et al. [29], heating a whey protein solution in a narrow pH range (5.7 – 6.2) leads to the formation of dense, disulfide-stabilized aggregates or "microgels". In this research, we used similar conditions to prepare covalently-stabilized whey protein aggregates as building blocks for oleogelation.

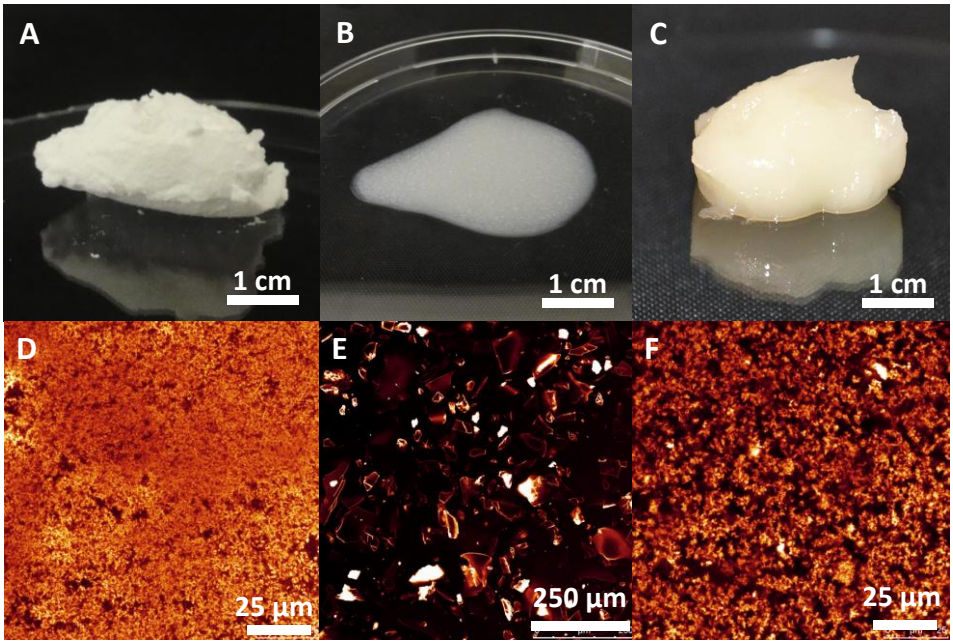

Figure 3.1. (A) Appearance of heat-set WPI aggregates after centrifugation, (B) dispersion of freeze-dried WPI aggregates in sunflower oil and (C) WPI aggregates in sunflower oil via a solvent exchange with corresponding CLSM micrographs (D-F). To visualize the protein aggregates, the used stain was rhodamine B.

To prepare such aggregates, a WPI solution at pH 5.7 was heated at 85 °C. After heat treatment, the WPI solution turned into a weak gel. For similar conditions, Schmitt and co-workers [29] reported on the formation of a liquid suspension instead of a gel. Since in protein aggregate and gel formation the exact mineral and protein composition is important, a slight variation between batches or preparation procedure might be responsible for the difference between a suspension or weak gel. The weak gel we obtained could easily be broken by shaking and vortexing to create a suspension of protein aggregates. Upon densification of the aggregates by centrifugation, the protein concentration increased to 9.6% w/w (as determined by Dumas). The appearance of the

resulting gel-like pellet and a representative confocal micrograph are shown in Figure 3.1A and D, respectively. The confocal micrograph shows a densely packed network of the protein aggregates. As is well-known, heat-induced unfolding of proteins leads to exposure of hydrophobic side groups originally buried inside the globular structure of the protein. As a result of an increased hydrophobicity, it was attempted to use the obtained aggregates as building blocks to gel liquid oil via a freeze-drying step. To this end, the obtained aggregates were transferred to the oil phase by first freeze-drying the pellet (to remove the water), followed by re-dispersing the dried aggregates in sunflower oil using a rotor-stator homogenizer. The resulting suspension of protein aggregates in oil was then centrifuged to collect the aggregates. As can be seen from Figure 3.1B, the resulting material did not have gel-like properties. The confocal micrograph shows a large increase in particle size (Figure 3.1E) compared to the initial protein aggregates. The large particle size is most likely responsible for the poor gel forming ability of the dispersed particles.

Subsequently, we attempted to disperse the protein aggregates in the oil through a solvent exchange procedure using an intermediate solvent. The appearance of the final pellet and the according confocal micrograph is shown in Figure 3.1C and Figure 3.1F, respectively. Interestingly, and in contrast to the freeze-dried sample, the pellet now shows gel-like properties due to network formation of the protein aggregates. From the confocal micrograph it can be seen that the aggregates are better dispersed compared to the freeze-dried sample and are similar in size as the WPI aggregates in water. Storage of the oleogel for several weeks showed minimal oil leakage, demonstrating the oil was effectively entrapped by the protein network. To confirm that the WPI aggregates formed an interconnected network, several scans were made in the z-direction and the resulting micrograph (Figure 3.2) confirms that the aggregates formed a 3-D network throughout the liquid oil.

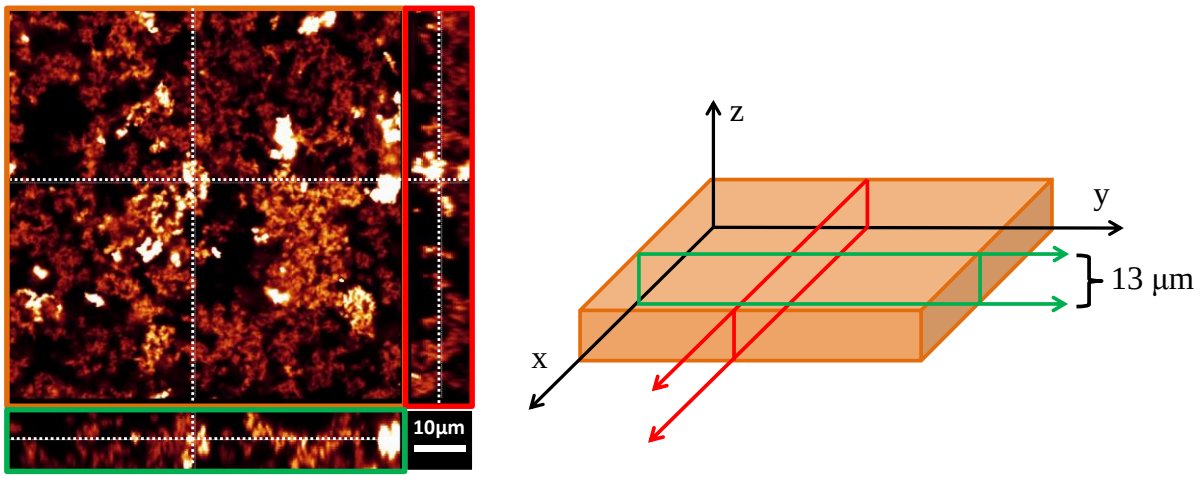

Figure 3.2. z-scan of an oleogel stabilized by WPI aggregates. The dotted lines indicate the position of view in the z-direction.

As can be observed in Figure 3.1B, drying the protein aggregates had a large influence on the gel forming ability of the aggregates in the oil phase. Upon drying, the aggregates clustered into larger particles. When dispersing these large particles into an oil phase, the strong interactions between the aggregates apparently prevent re-dispersion. Alternatively, when the aggregates are dispersed into an organic solvent to replace water as the continuous phase, the drying step is avoided. Since acetone is miscible with both water and sunflower oil, the aggregates were always in a wet condition, and dispersed evenly throughout the suspending medium, which was changed slowly from hydrophilic to hydrophobic. These conditions probably prevented agglomeration of the aggregates. In a similar way Tang et al. [30] found that MoS_2 sheets were dispersible in a wide range of solvents when a solvent exchange technique was applied.

Composition of whey protein oleogels

The protein concentration of the oleogel obtained as shown in Figure 3.1C was 6.8 wt% (± 0.3%) according to Dumas measurements. The water content was found to be 0.8 wt% (± 0.03%) determined by oven drying, indicating an effective removal of water by the applied solvent exchange procedure. The concentration of acetone was measured as a function of evaporation time and is given in Figure 3.3. After 16 h (overnight) evaporation, the acetone concentration was found to be < 2 ppm. Prolonged evaporation time decreased the acetone concentration in the oil phase even further to < 0.5 ppm after 48 h. Since the remaining acetone content was already almost negligible after 16 h, and in order to minimize lipid oxidation, overnight evaporation was taken as the standard for the remainder of the experiments.

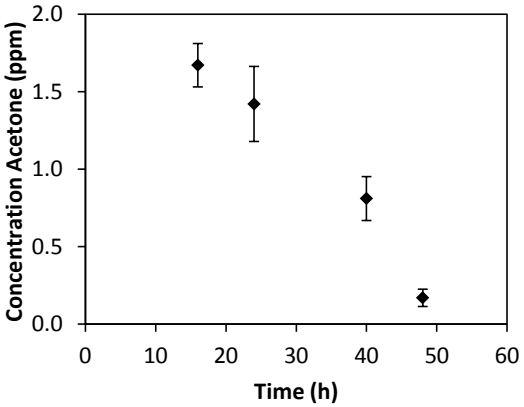

Figure 3.3. Acetone concentration in the WPI aggregate in oil dispersion as function of evaporation time.

Particle size of WPI aggregates in water and oil

The particle size of the WPI aggregates was determined by diluting the pellet either with demineralized water or sunflower oil followed by homogenization. The resulting particle size distribution is given in Figure 3.4. The WPI aggregates in water had an average particle size of 20 μm after homogenization (Figure 3.4A). Using sonication, a high energy dispersing technique, the particle size decreased to 200 nm with a small noticeable shoulder towards larger particle sizes of around 1 μm. The size of 200 nm was expected for the aggregates and is in good agreement with other research [29]. Increasing the sonication time did not lead to further decrease in particle size (results not shown), indicating that the aggregates of 200 nm could not be broken down further. Most likely, the measured particle size of 20 μm is a result of clustering of the aggregates, which are stabilized by (physical) hydrophobic interactions.

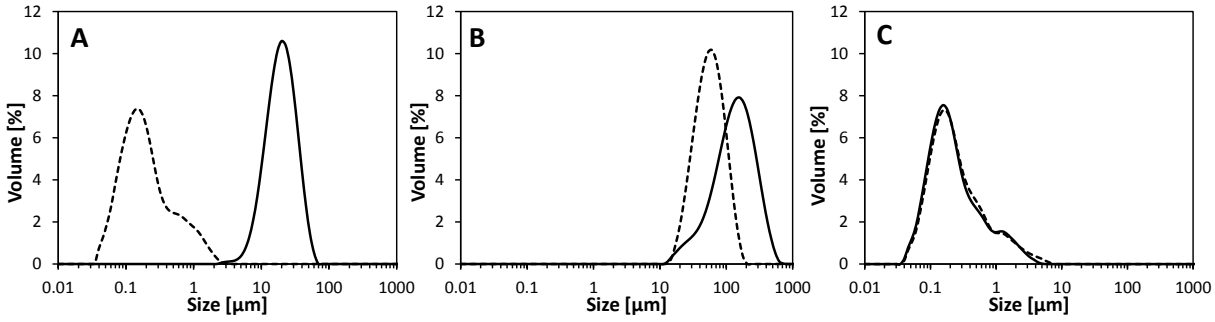

Figure 3.4. (A) particle size distribution of WPI aggregates in water, (B) freeze-dried aggregates dispersed in sunflower oil, (C) WPI aggregates in sunflower oil after solvent exchange. Solid lines indicate particle size after homogenization and dashed lines indicate particle size after sonication for 5 min.

The particle size of the freeze-dried WPI aggregates in oil after homogenization was found to be ~ 100 μm (Figure 3.4B). Sonication decreased the particle size to some extent to ~ 60 μm, but no particles of 200 nm were observed. This shows that the aggregates after freeze-drying were tightly bound and could not be broken. Alternatively, when the aggregates remained in a wet state throughout the solvent exchange procedure, an average particle size in oil of 200 nm was already achieved after homogenization, similar to the particle size in water after high energy input. This means that clustering was prevented and the aggregates were already dispersed well after mild shear treatments. When present in oil, the exposed hydrophobic patches on the protein aggregates have interactions with the surrounding apolar solvent (oil) that are favorable over interactions between the protein aggregates, facilitating the disintegration of initial larger clusters. The results show that by following a simple solvent exchange procedure, clustering of the heat-set WPI aggregates is prevented, and allows the small aggregates to be used as effective building blocks to create protein-based oleogels.

Rheological characterization WPI oleogels

To gain more information about the interactions between the protein aggregates within the network in sunflower oil, oscillatory rheology experiments were performed. To this end, the obtained dense pellet of WPI aggregates in sunflower oil was diluted to adjust the protein concentration. Frequency and amplitude sweeps were performed to examine the gel network structures.

Frequency and strain dependence

Figure 3.5 shows the storage modulus, G', and loss modulus, G", of WPI oleogels at two different protein concentrations in the frequency range of 0.01 to 10 Hz. Increasing the protein concentration from 4.1 (Figure 3.5A) to 6.1% w/w (Figure 3.5B) resulted in an increase of roughly one order of magnitude in G', indicating a stronger gel was formed. Both gels show G' > G" over the examined frequency range, for which the relative importance of elasticity in the system is reflected by the loss tangent ($\tan\delta = G'' / G'$). Figure 3.6A shows the $\tan\delta$ at $\gamma = 0.01\%$ and $\omega = 1$ Hz as a function of the protein concentration in the oleogel. Already at low protein concentration (~ 3 wt%), predominant elastic behavior was obtained as $\tan\delta$ was found to be ~ 0.4. Upon increasing the protein concentration, $\tan\delta$ decreased to ~ 0.07, which indicates a more solid-like behavior of the protein oleogels at higher protein concentrations.

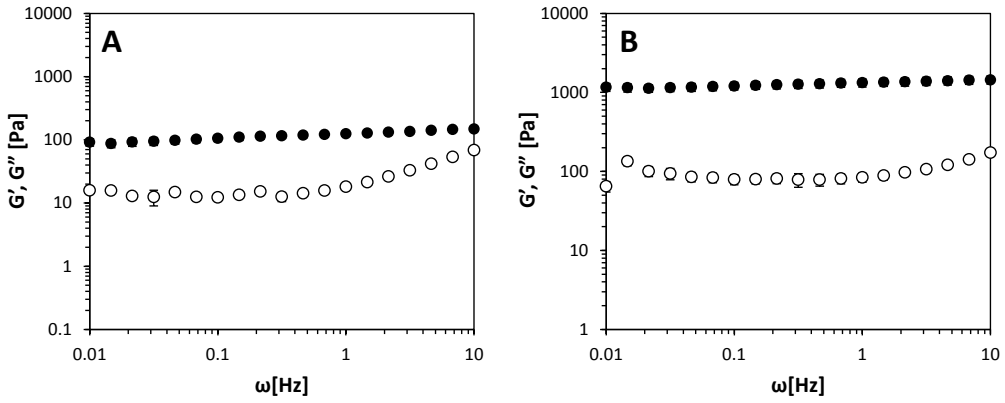

Figure 3.5. Frequency sweeps of a (A) 4.1 and (B) 6.1 wt% WPI aggregate oleogel. G': filled symbols, G": open symbols. Error bars indicate standard deviation of duplicate measurements.

Over the examined range, G' was only slightly dependent on frequency, which is typical behavior for elastic networks. From the frequency dependence of G', information on the network structure can be obtained. Determining the frequency dependence as $G' \sim \omega^n$, the exponent, n, can be obtained from a log-log plot of G' versus oscillation frequency. A covalent gel has an exponent $n = 0$ and for a physical gel $n > 0$ [31]. Therefore, the slope is indicative of a resemblance of an elastic covalent gel and can be used to examine protein gel network structures [32-34]. When plotted against the protein concentration, the value for n decreased from 0.15 to 0.04, as shown in Figure 3.6B. Since $n > 0$, this indicates that the gels classify as physical gels. However, upon increasing the amount of protein aggregates, the value for n decreases, which shows a higher resemblance of an elastic covalent gel. As both the tanδ and the exponent n decreases as a function of increasing protein concentration in the oleogel, it shows that the added particles are effectively contributing to a more elastic behavior of the gel [31, 35].

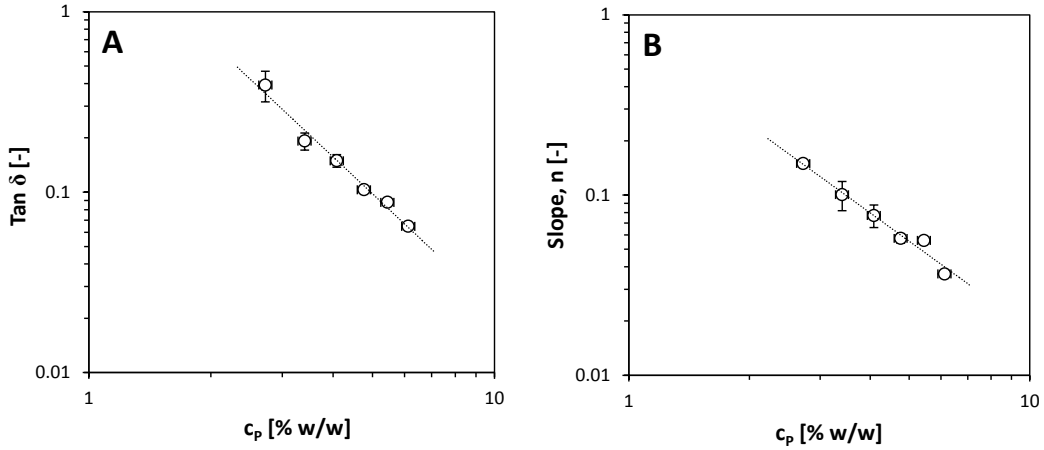

Figure 3.6. (A) tanδ and (B) the slope n as function of protein concentration (c_P) in the oleogel. Dotted lines were added to guide the eye.

To gain more insight in the rheological behavior at larger strains, strain sweeps were performed at different protein concentration over the strain range 0.001 – 100%. In Figure 3.7, the results are given for two protein concentrations (4.1 and 6.1 wt%). For both gels, a typical behavior of G' and G" as a function of increasing strain is observed. At low deformation, both systems can be classified as a gel since G' is roughly an order of magnitude larger than G". At the limit of linearity (γ_0), the elastic response starts to drop and diverges from linear behavior. What can be observed is that G' decreases more rapidly than G" resulting in a cross-over from elastic to viscous behavior. The G" shows a small strain overshoot around γ_0, indicating rearrangements in the network structure [36].

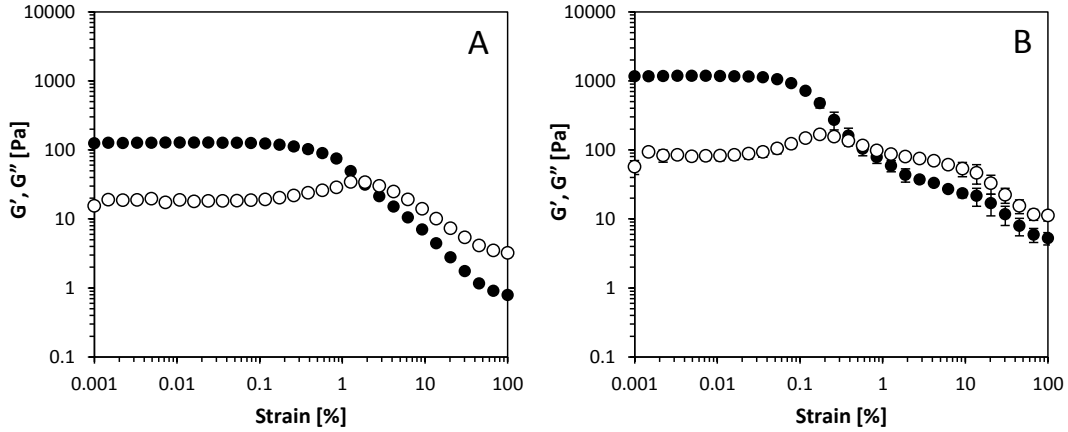

Figure 3.7. Oscillatory strain sweeps of a (A) 4.1 wt% and (B) 6.1 wt% WPI aggregate oleogel. G': filled symbols, G": open symbols. Error bars indicate standard deviation of duplicate measurements.

Fractal dimension

Rheological data are used to estimate the fractal dimensions (d_f) in protein gels. As described in the materials and method section of this chapter, fractal networks can be either in a strong-link or a weak-link regime depending on the strength of the interactions within and between the flocs [26]. As can be seen in Figure 3.8A, γ_0 decreases as a function of protein concentration. This indicates that the fractal flocs in the gel network can be best described using the strong-link regime (eq. 3.1 and 3.2), which will be used below. Figure 3.8B shows the elastic modulus, G', as a function of the protein concentration, from which the best fit of $G' \sim c_p^{5.3}$ through the data points is found. Using the exponent and equation 3.1 (i.e. the strong-link regime), we calculated d_f to be 2.2 (± 0.1) when assuming the fractal dimension of the backbone, *x*, to be between 1 – 1.3 [26].

The preparation of the protein-based oleogels resembles that of cold-set protein gelation in aqueous environments in the sense that first aggregates are formed that are allowed to interconnect to form elastic networks. By acidification of a suspension of WPI aggregates in aqueous media, values for d_f ~ 2.2 – 2.3 were found using permeability measurements and image analysis [24]. Other examples of whey protein cold-set gelation by the addition of salt, using rheological data, typical values for d_f are found in the range of 2.3 – 2.7. In these cases, the fractal dimension depended on salt type and ionic strength, and were found to be in the weak-link regime [25, 37, 38]. Our data of the protein network in oil, however, were best described using the strong-link regime. A possible explanation for this difference might be found in the fact that in our case, the used protein concentration range was quite low compared to other studies of protein networks in aqueous media. When using low concentrations, one allows the fractal flocs to grow larger in size, which may result in strong-link behaviour [26]. Nevertheless, the similarity of d_f values found in our protein networks in oil (d_f ~ 2.2) and for cold-set gelation in aqueous environments, indicates that the aggregation process results in similar gel network structure in both water and oil. Even though the applicability of a fractal model for protein gels can be questionable given their heterogeneity and possible limited self-similarity over different length scales [39], the obtained values for d_f are in agreement with other protein networks.

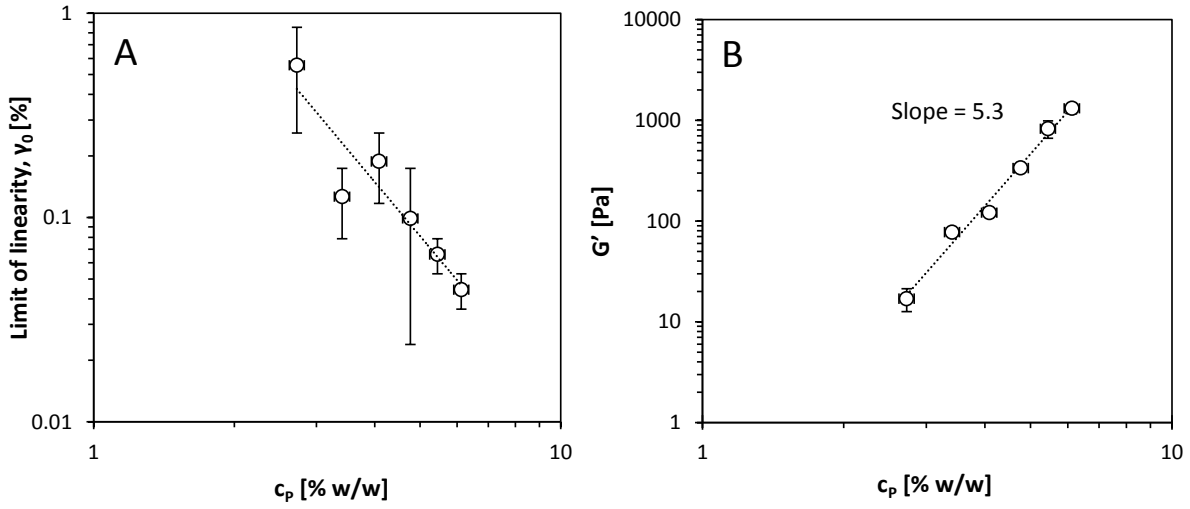

Figure 3.8. Log-log plots of (A) limit of linearity (γ_0) and (B) G' versus protein concentration (c_P). The dotted line in figure A was added to guide the eye, in figure B it represents the best fit through the experimental data points.

Overall, it was shown that heat-set WPI aggregates are remarkably well able to gelate liquid oil into oleogels. Upon increasing the concentration, the protein aggregates are effectively incorporated into a network as evidenced by the decreasing frequency dependence of G' and decreasing tanδ. Moreover, since the results suggest that the fractal flocs are in the strong-link

regime, G' increased rapidly as a function of protein concentration. From the rheological data it is clear that the protein aggregates have an effective particle-particle interaction in the oil. The nature of these interactions, however, remains uncertain. In aqueous systems, protein aggregate network formation is dominated by hydrophobic interactions, hydrogen bonding, van der Waals interactions and disulfide bonds [24, 40]. We hypothesize that in liquid oils, hydrophobic interactions between the protein aggregates will not play a role since exposed hydrophobic patches have favorable interactions with the apolar solvent. Instead, we hypothesize that the gelation of oil using protein aggregates is mainly governed by interactions of hydrophilic nature, i.e. interactions between exposed hydrophilic side groups. Such interactions can be formed through hydrogen bonding, which have already been discussed in the case of silica particles in apolar media by Raghavan [41, 42]. In their studies, it was shown that when the dispersed particles do not have the possibility for hydrogen bonding with the surrounding solvent, particles interact with themselves through hydrogen bonding to form elastic networks. Since proteins are amphiphilic by nature, the exposed side groups on the surface of the aggregate and their hydrophobicity determine the balance between protein-protein and protein-solvent interactions.

Conclusion

In this Chapter, we report on the successful gelation of liquid oil by using heat-set whey protein aggregates. Starting from an aqueous suspension, replacing the water for an oil miscible solvent, agglomeration of the protein aggregates was prevented and similar particle size (diameter ~ 200 nm) was measured in both water and oil. Due to the submicron particle size, the aggregates showed to be capable of forming a gel network in liquid oil. Gel-like behavior, where G' > G", was already observed at low protein concentration (~ 3%). Relating G' to protein concentration shows that $G' \sim c_p^{5.3}$, from which a fractal dimension of roughly 2.2 was obtained, similar to fractal dimensions found for protein networks in aqueous media [24, 25].

In summary, we have shown for the first time that submicron protein aggregates can form a network in liquid oil, similar to their well-known ability to form a network in water. This finding introduces a new conceptual tool in colloid science; using protein aggregates to structure oil and control its viscoelastic properties. The insights in the protein network formation extends the work in Chapter 2, in which we showed that the solvent exchange procedure can be used as an effective tool to create protein oleogels from macroscopic hydrogel templates [43].

The functionality of protein aggregates is well-known in aqueous environments. However, until now, no studies were done on oil structuring ability in the form of directly dispersed aggregates in

liquid oil. Our novel route extends protein functionality beyond gelling ability of water, emulsifying, or foaming ability. Although examples of polymer oleogelation exist [14, 22], for applications in the field of foods, pharmaceuticals or cosmetics, protein oleogels could provide significant advantages such as a low gelation concentration, cost effectiveness, and a widespread availability. In addition, in water-based systems many possible routes to create aggregates from different protein sources have been reported [44-46], which results in a wide variety of protein aggregates with different physical and chemical properties. The diversity to tune the initial protein building blocks provides opportunities to alter the interactions between the protein aggregates in oil-based systems and resulting network formation. Further research could be dedicated to a more detailed understanding of the interactions involved in protein aggregate network formation in oil-based systems, as limited knowledge is available on protein behavior in hydrophobic environments. This will provide new insights in the structure-function relationship of specific protein-protein interactions and physico-chemical properties of proteins oleogels. Since the topic of oleogelation is of growing interest in different fields of science, we envision that protein-based oleogels have great potential.

References

1. Kumar, R. and O.P. Katare, *Lecithin organogels as a potential phospholipid-structured system for topical drug delivery: A review.* AAPS PharmSciTech, 2005. **6**(2): p. E298-E310.
2. Vintiloiu, A. and J.C. Leroux, *Organogels and their use in drug delivery - A review.* Journal of controlled release, 2008. **125**(3): p. 179-192.
3. Basak, S., J. Nanda, and A. Banerjee, *A new aromatic amino acid based organogel for oil spill recovery.* Journal of Materials Chemistry, 2012. **22**(23): p. 11658-11664.
4. Wicklein, A., et al., *Self-assembly of semiconductor organogelator nanowires for photoinduced charge separation.* ACS Nano, 2009. **3**(5): p. 1107-1114.
5. Marangoni, A., *Organogels: An Alternative Edible Oil-Structuring Method.* Journal of the American Oil Chemists' Society, 2012. **89**(5): p. 749-780.
6. Patel, A.R., et al., *Edible applications of shellac oleogels: Spreads, chocolate paste and cakes.* Food and Function, 2014. **5**(4): p. 645-652.
7. Gandolfo, F.G., A. Bot, and E. Flöter, *Structuring of Edible Oils by Long-Chain FA, Fatty Alcohols, and Their Mixtures.* Journal of the American Oil Chemists' Society, 2004. **81**(1): p. 1-6.
8. Hwang, H.S., et al., *Organogel formation of soybean oil with waxes.* Journal of the American Oil Chemists' Society, 2012. **89**(4): p. 639-647.
9. Toro-Vazquez, J.F., et al., *Physical properties of organogels and water in oil emulsions structured by mixtures of candelilla wax and monoglycerides.* Food Research International, 2013. **54**(2): p. 1360-1368.
10. Bot, A. and W.G.M. Agterof, *Structuring of edible oils by mixtures of γ-oryzanol with β-sitosterol or related phytosterols.* Journal of the American Oil Chemists' Society, 2006. **83**(6): p. 513-521.
11. Sawalha, H., et al., *Organogel-emulsions with mixtures of β-sitosterol and γ-oryzanol: Influence of water activity and type of oil phase on gelling capability.* Journal of Agricultural and Food Chemistry, 2012. **60**(13): p. 3462-3470.
12. Gong, R., et al., *A clickable, highly soluble oligopeptide that easily forms organogels.* Supramolecular Chemistry, 2013. **25**(5): p. 269-275.
13. Nikiforidis, C.V. and E. Scholten, *Self-assemblies of lecithin and α-tocopherol as gelators of lipid material.* RSC Advances, 2014. **4**(5): p. 2466-2473.
14. Davidovich-Pinhas, M., S. Barbut, and A.G. Marangoni, *The gelation of oil using ethyl cellulose.* Carbohydrate Polymers, 2015. **117**: p. 869-878.
15. Zetzl, A.K., A.G. Marangoni, and S. Barbut, *Mechanical properties of ethylcellulose oleogels and their potential for saturated fat reduction in frankfurters.* Food and Function, 2012. **3**(3): p. 327-337.
16. Gravelle, A.J., et al., *Towards the development of a predictive model of the formulation-dependent mechanical behaviour of edible oil-based ethylcellulose oleogels.* Journal of Food Engineering, 2014. **143**: p. 114-122.

17. Davidovich-Pinhas, M., S. Barbut, and A.G. Marangoni, *The role of surfactants on ethylcellulose oleogel structure and mechanical properties.* Carbohydrate Polymers, 2015. **127**: p. 355-362.
18. Nikiforidis, C.V. and E. Scholten, *Polymer organogelation with chitin and chitin nanocrystals.* RSC Advances, 2015. **5**(47): p. 37789-37799.
19. Huang, Y., et al., *Hydrophobic modification of chitin whisker and its potential application in structuring oil.* Langmuir, 2015. **31**(5): p. 1641-1648.
20. Romoscanu, A.I. and R. Mezzenga, *Emulsion-templated fully reversible protein-in-oil gels.* Langmuir, 2006. **22**(18): p. 7812-7818.
21. Patel, A.R., et al., *A foam-templated approach for fabricating organogels using a water-soluble polymer.* RSC Advances, 2013. **3**(45): p. 22900-22903.
22. Patel, A.R., et al., *Biopolymer-based structuring of liquid oil into soft solids and oleogels using water-continuous emulsions as templates.* Langmuir, 2015. **31**(7): p. 2065-2073.
23. Ako, K., T. Nicolai, and D. Durand, *Salt-induced gelation of globular protein aggregates: Structure and kinetics.* Biomacromolecules, 2010. **11**(4): p. 864-871.
24. Alting, A.C., et al., *Cold-set globular protein gels: Interactions, structure and rheology as a function of protein concentration.* Journal of Agricultural and Food Chemistry, 2003. **51**(10): p. 3150-3156.
25. Marangoni, A.G., et al., *On the structure of particulate gels—the case of salt-induced cold gelation of heat-denatured whey protein isolate.* Food Hydrocolloids, 2000. **14**(1): p. 61-74.
26. Shih, W.H., et al., *Scaling behavior of the elastic properties of colloidal gels.* Physical Review A, 1990. **42**(8): p. 4772-4779.
27. Wu, H. and M. Morbidelli, *A Model Relating Structure of Colloidal Gels to Their Elastic Properties.* Langmuir, 2001. **17**(4): p. 1030-1036.
28. Hagiwara, T., H. Kumagai, and T. Matsunaga, *Fractal Analysis of the Elasticity of BSA and β-Lactoglobulin Gels.* Journal of Agricultural and Food Chemistry, 1997. **45**(10): p. 3807-3812.
29. Schmitt, C., et al., *Influence of protein and mineral composition on the formation of whey protein heat-induced microgels.* Food Hydrocolloids, 2011. **25**(4): p. 558-567.
30. Tang, Z., Q. Wei, and B. Guo, *A generic solvent exchange method to disperse MoS2 in organic solvents to ease the solution process.* Chemical Communications, 2014. **50**(30): p. 3934-3937.
31. Clark, A.H. and S.B. Ross-Murphy, *Structural and mechanical properties of biopolymer gels*, in *Advances in Polymer Science*. 1987, Springer Berlin Heidelberg: Berlin, Heidelberg. p. 57-192.
32. Egelandsdal, B., K. Fretheim, and O. Harbitz, *Dynamic rheological measurements on heat-induced myosin gels: An evaluation of the method's suitability for the filamentous gels.* Journal of the Science of Food and Agriculture, 1986. **37**(9): p. 944-954.
33. Stading, M. and A.-M. Hermansson, *Viscoelastic behaviour of β-lactoglobulin gel structures.* Food Hydrocolloids, 1990. **4**(2): p. 121-135.
34. Creusot, N., et al., *Rheological properties of patatin gels compared with β-lactoglobulin, ovalbumin, and glycinin.* Journal of the Science of Food and Agriculture, 2011. **91**(2): p. 253-261.

35. Rao, A., *Rheology of Fluid and Semisolid Foods: Principles and Applications*. 2 ed. Food Engineering Series. 2007: Springer US: p. 339 - 401.
36. Hyun, K., et al., *Large amplitude oscillatory shear as a way to classify the complex fluids.* Journal of Non-Newtonian Fluid Mechanics, 2002. **107**(1-3): p. 51-65.
37. Kuhn, K.R., Â.L.F. Cavallieri, and R.L. da Cunha, *Cold-set whey protein gels induced by calcium or sodium salt addition.* International Journal of Food Science and Technology, 2010. **45**(2): p. 348-357.
38. Hongsprabhas, P., S. Barbut, and A.G. Marangoni, *The structure of cold-set whey protein isolate gels prepared with calcium.* LWT - Food Science and Technology, 1999. **32**(4): p. 196-202.
39. Nicolai, T., *Structure of Self-Assembled Globular Proteins*. Food Colloids: Self-Assembly and Material Science. 2007: The Royal Society of Chemistry: p. 35-56.
40. Remondetto, G.E. and M. Subirade, *Molecular mechanisms of Fe-induced β-lactoglobulin cold gelation.* Biopolymers, 2003. **69**(4): p. 461-469.
41. Raghavan, S.R., H.J. Walls, and S.A. Khan, *Rheology of silica dispersions in organic liquids: New evidence for solvation forces dictated by hydrogen bonding*. Langmuir, 2000. **16**(21): p. 7920-7930.
42. Raghavan, S.R. and S.A. Khan, *Shear-Thickening Response of Fumed Silica Suspensions under Steady and Oscillatory Shear.* Journal of Colloid and Interface Science, 1997. **185**(1): p. 57-67.
43. De Vries, A., et al., *Protein Oleogels from Protein Hydrogels via a Stepwise Solvent Exchange Route.* Langmuir, 2015. **31**(51): p. 13850-13859.
44. Maltais, A., G.E. Remondetto, and M. Subirade, *Mechanisms involved in the formation and structure of soya protein cold-set gels: A molecular and supramolecular investigation.* Food Hydrocolloids, 2008. **22**(4): p. 550-559.
45. Donato, L., E. Kolodziejcyk, and M. Rouvet, *Mixtures of whey protein microgels and soluble aggregates as building blocks to control rheology and structure of acid induced cold-set gels.* Food Hydrocolloids, 2011. **25**(4): p. 734-742.
46. Mession, J.L., et al., *Effect of globular pea proteins fractionation on their heat-induced aggregation and acid cold-set gelation.* Food Hydrocolloids, 2015. **46**: p. 233-243.

Chapter 4

The effect of oil type on network formation by protein aggregates into oleogels

This chapter is based on: de Vries, A., Lopez Gomez, Y., van der Linden, E., Scholten, E., *The effect of oil type on network formation by protein aggregates into oleogels.* [submitted]

Introduction

In foods, the phenomenon of gelation is governed by network formation of specific 'building blocks'. In aqueous phases, many biopolymers such as proteins and polysaccharides are able to associate into networks, and provide ample opportunities to create desired textures by varying or combining gelling agents, changing solvent conditions, processing conditions, etc [1]. In oil phases, traditionally, structure formation is less diverse and relies on the crystallization of saturated and *trans* fatty acids in triglycerides into a space-spanning network, entrapping the liquid oil. Varying the crystallization rate, shearing conditions, and the composition or amount of saturated fatty acids provide ways to alter the network formation and the physico-chemical properties of the resulting solid-like fat [2]. Although such fatty acids are very useful in food products as they provide oxidative stability, hardness, and plastic deformation, they are also debated because of a possible negative impact on human health by changing the blood cholesterol profile [3]. Although research concerning these health implications of the various fatty acids is still on-going [4], legislative actions have been taken to ban partially hydrogenated oils in food products. Additionally, with regard to the cholesterol composition in the blood, it has been shown that replacement of saturated fats with poly unsaturated fatty acids, as ubiquitously present in liquid oil, has clear health benefits [5, 6]. The use of unsaturated fats is therefore highly promoted. The replacement of saturated fats by unsaturated oils, however, is not straightforward as liquid oil can negatively affect the texture of food products [7, 8].

One approach to replace saturated or *trans* fatty acids, which has gained much attention over the last few years, is to use other structuring agents to provide a solid character to liquid oil by the formation of so-called 'oleogels' [9-12]. In many of these oleogels, gelation is achieved by low molecular weight organogelators (LMOGs) such as waxes [13], lecithins [14, 15], phytosterols [16] or monoglycerides [17]. Besides LMOGs, the cellulose derivative ethylcellulose (EC) is studied for its gelling properties in liquid oil. Being hydrophobically modified, this polymer is dispersible in liquid oil at high temperature and forms gels upon cooling [18].

In the formation of oleogels, the nature of the gelling agent and the nature of the solvent can greatly affect the rheological behaviour. For example, oleogels formed by self-assembly of γ-oryzanol and β-sitosterol into tubules have been shown to be affected by the polarity of the oil [19]. Other researchers, using the same gelators, concluded that next to polarity, also the viscosity of the oil phase affected the self-assembly of the structuring molecules and therefore affected gelation time and the final gel strength [20]. Also in monoglyceride-based oleogels, the use of oils with different polarity and viscosity have shown to affect crystallization and gelation behaviour

[21]. Additionally, the fatty acid chain length in the oil affected the rheological behaviour based on a difference in special orientation of the fat crystals [22]. In general, gel strength is decreased when the interactions between the gelator molecules and the oil are enhanced. The interactions depend largely on the chemical composition and the polarity of the oil. In ricinelaidic acid based oleogels, a decrease in the gelation efficiency was observed when the molecules were able to form hydrogen bonding with moieties on different oils [23]. Alternatively, in EC oleogels, an increase in oil polarity or polar compounds increased gel hardness [24]. This effect was related to the better solubility of the EC polymers during heating.

In Chapter 3, it was demonstrated how heat-set whey protein aggregates can be used as effective building blocks for oil gelation. Efficient network formation was achieved by sufficient interactions of hydrophilic nature between the submicron protein aggregates in hydrophobic oil. In general, network formation of such colloidal particles is affected by both particle-particle and particle-solvent interactions. Therefore, a change in solvent type can be used to alter the network formation and the resulting rheological properties. To assess the effect of different solvent conditions, the oil type was varied and the rheological properties of the resulting protein oleogels were investigated. For comparison with other colloidal systems, also the rheological behaviour of gels prepared with colloidal silica particles with well-defined surface properties were examined.

Materials and methods

Materials

Whey protein isolate (WPI, BiPro) was obtained from Davisco Foods International (Le Sueur, MN, USA) with a protein concentration of 93.2% (N x 6.38) and was used as received. Acetone (AR grade) was supplied by Actu-All Chemicals (Oss, the Netherlands). Two types of silica particles were used in this study, a hydrophilic and a hydrophobic fumed silica. Fumed silica, prepared by flame hydrolysis, consists of small, nanometer-sized primary particles that form branched and stable aggregates. Hydrophilic fumed silica (A200) was obtained from Sigma Aldrich and its surface chemistry consists of a high degree of hydroxyl groups. According to the supplier specification, the particles consist of agglomerated, highly branched aggregates of ~ 0.2 – 0.3 μm. Hydrophobic silica (R972) was obtained from Evonik Industries (Essen, Germany), for which about 70% of the hydroxyl groups on the surface of the particles were modified by attachment of methyl groups [25]. Both silica particles consisted of agglomerates of small primary particles (Figure 4.1) with a specific surface area of 200 m^2/g and 130 m^2/g for the hydrophilic and hydrophobic silica

particles, respectively. For convenience, hydrophobic silica will be referred to as R972 and hydrophilic silica as A200. Four different oils were used in the current study. Extra virgin olive oil (EVO) and sunflower oil were purchased at a local supermarket and used without purification. Medium chain triglyceride oil (MCT) was obtained from Cremer Oleo GmbH (Hamburg, Germany). This highly refined oil consisted predominantly of C8 and C10 fatty acids. Castor oil was obtained from Sigma Aldrich.

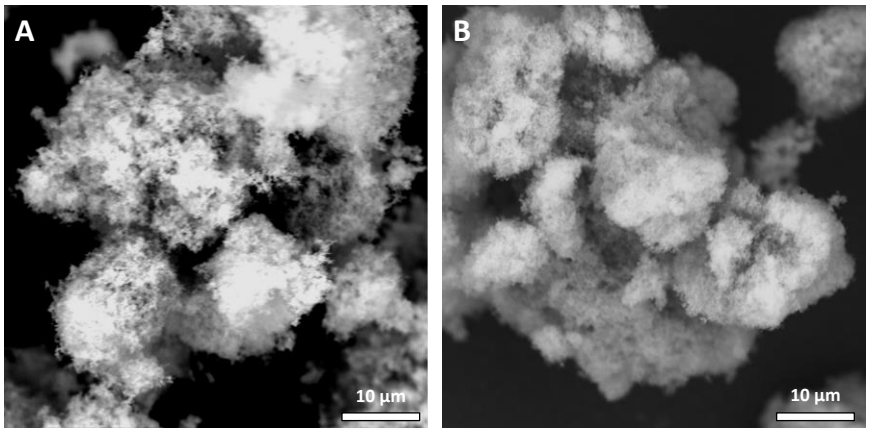

Figure 4.1. Scanning Electron Microscopy (SEM) image of silica particles, A) hydrophobic R972 silica, B) hydrophilic A200 silica.

Methods

Oil properties

Viscosity. The viscosity of the oils was determined using a stress-controlled rheometer (AP502, Anton Paar GmbH, Graz, Austria) with a double gap geometry (DG26.7, internal diameter: 24.7 mm, external diameter 26.7 mm). After sample loading, the shear rate was increased from 0.1 to 100 s^{-1}. Measurements were performed in duplicate and all oils behaved as Newtonian liquids.

Interfacial tension. The oil-water interfacial tension was determined using an automated drop tensiometer (ADT, Teclis Tracker, ITCONCEPT, Longessaigne, France). A water droplet (milli-Q, Millipore) with a surface area of 50 mm^2 was created in the different oils. The contact angle was measured under static conditions by keeping the surface area constant, and the interfacial tension was calculated using the available software. Measurements were performed at 20 °C (± 0.1 °C), which was maintained by a temperature-controlled water bath. The development of the interfacial tension was followed for 1 h, until a stable value was reached.

Preparation of protein aggregates

WPI powder (4% w/w) was dissolved in demineralized water under continuous stirring at room temperature for 2 h. Afterwards, the pH of the stock solution was adjusted to 5.7 using a 1 M HCl solution. To induce aggregate formation, samples were heated at 85 °C for 15 min using a temperature-controlled water bath. After cooling, the resulting protein dispersion was homogenized using a rotor stator homogenizer (Ultra Turrax, T25, IKA Werke, Germany) at 13000 rpm for 3 min. The protein aggregates were then collected by centrifugation at 4000 g (Hermle Z383K, Hermle Labortechnik GmbH, Wehingen, Germany) for 20 min at 20 °C. Hereafter, the pellet was re-dispersed and centrifuged twice with demineralized water to remove remaining soluble protein material.

Preparation of protein oleogels and silica oleogels

To prepare the protein oleogels, the WPI aggregates were transferred to the 4 different oil types using a solvent exchange procedure as described in Chapter 3. In this procedure, the polarity of the solvent was changed gradually to remove the surrounding water from the WPI aggregates and replace the continuous phase for oil. In short, 15 g of aqueous pellet, containing the WPI aggregates, was re-dispersed in 150 mL acetone, and mixed thoroughly using rotor stator homogenization at 13000 rpm for 3 min. Afterwards, the sample was centrifuged at 4000 g for 20 min at 20 °C. Excess acetone was removed by decanting and the pellet, containing the protein aggregates, was collected. The pellet was then re-dispersed, homogenized and centrifuged as described above once more using acetone to assure water removal, and twice using one of the four oils. The obtained pellet of WPI aggregates in oil was diluted in a ratio of 1:10 with oil and left overnight under continuous stirring to allow for evaporation of the remaining acetone. The next day, the protein aggregates were collected by centrifugation at 4000 g for 20 min at 20 °C. The protein concentration was determined by Dumas (Dumas Flash EA 1112 Series, N Analyser, Thermo Scientific) using a nitrogen conversion factor of 6.38.

To prepare the protein oleogels, the protein concentration was adjusted to 10% w/w by adding the appropriate amount of oil and mixed thoroughly for 3 minutes using a rotor stator homogenizer (3 min, 13000 rpm). To prepare the silica suspensions, silica powder was added to the liquid oil and mixed thoroughly using rotor stator homogenization for 3 min at 13000 rpm (the same conditions as for the protein oleogels) to produce a 10% w/w suspension. Hereafter, all samples were degassed using a vacuum pump to remove entrapped air. All values for protein or silica concentration are given in % w/w.

Rheology

To analyze gel formation, oscillatory rheology experiments were performed using a stress-controlled rheometer (AP502, Anton Paar, GmbH, Graz, Austria). All measurements were performed at 20 °C using a parallel plate (ø = 49.978 mm) setup with sandblasted plates to avoid slip. Before any measurement started, the samples were allowed to equilibrate for 60 – 120 min at a fixed frequency of 1 Hz and a strain (γ) of 0.01% (which was within the linear viscoelastic region). Frequency sweeps were performed by increasing the frequency logarithmically from 0.01 to 10 Hz at γ = 0.01%. Amplitude sweeps were performed by increasing the strain logarithmically from 0.001 to 100% at a fixed frequency of 1 Hz. To determine the ability of the network to recover, first large deformation was applied at a strain of 100%, and then reduced to 0.01%. The recovery of G' was then monitored for 30 minutes. All measurements were performed in duplicate.

Confocal Laser Scanning Microscopy (CLSM)

The network structure of the protein and silica suspensions was visualized using CLSM. Here, the samples were gently mixed with a drop of rhodamine B solution (0.2%) in ethanol to stain the protein aggregates and silica particles. The resulting network structure was visualized using a Confocal Laser Scanning Microscope (Leica tcs sp5, Leica Microsystems, Wetzlar, Germany).

Scanning Electron Microscopy (SEM)

To visualize the structure of the silica powders, a Scanning Electron Microscope (Phenom G2 Pro, Phenom-World BV, Eindhoven, and The Netherlands) was used. Using carbon tabs, the powder was fixed onto aluminium stubs (SPI Supplies/Structure Probe Inc., West Chester, USA). The appearance of the powders could be visualized directly without sample pre-treatment due to the low voltage used (5kV).

Results and discussion

Appearance and microstructure

In the current study, heat-set whey protein aggregates were used as building blocks for network formation in liquid oil. The protein aggregates were obtained by heating the whey proteins at a pH close to their isoelectric point in aqueous conditions, and the final protein aggregates had a surface averaged diameter ($d_{3,2}$) of 150 nm. These results are in agreement with other papers reporting similar conditions [26, 27]. Following their preparation, the protein aggregates were transferred to the oil phase using a solvent exchange procedure, which did not alter their particle size (cf. Chapter 3).

At a protein concentration of 10%, self-supporting oleogels had formed, where the liquid oil is entrapped by a network of protein aggregates. The appearance of such a protein oleogel in sunflower oil can be seen in Figure 4.2A. To compare the gelling ability of the colloidal protein aggregates with other colloidal particles, two types of fumed silica particles were dispersed in sunflower oil at the same concentration. Hydrophobic R972 silica formed a gel at 10% w/w in sunflower oil, but the network was disrupted when the sample was taken out of the container as the material started to flow (Figure 4.2B). In contrast, hydrophilic A200 silica formed a rigid, paste-like structure in sunflower oil at 10% (Figure 4.2C). This immediate difference in gelling ability in nonpolar solvents is related to the surface chemistry of the silica particles. The surface of A200 silica consist of hydroxyl groups, whereas for R972 silica, these hydroxyl groups are replaced with methyl groups. In liquid oil, hydrophilic silica is able to from strong particle-particle interactions via hydrogen bonds between the hydroxyl groups at the particle surface. Due to the methyl groups on the surface, hydrophobic silica particles have favourable particle-solvent interactions with the surrounding oil and a decreased amount of hydrogen bonds between the particles [28, 29].

The microstructure of the network created by the different particles is visualized by CLSM and shown in Figure 4.2D, E, and F for the protein aggregates, R972, and A200 respectively. Here, dispersions of 5% were visualized in order to observe the differences in their network structure more clearly. The CLSM image of the protein oleogel (Figure 4.2D) shows that the aggregates formed a fractal-like network in the liquid oil, resulting in gel formation. The R972 silica particles, on the other hand, were distributed homogeneously throughout the suspending oil, which can be attributed to the more hydrophobic character of the particles (Figure 4.2E). Due to the presence of strong hydrogen bonds between the hydrophilic particles, A200 silica (Figure 4.2F) formed a

fractal-like network structure. Compared with both silica particles, the protein aggregates seem to form a network consisting of denser clusters. Most likely, the silica particles have a higher porosity and a larger surface area compared to the protein aggregates, which resulted in a finer network. Nevertheless, the tendency for network formation is attributed to the balance between particle-solvent and particle-particle interactions and in this regard, protein aggregates show a higher similarity to the hydrophilic silica particles.

Another interesting feature is that the protein oleogel was opaque, whereas both silica oleogels were transparent. This difference in appearance can be explained by taking the refractive indices (RI) of the materials into account. Silica particles have a RI of ~ 1.47, which is close to that of sunflower oil (~ 1.46 – 1.47). For protein solutions, the RI depends on the concentration, and for largely dehydrated proteins, the RI is ~ 1.54 [30].

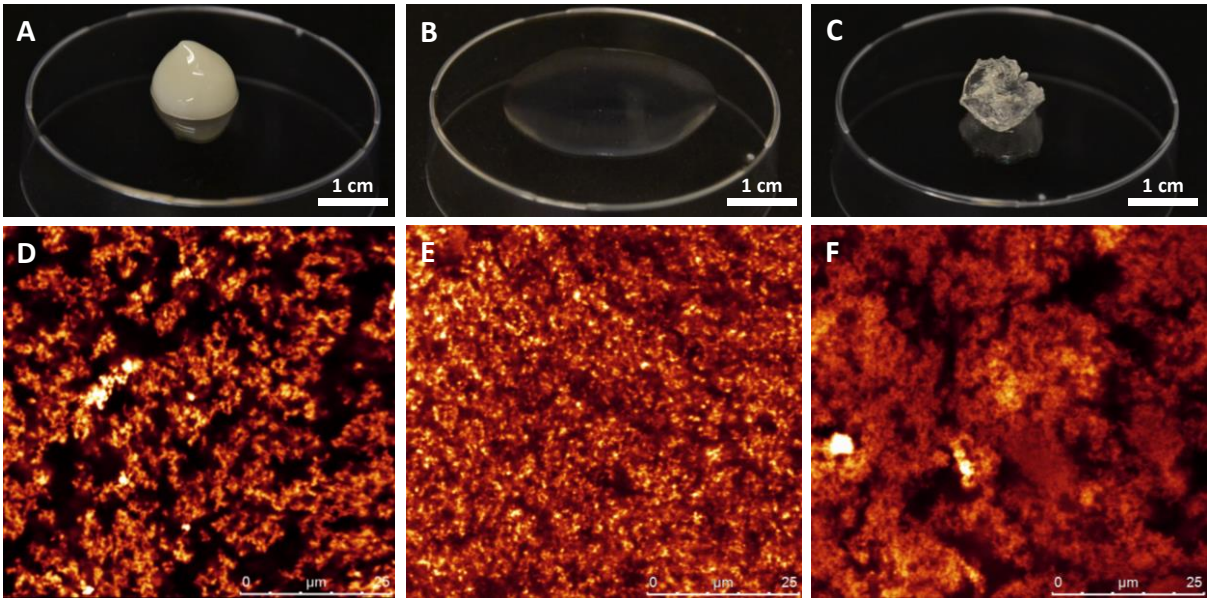

Figure 4.2. Appearance of 10% dispersions in sunflower oil of whey protein aggregates (A), hydrophobic silica R972 (B), hydrophilic silica A200 (C) and corresponding CLSM images (D-F). Samples for CLSM were diluted to 5%.

Solvent characteristics

Network formation by colloidal particles suspended in a solvent is largely dependent on the surface chemistry of the particles and the nature of the solvent. Therefore, four different oil types were chosen to prepare the oleogels; medium chain glyceride oil (MCT), extra virgin olive oil (EVO), sunflower oil, and castor oil. Characteristics of these oils can be found in Table 4.1. MCT oil consists mainly of medium chain (C:8 and C:10) saturated fatty acids, is highly refined and has

a relative low viscosity. Sunflower oil and EVO both mainly consist of oleic (C18:1) and linoleic (C18:2) acid, where EVO can also contain up to 20% palmitic acid (C16:0) [31]. The main difference between sunflower oil and EVO is the degree of refinement. Sunflower oil is a refined oil with minor polar components, with the exception of tocopherols. EVO on the other hand is a cold pressed, unrefined oil which can contain a substantial amount (up to 2%) of polar molecules such as polyphenols, phosphatides, pigments, and sterols [31]. Given the different composition, we propose that this has an influence on the polarity of the different oils. Here, we use the oil-water interfacial tension as a measure for the polarity. Due to the high level of refinement of the MCT oil, the polarity of this oil is the lowest, which is evidenced by the highest oil-water interfacial tension among the used oils in this study (Table 4.1). Both sunflower oil and EVO are less pure, and therefore have a slightly higher polarity. As seen by the difference in interfacial tension, EVO had a lower interfacial tension than sunflower oil, as expected by the larger amount of minor components present. Castor oil consists mainly of ricinoleic acid, a C18:1 carbon fatty acid with a hydroxyl group at the C12 position. As a result of these hydroxyl groups, this oil is more polar than the other oils studied, as seen by the lowest value for the interfacial tension. The viscosities of the oils differ significantly, where MCT has the lowest viscosity and castor oil is the most viscous oil as shown in Table 4.1. Based on the interfacial tension, the polarity of the oils studied range from low to high polarity as MCT < sunflower oil < EVO < castor oil.

Table 4.1. Viscosity and oil-water interfacial tension of the oils used to form oleogels.

Oil type	Viscosity at 20 °C [mPa.s]	Oil-water interfacial tension at 20 °C [mN/m]
MCT oil	29.8 (± 0.1)	26.5 (± 0.4)
Sunflower oil	63.3 (± 0.1)	24.4 (± 0.1)
EVO	80.1 (± 0.1)	14.7 (± 0.1)
Castor oil	1045.0 (± 5.0)	11.7 (± 0.1)

Small amplitude oscillatory rheology

Using these oils, protein aggregates were dispersed at a concentration of 10% to create oleogels and we examined their rheological behaviour. First, we focus on the protein oleogels prepared in MCT, EVO and sunflower oil, since castor oil had a large impact on the rheological behaviour due to its different chemical composition, as will be discussed in detail below. The storage modulus, G', and the loss modulus, G", as a function of the frequency are shown in Figure 4.3. Since G' is larger than G" in all cases and G' is largely independent of the applied frequency, this indicates

that all systems can be classified as gels. For the two types of silica particles, regardless of the type of oil used, G' was found to be much higher for the hydrophilic A200 silica than the hydrophobic R972 silica. The G' of the oleogel prepared with A200 silica was independent on the applied frequency, whereas for R972 silica, G' was distinctly more frequency dependent. For R972 silica, a cross-over between G' and G" at high frequencies can be seen, indicating weaker gel network formation than in the case A200 silica particles were used. Due to the methyl groups on the surface of the particles, R972 silica has increased favourable interactions with the surrounding nonpolar solvents and a lower ability for particle-particle hydrogen bonds. In contrast, A200 silica has less favourable interactions with the surrounding solvent, and an increased ability for particle-particle interactions through hydrogen bonds. This is in accordance with other reports on the gelling behaviour of these two types of silica particles [28, 32].

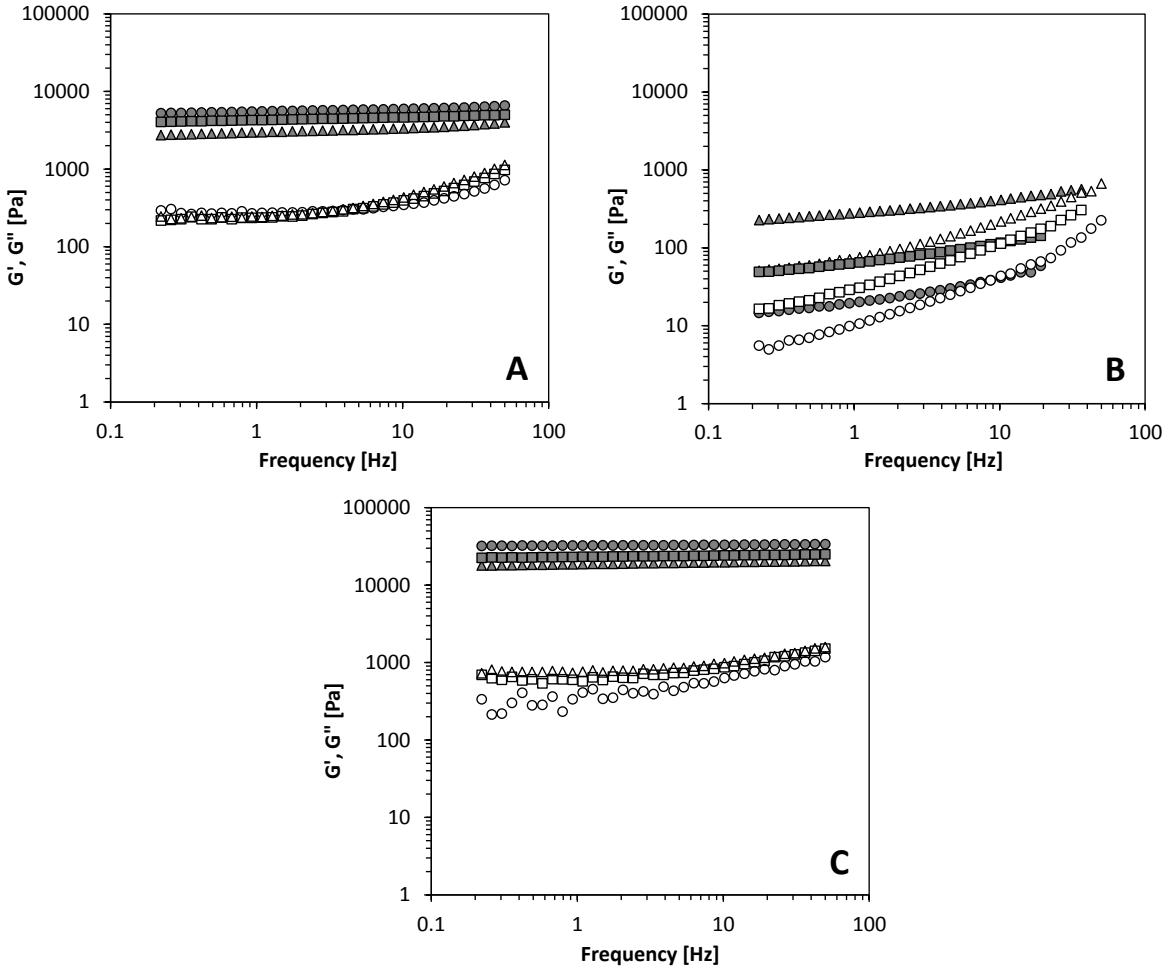

Figure 4.3. Frequency sweeps of 10% protein aggregates (A), hydrophobic R972 silica (B), and hydrophilic A200 silica (C) in MCT oil (○), sunflower oil (□) and olive oil (△). Filled symbols: G', open symbols: G".

Protein aggregates at the same concentration formed gels with a gel strength in between that of the two types of silica particles, both in magnitude of G' as well as in the frequency dependency of G'. Since protein aggregates are amphiphilic, the ability for network formation in oil compared to the hydrophilic A200 silica is lower, due to fewer particle-particle interactions, but higher compared to the hydrophobic R972 silica. Another reason for the lower gel strength of the protein aggregates compared to A200 silica could be the difference in density of the network. Looking at the CLSM images (Figure 4.2), the protein aggregates formed a coarser, more open network compared to the more finely dispersed A200 silica. Colloidal silica consist of highly porous particles with a high surface area, which could lead to more particle-particle interactions compared to the protein aggregates and hence higher gel strength.

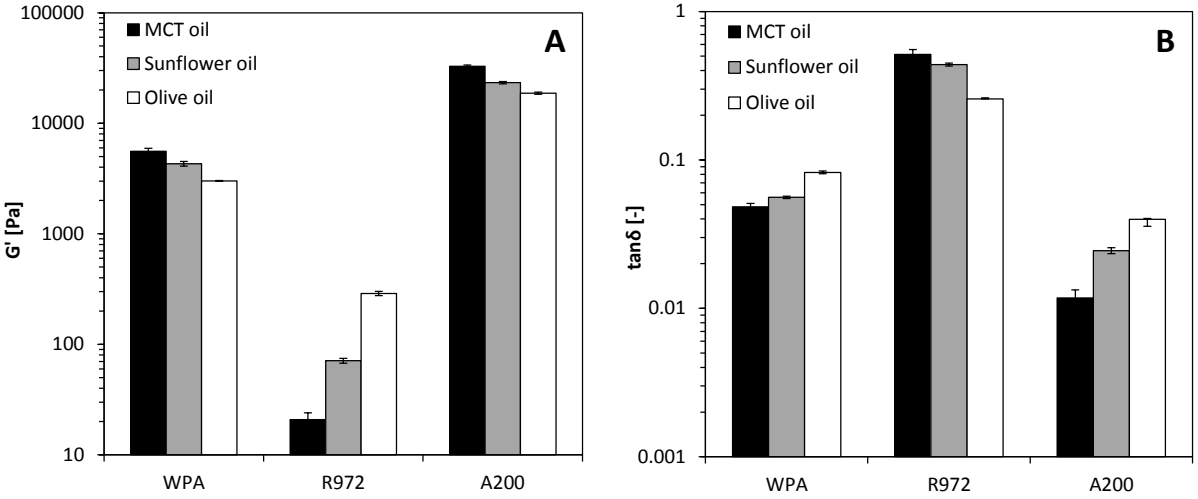

Figure 4.4. G' (A) and tanδ (B) of 10% whey protein aggregates (WPA), hydrophobic silica (R972,) and hydrophilic silica (A200) in different oils.

Besides the surface chemistry of the particles, also the nature of the solvent has an effect on the ability to form colloidal networks. For better comparison, values for G' and the loss tangent (tanδ, G"/G' i.e. the solid-like character of the gel) for the different gel systems is summarized in Figure 4.4. For A200 silica, using a polar EVO decreased G' and increased tanδ, indicating a weaker network formation compared to gels made with the apolar MCT oil. Interestingly, for R972 silica this effect is reversed, i.e. G' increased and tanδ decreased with increasing polarity. Notice that the change in polarity has a larger effect on the hydrophobic then the hydrophilic particles. G' decreases roughly a factor 2 for A200 silica, whereas for R972 silica at the same concentration, G' increased roughly with a factor 13. The decrease in gel strength for the hydrophilic A200 silica particles can be explained by the increase in particle-solvent interactions as a function of increased polarity changing from MCT to EVO. Similarly, an increase in gel strength for hydrophobic R972

particles is obtained as a function for increasing polarity, as the more apolar MCT oil favours more particle-solvent interactions than the more polar EVO.

Using different oil types for structure formation by the protein aggregates, G' increased and tanδ decreased as EVO < sunflower oil < MCT oil, indicating a higher amount of protein-solvent interactions in a more polar environment, giving weaker gel strength. Similar to A200 silica, G' decreased roughly two-fold as the polarity of the oil type increases. The results indicate that the strength of the network formed by protein aggregates is affected by the polarity of the solvent, resulting in weaker gels in more polar oils.

The most polar oil used in this study was castor oil, as shown by the lowest oil-water interfacial tension. This high polarity is caused by ricinoleic acid, which has a hydroxyl group at the C12 position. When attempting to create oleogels in castor oil using the protein aggregates, we were not able to acquire a dispersion of sufficient concentration, and therefore the rheological behaviour could not be determined. For both silica particles, as shown in Figure 4.5A, no gel formation was observed as G" > G' for most of the frequencies studied and G" was almost proportional to the applied frequency. Hydrophilic A200 silica showed a cross-over between G' and G" at low frequency, but G" was larger than G' for the entire frequency range for the hydrophobic R972 silica. This indicates that no network formation was achieved by either of the silica particles. As shown in the CLSM micrographs in Figure 4.5B and C, both silica particles were dispersed evenly throughout the castor oil, indicating few particle-particle interactions and poor network formation.

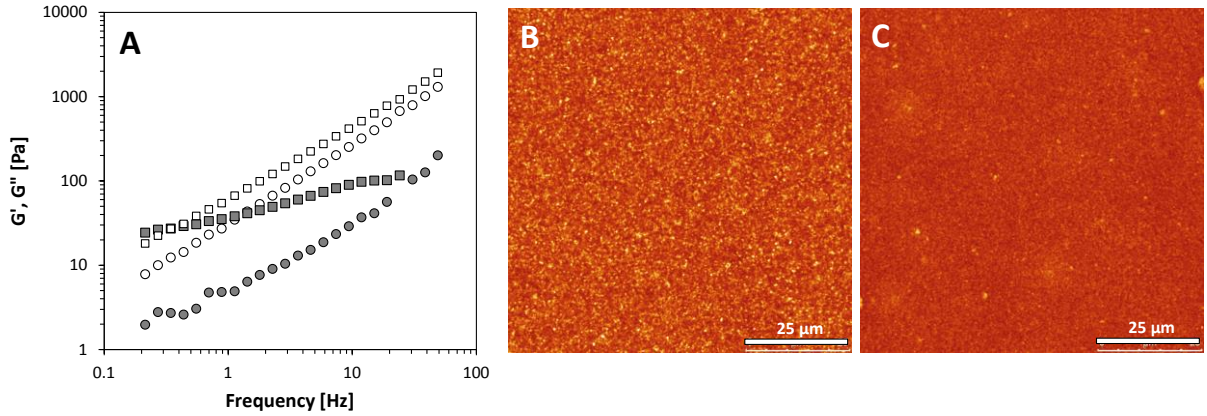

Figure 4.5. Frequency sweep (A) of 10% hydrophilic A200 silica (□) and hydrophobic R972 silica (○) in castor oil. Filled symbols: G', open symbols: G". CLSM image of (B) 5% R972 and (C) 5% A200 in castor oil.

Based on the increased polarity, we would indeed expect a decrease in gel strength for the hydrophilic silica. As shown by Raghavan and co-workers [29], the main driving force for network formation between silica particles is the formation of particle-particle interactions through hydrogen bonds. Instead of strong particle-particle interactions, the high content of hydroxyl groups in castor oil favoured particle-solvent interactions, causing a 'solvation layer' around the particles and therefore inhibited gel formation. For the hydrophobic silica, on the other hand, we would expect an increase in gel strength based on the results discussed previously. In the case of castor oil, hydrogen bonds can also occur between the predominantly hydrophobic particles and the solvent, even if the high polarity of the solvent would favour less particle-solvent interactions. For all types of particles, the increased particle-solvent hydrogen bond formation prevented gel formation. The network formation can therefore not only be controlled by the polarity, but also by the presence of specific chemical groups on the solvent molecules.

Large deformation and structure recovery

Besides the formation of elastic networks, depending on the interactions between the colloidal particles to build a structure, properties like resistance against structure breakdown and structure recovery are important aspects for different applications. Therefore, we examined the structure breakdown of the different particles using large deformation rheology. Figure 4.6 shows the rheological behaviour of the oleogels as a function of the applied strain, where the linear viscoelastic regime (LVR) is defined as the strain value where G' is independent on the applied strain until a certain critical value (γ_c).

As shown in Figure 4.6B and C, A200 silica oleogels show a somewhat longer LVR compared to R972 silica, indicating the network is less prone to yielding. Most likely, this can be attributed to the higher surface area of the A200 silica and the increased ability to form particle-particle interactions through hydrogen bonds in nonpolar media, giving rise to a more rigid network. Compared to both silica particles, the gels prepared with protein aggregates had a distinct lower γ_c. Based solely on their amphiphilic nature, we would expect that structure breakdown by yielding would be an intermediate between the hydrophilic and hydrophobic particles. The results show that the amphiphilicity of the protein aggregates is not the only parameter to determine the yielding behaviour of the network. Looking again at the microstructure of the gels in Figure 4.2, the more densely packed network by the protein aggregates compared to the silica particles could explain this different behaviour, as the larger mesh sizes and the lower amount of connections between larger flocs in the colloidal network would be more prone to yielding phenomena. Similar

effects were observed for Ca^{2+}-induced WPI gels, where coarser networks were formed for increasing Ca^{2+} concentration, which resulted in gels with a lower fracture strain [33].

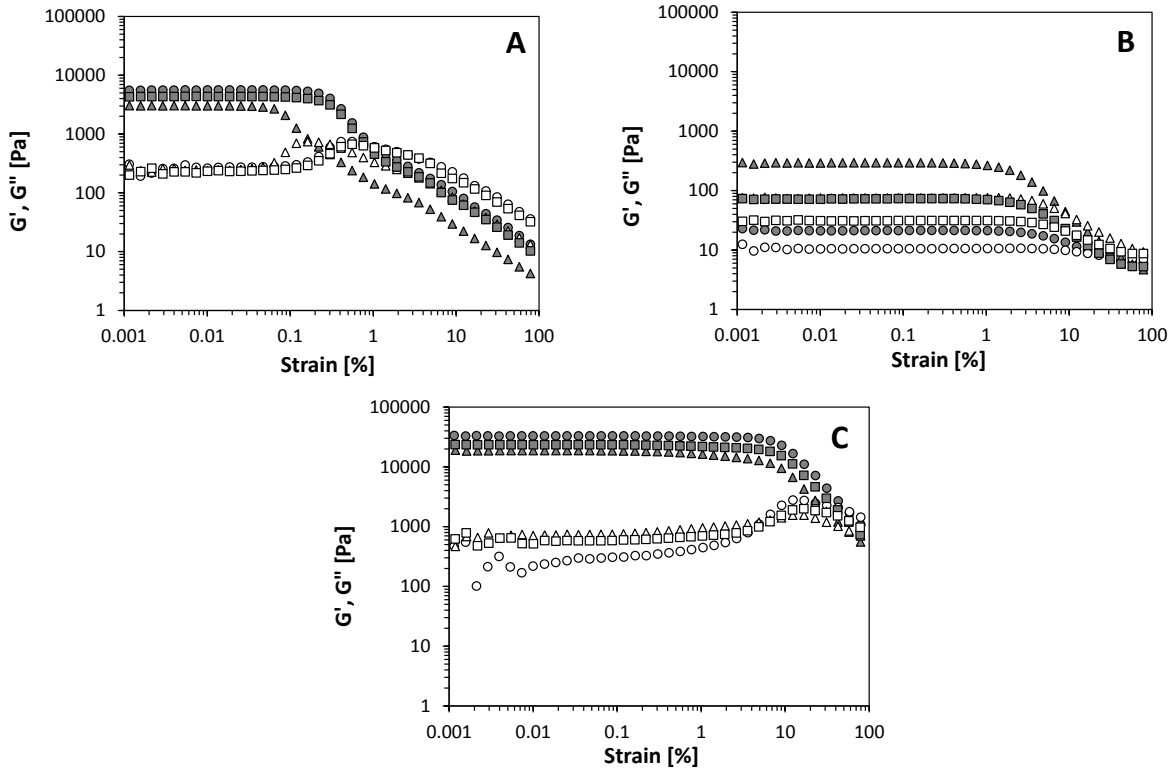

Figure 4.6. Large deformation properties of 10% WPA oleogels (A), hydrophobic R972 silica oleogels (B) hydrophilic A200 silica oleogels (C), in MCT oil (○), sunflower oil (□) and olive oil (△). Filled symbols: G', open symbols: G".

As shown in Figure 4.6, γ_c was not substantially affected by the oil type, indicating that indeed the network structure is more dominant for yielding phenomena. An exception is seen in the case for EVO, where a lower γ_c is observed for both the A200 silica and the protein aggregates. As EVO is not a very pure oil, the structure breakdown might be related to the presence of polar components having a high affinity for the particle surface, leading to fewer or less strong interactions.

An interesting feature is observed for strain amplitudes around γ_c. For the gels made with A200 silica and protein aggregates, G" shows a weak strain overshoot in the region of γ_c, which is not detected in the R972 gels. This overshoot for G" is characteristic for many flocculated gel structures [34, 35]. Deformation of a network, as is done in these experiments, is a process where two phenomena, structure loss and structure creation, simultaneously occur due to breakage and reformation of network junctions. The type of behaviour observed when increasing the strain amplitude depends on which of these two phenomena is dominant. Although difficult to quantify

the magnitude of these processes, the change in the moduli can provide qualitative information as described in a paper by Hyun and co-workers [36], where the authors define a loss rate parameter and a creation rate parameter. Strain thinning behaviour, or 'type I' behaviour, is observed when the loss parameter is positive and the creation parameter is negative, giving rise to a decrease in both moduli. In this case, the structural elements align with the applied flow field and lose network junctions that do not reform during deformation, as we observe for the hydrophobic R972 samples. In 'type III' behaviour, both parameters are positive, but the creation parameter is smaller than the loss parameter, giving rise to a weak strain overshoot for G" as we observe for both the protein aggregate gels and the A200 gels. As the two types of silica show a different behaviour during deformation, this indicates that the rate of structure loss and structure formation is dependent on the surface chemistry of the particles and the strength of the particle-particle interactions. Since a weak strain overshoot is observed for the more hydrophilic particles, rapid structure formation is most likely due to the rate of hydrogen bond formation between the particles. To further assess the ability of the network to restore after deformation is applied, we examined the structure reformation over time at low deformation after the network was subjected to high strains.

Structure recovery

After subjecting the different gels to large deformation (γ = 100%) to induce structure breakdown, the strain was reduced to γ = 0.01% (which was within the linear viscoelastic regime) to examine the structure recovery, or thixotropic behaviour, over time. During structure breakdown, network junctions between interacting colloidal particles or fractal flocs of these particles are broken due to the applied large deformations. Under subsequent non-destructive low deformations, these junctions are then reformed, restoring the network.

Table 4.2. Exponent n for structure recovery after deformation, determined by the best fit of $G' \sim t^n$.

Oil type	**Structure recovery exponent *n*** **Particle type**		
	WPA	R972	A200
MCT	0.09 (± 0.00)	0.44 (± 0.05)	0.05 (± 0.01)
Sunflower	0.09 (± 0.00)	0.56 (± 0.01)	0.04 (± 0.00)
EVO	0.14 (± 0.00)	0.72 (± 0.01)	0.05 (± 0.00)

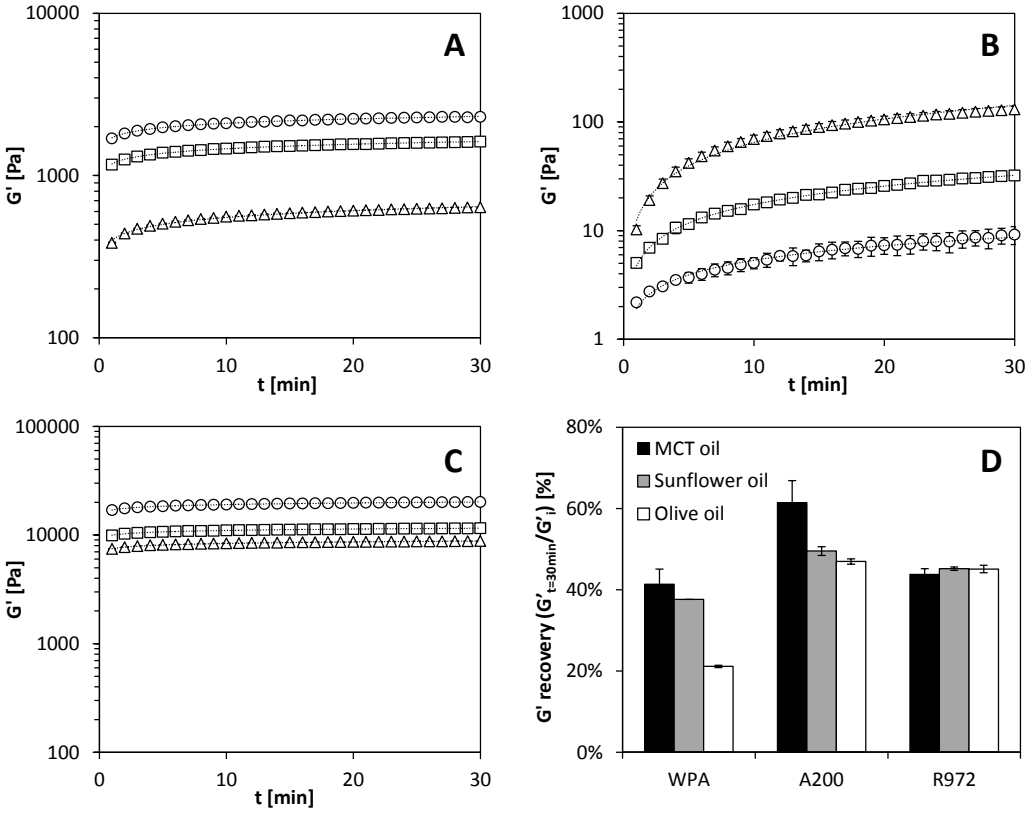

Figure 4.7. Structure recovery over time after deformation at 100% strain for oleogels prepared with (A) 10% whey protein aggregates (WPA), (B) 10% hydrophobic R972 silica, (C) 10% hydrophilic A200 silica. Used oils: MCT oil (○), sunflower oil (□) and olive oil (△). The solid lines represent the best fit to $G' \sim t^n$. Fig D summarizes the obtained values for G' recovery after 30 minutes as %.

The recovery of G' was followed for 30 minutes and the results can be found in Figure 4.7A-C. As shown, the development of G' over time showed a power law dependence over time for all samples following $G' \sim t^n$. In all samples, it was found that n < 1 (Table 4.2), which indicates a self-delaying process where the rate of change, dG'/dt, decreases over time. This power law dependency was also observed for other systems, such as clay dispersions [37] and fat crystals [38]. Important to note is that during recovery, gels were re-formed for which G' > G" in all samples.

Figure 4.7A shows a rapid structure recovery for the protein aggregates, where most of the recovery occurred in the first minute after reduction of the strain amplitude. In literature, a rapid structure recovery was also observed for silica particles and nano-diamond particles in mineral oil [39, 40] or fat crystal networks [38]. Similar to the case of protein aggregates, the structure recovery of the A200 silica network was fast (Figure 4.7C) and can be described by a power law exponent n close to zero (Table 4.2). Therefore, most of the disrupted network, as a result of detachment of the particles or clusters of particles from the network by applying high strains,

almost instantaneously reformed by creating new junctions. For the hydrophobic R972 silica particles, however, the network recovery was slower (Figure 4.7B) compared to that of the hydrophilic A200 silica or protein aggregates. These results can most likely be related to the affinity of the particles for the solvent. In the case of the hydrophilic silica particles and the protein aggregates, the low affinity for the solvent leads to particle-particle interactions that dominate over particle-solvent interactions in oil. The strong particle-particle interactions gave rise to a rapid G' recovery for both A200 silica and protein aggregates upon lowering the strain.

Using a different oil type did not result in an observable difference for the structure recovery rate for A200 silica and for the protein oleogels. Since the recovery is almost instantaneous, it is likely that the differences could not be seen with the current experimental setup. In contrast, the characteristics of the different oils did have an effect on the recovery rate for gels made with R972 silica. In these gels, the recovery rate over time (dG'/dt) was lower for apolar MCT oil than for the polar EVO. This effect is most likely related to more favourable particle-particle interactions in the polar EVO, compared to more particle-solvent interactions in the apolar MCT oil.

Figure 4.7D shows the amount of G' recovery for different oil types after 30 minutes, which was defined as the G' after 30 minutes recovery time divided over the initial gel strength (G'_i) before large deformation. The network of protein aggregates recovered towards 20 – 40% of their original G' after 30 minutes, depending on the oil type used. Largest recovery was measured for MCT oil, followed by sunflower oil and EVO. Similar behaviour was measured for A200 silica, where the same effect of oil type on the extend of structure recovery was measured, although the recovery was higher (50 – 60%). This effect of oil type is consistent with the larger amount of particle-particle interactions observed for a more apolar oil and more hydrophilic particles. The network of the hydrophobic silica particles recovered to about 45% of their original value for G', but their recovery did not depend on oil type within the timeframe of the experiment. The lower G' recovery for the protein aggregates compared to the two types of silica particles may be explained by the denser network structure of the protein aggregates. Upon deformation of such a dense network with larger clusters and a relative large mesh size, less bonds are re-formed between the proteins aggregates compared to the finer network of silica particles. This could be due to the larger surface area of the silica particles and subsequently more contact points between the particles. However, given that protein oleogels are able to flow under large deformation, but regenerate its elastic network quickly after deformation is reduced, this behaviour could provide benefits to a variety of food applications.

Conclusions

Whey protein based oleogels (10% protein) were prepared using heat-set whey protein aggregates. Since the particle-particle interactions between the aggregates in oil can be affected by oil composition, we prepared protein oleogels in different oil types; MCT oil, sunflower oil, extra virgin olive oil (EVO) and castor oil. The oils varied in polarity and chemical composition. For comparison, we used two types of silica particles of known surface chemistry, i.e. hydrophilic and hydrophobic silica, to prepare silica oleogels at the same concentration. All particles were able to provide structure to MCT, sunflower and EVO, where G' > G''. The change in oil type resulted in a difference in particle-particle and particle-solvent interactions, which in turn affected the rheological behaviour. For protein aggregates, an increase in oil polarity resulted in a decrease in G' due to more favourable particle-solvent interactions. In castor oil, we were unable to create gels with either silica particles or protein aggregates. This effect can be attributed to the ability of the oil to form hydrogen bonds with the particles, preventing particle-particle interactions. Large deformation behaviour of protein oleogels showed structure breakdown and yielding behaviour of the gels followed by rapid recovery of the network after deformation was reduced. Rapid recovery after deformation and the fact that the interactions between the protein aggregates in oil can be tuned by changing the characteristics of the oil, may be interesting features for various applications in foods.

References

1. Banerjee, S. and S. Bhattacharya, *Food gels: gelling process and new applications.* Crit Rev Food Sci Nutr, 2012. **52**(4): p. 334-346.
2. Marangoni, A.G., et al., *Structure and functionality of edible fats.* Soft Matter, 2012. **8**(5): p. 1275-1300.
3. Mensink, R.P. and M.B. Katan, *Effect of dietary trans fatty acids on high-density and low-density lipoprotein cholesterol levels in healthy subjects.* New England Journal of Medicine, 1990. **323**(7): p. 439-445.
4. Mensink, R.P., et al., *The Increasing Use of Interesterified Lipids in the Food Supply and Their Effects on Health Parameters.* Adv Nutr, 2016. **7**(4): p. 719-729.
5. Hu, F.B. and W.C. Willett, *Optimal diets for prevention of coronary heart disease.* Journal of the American Medical Association, 2002. **288**(20): p. 2569-2578.
6. Mensink, R.P., et al., *Effects of dietary fatty acids and carbohydrates on the ratio of serum total to HDL cholesterol and on serum lipids and apolipoproteins: A meta-analysis of 60 controlled trials.* American Journal of Clinical Nutrition, 2003. **77**(5): p. 1146-1155.
7. Akoh, C.C., *Fat replacers.* Food Technology, 1998. **52**(3): p. 47-53.
8. Sudha, M.L., et al., *Fat replacement in soft dough biscuits: Its implications on dough rheology and biscuit quality.* Journal of Food Engineering, 2007. **80**(3): p. 922-930.
9. Marangoni, A., *Organogels: An Alternative Edible Oil-Structuring Method.* Journal of the American Oil Chemists' Society, 2012. **89**(5): p. 749-780.
10. Patel, A.R. and K. Dewettinck, *Edible oil structuring: an overview and recent updates.* Food & Function, 2016. **7**(1): p. 20-29.
11. Rogers, M.A., *Novel structuring strategies for unsaturated fats – Meeting the zero-trans, zero-saturated fat challenge: A review.* Food Research International, 2009. **42**(7): p. 747-753.
12. Rogers, M.A., A.J. Wright, and A.G. Marangoni, *Oil organogels: the fat of the future?* Soft Matter, 2009. **5**(8): p. 1594-1596.
13. Blake, A.I., E.D. Co, and A.G. Marangoni, *Structure and physical properties of plant wax crystal networks and their relationship to oil binding capacity.* JAOCS, Journal of the American Oil Chemists' Society, 2014. **91**(6): p. 885-903.
14. Nikiforidis, C.V. and E. Scholten, *Self-assemblies of lecithin and α-tocopherol as gelators of lipid material.* RSC Advances, 2014. **4**(5): p. 2466-2473.
15. Pernetti, M., et al., *Structuring edible oil with lecithin and sorbitan tri-stearate.* Food Hydrocolloids, 2007. **21**(5-6): p. 855-861.
16. Bot, A. and W.G.M. Agterof, *Structuring of edible oils by mixtures of γ-oryzanol with β-sitosterol or related phytosterols.* Journal of the American Oil Chemists' Society, 2006. **83**(6): p. 513-521.
17. Da Pieve, S., et al., *Shear Nanostructuring of Monoglyceride Organogels.* Food Biophysics, 2010. **5**(3): p. 211-217.

18. Davidovich-Pinhas, M., S. Barbut, and A.G. Marangoni, *The gelation of oil using ethyl cellulose.* Carbohydrate Polymers, 2015. **117**: p. 869-878.
19. Sawalha, H., et al., *The influence of the type of oil phase on the self-assembly process of γ-oryzanol + β-sitosterol tubules in organogel systems.* European Journal of Lipid Science and Technology, 2013. **115**(3): p. 295-300.
20. Calligaris, S., et al., *Effect of Oil Type on Formation, Structure and Thermal Properties of γ-oryzanol and β-sitosterol-Based Organogels.* Food Biophysics, 2013. **9**(1): p. 69-75.
21. Valoppi, F., et al., *Influence of oil type on formation, structure, thermal and physical properties of monoglyceride-based organogel.* European Journal of Lipid Science and Technology, 2016 [in press].
22. Martins, A.J., et al., *Beeswax organogels: Influence of gelator concentration and oil type in the gelation process.* Food Research International, 2016. **84**: p. 170-179.
23. Wright, A.J. and A.G. Marangoni, *Formation, structure, and rheological properties of ricinelaidic acid-vegetable oil organogels.* JAOCS, Journal of the American Oil Chemists' Society, 2006. **83**(6): p. 497-503.
24. Gravelle, A.J., et al., *Influence of solvent quality on the mechanical strength of ethylcellulose oleogels.* Carbohydr Polym, 2016. **135**: p. 169-179.
25. Ferch, H., *The use of hydrophobic AEROSIL in the coatings industry.* Technical Bulletin Pigments No. 18, 1993.
26. Schmitt, C., et al., *Influence of protein and mineral composition on the formation of whey protein heat-induced microgels.* Food Hydrocolloids, 2011. **25**(4): p. 558-567.
27. Schmitt, C., et al., *Internal structure and colloidal behaviour of covalent whey protein microgels obtained by heat treatment.* Soft Matter, 2010. **6**(19): p. 4876-4884.
28. Patel, A.R., et al., *Fumed silica-based organogels and 'aqueous-organic' bigels.* RSC Adv., 2015. **5**(13): p. 9703-9708.
29. Raghavan, S.R., et al., *Colloidal interactions between particles with tethered nonpolar chains dispersed in polar media: Direct correlation between dynamic rheology and interaction parameters.* Langmuir, 2000. **16**(3): p. 1066-1077.
30. Barer, R. and S. Tkaczyk, *Refractive Index of Concentrated Protein Solutions.* 1954. **173**(4409): p. 821-822.
31. Inglese, P., et al., *Factors Affecting Extra-Virgin Olive Oil Composition*, in *Horticultural Reviews*. 2011. **38**: p. 83-147.
32. Khan, S.A. and N.J. Zoeller, *Dynamic rheological behavior of flocculated fumed silica suspensions.* Journal of Rheology, 1993. **37**(6): p. 1225-1235.
33. Barbut, S., *Effects of calcium level on the structure of pre-heated whey protein isolate gels.* LWT - Food Science and Technology, 1995. **28**(6): p. 598-603.
34. Kawaguchi, M., M. Okuno, and T. Kato, *Rheological properties of carbon black suspensions in a silicone oil.* Langmuir, 2001. **17**(20): p. 6041-6044.

35. Derec, C., et al., *Aging and nonlinear rheology in suspensions of polyethylene oxide-protected silica particles.* Phys Rev E Stat Nonlin Soft Matter Phys, 2003. **67**(6 Pt 1): p. 061403/1-061403/9.
36. Hyun, K., et al., *A review of nonlinear oscillatory shear tests: Analysis and application of large amplitude oscillatory shear (LAOS).* Progress in Polymer Science, 2011. **36**(12): p. 1697-1753.
37. Willenbacher, N., *Unusual thixotropic properties of aqueous dispersions of Laponite RD.* Journal of Colloid and Interface Science, 1996. **182**(2): p. 501-510.
38. Macias-Rodriguez, B. and A.G. Marangoni, *Rheological characterization of triglyceride shortenings.* Rheologica Acta, 2016. **55**(9): p. 767-779.
39. Raghavan, S.R., *Shear-induced microstructural changes in flocculated suspensions of fumed silica.* Journal of Rheology, 1995. **39**(6): p. 1311-1325.
40. Burns, N.A., et al., *Nanodiamond gels in nonpolar media: Colloidal and rheological properties.* Journal of Rheology, 2014. **58**(5): p. 1599-1614.

Chapter 5

Tuning the rheological properties of protein-based oleogels by water addition and heat treatment

This chapter is based on: de Vries, A., Jansen, D., van der Linden, E., Scholten, E., *Tuning the rheological properties of protein-based oleogels by water addition and heat treatment.* [submitted]

Introduction

Rheological properties of colloidal gels are mainly determined by the inter-particle interactions and the size and volume fraction of the dispersed colloidal particles [1]. Inter-particle attraction can be controlled by various means, such as reducing the electrostatic repulsive barrier [2], changing hydrophobic interactions, and inducing bridging [3] or depletion flocculation [4]. The ability to control aggregation of such particles and the resulting rheological properties of the network structure is a challenge, but important for various applications such as paints, inks, personal care products, pharmaceuticals, or foodstuffs [5]. In non-polar solvents, interactions between colloidal particles are mainly governed by steric interactions and hydrogen bonding. As shown by Trappe and Weitz [6], the critical concentration or interaction energy for network formation by carbon black particles in mineral oil depends on both the volume fraction and the interaction between the particles, which was altered by surfactant concentration. Interactions between particles in non-polar solvents also depend on the nature of the solvent and the surface chemistry of the particles. In the case of hydrophilic silica particles, gelation is achieved when the solvent is incapable of forming hydrogen bonds with the hydroxyl groups on the surface of the silica particles. Here, inter-particle hydrogen bond formation is responsible for the formation of a space-spanning network with elastic properties [7].

Another effective method to tune the interactions between colloidal particles is by the addition of small amounts of a secondary solvent. When the secondary solvent is immiscible in the primary solvent, so-called capillary suspensions can be obtained. Addition of small quantities of a secondary solvent (usually < 1%) can transform fluid suspensions into elastic gels with a high yield stress [8-10]. This is a well-known effect in wet granular media, where the inter-particle strength is greatly enhanced by the addition of a wetting fluid [11]. The mechanism behind this phenomenon is the formation of a liquid 'bridge' between two particles governed by wetting phenomena. The strength of the resulting capillary interaction exceeds other attractive interactions like van der Waals interactions and provide a strong network. Interestingly, both wetting and non-wetting fluids can be used for this purpose and result in the formation of gels in the pendular or capillary state, respectively [8]. Also for food applications, this mechanism can provide an effective route to alter the viscosity of oil-based suspensions [12].

In Chapters 3 and 4 the formation of a protein network in liquid oil to form so-called 'oleogels' was described. Sub-micron colloidal protein aggregates were prepared in an aqueous environment and subsequently the water was substituted for a liquid oil by a solvent exchange procedure. Dispersed in the oil, protein aggregates were shown to be capable of forming an effective network

with solid-like properties. For applications in different fields, it is desired to control the rheological properties of these oleogels. In Chapter 4, it was shown that the interactions between the protein aggregates can be changed by altering the polarity of the oil type. In the current research, the aim is to investigate different routes to induce interactions between colloidal protein aggregates and investigate the effect on the gel formation. The interactions between the aggregates in liquid oil are changed by adding small amounts of water and/or applying a heat treatment.

Materials and methods

Materials

Whey protein isolate (WPI, BiPro) was obtained from Davisco Foods International (Le Sueur, MN, USA). The protein concentration was 93.2% (N x 6.38) and was used as received. *N*-Ethylmaleimide (NEM) was purchased from Sigma-Aldrich (Steinheim, Germany). Acetone was supplied by Actu-All Chemicals (Oss, the Netherlands). Refined sunflower oil (Vandermoortele NV, Breda, the Netherlands) was bought at a local supermarket and was used without further purification. Demineralized water was used throughout the experiments.

Methods

Preparation of WPI aggregates

WPI aggregates were prepared by heat-induced aggregation as described in Chapter 3. Briefly, a protein stock solution was prepared by adding WPI powder (4% w/w) in demineralized water under continuous stirring, followed by adjusting the pH of this stock solution to 5.7 using a 1 M HCl solution. The resulting solution was heated in 50 mL plastic tubes at 85 °C for 15 minutes using a temperature-controlled water bath. After cooling, the resulting WPI aggregate dispersion was homogenized by using a rotor stator homogenizer (Ultra Turrax, T25, IKA Werke, Germany) at 13000 rpm for 3 min. The protein aggregates were then collected as a pellet by centrifugation at 4000 g (Hermle Z383K, Hermle Labortechnik GmbH, Wehingen, Germany) for 20 min at 20 °C. After collection, the pellet was re-dispersed and centrifuged twice with demineralized water to remove remaining soluble protein material. The resulting protein aggregates had a surface averaged diameter ($d_{3,2}$) of 190 (± 25) nm.

Free thiol blocking

After preparing the protein aggregates, the free thiol groups were blocked using NEM. To this end, NEM was added at 0.5 or 5 mM to a 4% WPI aggregate suspension in water. After NEM addition, the sample was gently stirred using a magnetic stirrer for 30 min, to allow for sufficient time for the reaction to take place. After this, the sample was washed twice using water and used to produce protein oleogels.

Preparation of the protein oleogels using a solvent exchange

To prepare protein oleogels, the WPI aggregates were transferred to sunflower oil by using a solvent exchange procedure, which has been described in Chapter 3. In short, the aqueous pellet, containing the WPI aggregates, was re-dispersed in acetone, and homogenized. Afterwards, the sample was centrifuged and re-dispersed once more using acetone to assure water removal. The pellet was then re-dispersed and centrifuged twice in sunflower oil. After evaporation of the remaining acetone, the suspension was centrifuged at 4000 g for 20 min at 20 °C to increase the concentration of the protein aggregates and induce gel formation. To prepare protein oleogels at different protein concentration and water addition, the dense pellet was diluted to the desired protein concentration using sunflower oil. Demineralized water was slowly added while vigorously stirring the protein suspension using rotor-stator homogenization at 13500 rpm. After the water was added, mixing was continued for 180 s to assure the formation of a homogeneous sample. Next, the entrapped air bubbles were removed using a vacuum pump for 5 min.

Composition

Protein content: The protein concentration was determined by measuring the nitrogen content using Dumas (Dumas Flash EA 1112 Series, N Analyser, Thermo Scientific). After weighing, the samples were dried overnight in an oven at 60 °C before analysis. To calculate the protein content, a nitrogen conversion factor of N x 6.38 was used.

Water content: Water content in the oleogel was determined by dry matter determination. Aluminium cups (ø = 5 cm) were first heated to 105 °C in an oven (Venticell, BMT Medical Technology, Brno, Czech Republic) to remove any water contamination. Afterwards, approximately 1 g of oleogel sample was added to the cup, and its weight was recorded before and after drying for 4 h at 105 °C.

Confocal Laser Scanning Microscopy (CLSM)

The microstructure of the oleogels was analysed by confocal laser scanning microscopy (CLSM). For visualization of the proteins and the oil, 0.05% nile blue was added to the oil. Thereafter, the protein and water concentrations were adjusted and the sample was homogenized as described above. CLSM images were obtained at room temperature on a LEICA TCS SP5 Confocal Laser Scanning Microscope (Leica Microsystems GmbH, Mannheim, Germany). Digital image files were acquired in 1024 x 1024 pixel resolution. Using different wavelengths, the protein signal could be separated from the oil signal.

Rheology

The rheological properties of the protein oleogels were determined by oscillatory deformation using a stress-controlled rheometer (MCR 501, Anton Paar GmbH, Graz, Austria) equipped with a peltier temperature controller. A cone and plate setup with a 1° angle (CP50-1) was used in all the experiments. The gap during the experiments was set to 0.05 mm. After sample loading, the sample was left to equilibrate for 30 minutes at a strain (γ) of 0.01% and 1 Hz (which was within the linear viscoelastic regime) to obtain a constant value for the elastic modulus, G'. Amplitude sweeps (at 20 °C) were performed by increasing the strain amplitude from 0.001% to 100% at 1 Hz. Temperature sweeps were performed at small deformation (1 Hz and γ = 0.01%) by increasing the temperature from 20 °C to 85 °C at 3 °C / min. After keeping the temperature constant at 85 °C for 15 min, the temperature was decreased to 20 °C at a rate of 3 °C / min.

Results and discussion

Macroscopic observations

Protein aggregates were formed by heat treatment in an aqueous environment and then suspended in oil using a solvent exchange procedure. After the solvent exchange, dry matter determination showed that the amount of water left in the oil-based gel is 0.081 (± 0.001) g / g protein. Adding extra water to the suspension of protein aggregates in sunflower oil had a noticeable effect on the viscosity as well as the appearance of the suspensions. The appearance of the samples after addition of water at different concentrations can be seen in Figure 5.1. The flow behaviour of the tilted samples indicate an increase in viscosity when water was added. Besides an increase in viscosity, the samples turned form opaque to transparent when water was added at a ratio of 0.5 g water / g protein. Apparently, with increasing water content, a point is reached where the refractive index (RI) of the dispersed phase matches that of the continuous phase. Since RI match occurs at a constant water-protein ratio, it was assumed that the water changes the refractive index of the protein aggregates and not that of the oil. A similar effect of refractive index matching was observed by Rickard et al. [13] while dehydrating a droplet of an aqueous protein solution against a solution of decanol. As water slowly dissolves in the surrounding fluid, the protein concentration in the shrinking droplet increases. At some point during the dehydration process, the RI of the droplet exactly matches that of the solvent and thereby becomes invisible. In our case, the water is most likely able to migrate into the protein aggregates. It is known that the RI increment (dn) of an aqueous protein solution depends on the protein concentration as $dn/dc \sim 0.002$ [13, 14]. The protein concentration at the point where the sample turns optically transparent, is calculated to be 65% taking the refractive index of oil as 1.46. This is in good agreement with the measured protein concentration of 63% at the point of the RI match. Apparently, the assumption that the added water migrates into the protein aggregates seems justified.

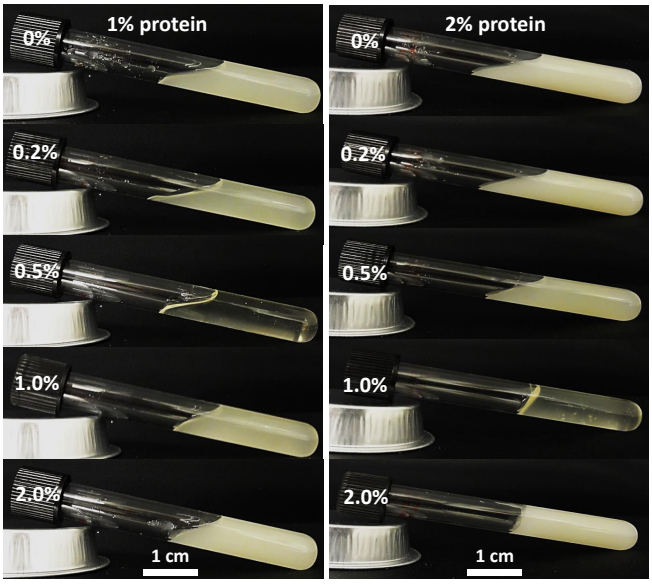

Figure 5.1. Appearance of protein aggregate suspensions in sunflower oil after addition of water (as indicated as weight% on the left hand side of the image).

Figure 5.2A shows the appearance of a 4% w/w WPI aggregate suspension in sunflower oil. In this case, insufficient attraction between the aggregates is present to allow for the formation of a self-supporting gel. When 0.5 g water / g protein was added, the suspension turned into a firm and transparent paste-like gel (Figure 5.2B). To determine the effect of water removal, the water was evaporated in an oven at 105 °C. After removal of the water by evaporation, the appearance of the gel returned turbid (Figure 5.2C). Interestingly, the gel-like structure of the sample remained. This indicates that water has a strong influence on the viscosity of the protein oleogels as a result of increased attractive interactions, but once removed, the increased interactions between the protein aggregates remained.

Figure 5.2. Appearance of a 4% protein aggregate dispersion in sunflower oil. A) before water addition, B) after 0.5 g water / g protein addition, C) after removal of the added water.

Microstructural observations

To determine the effect of water addition on the network formation at a smaller length scale, the samples were analysed using Confocal Laser Scanning Microscopy (CLSM). Figure 5.3 shows the CLSM micrographs of 2% protein aggregate suspensions in sunflower oil at increasing water concentration addition. In these images, the proteins are visualized in green, oil is coloured in red and water appears as black.

Without water addition, the protein aggregates are distributed evenly throughout the oil phase (Figure 5.3A). Addition of water induced clustering of the protein aggregates and larger structures can be observed (Figure 5.3B and C). The effect of clustering between the protein aggregates was seen up to an addition of 0.5 g water / g protein, the point of RI match. Adding more water led to the formation of free water droplets, as seen in Figure 5.3D-F by the dark spots. At concentrations higher than 0.5 g / g protein, the water is in excess, and water droplets are formed, resulting in a water-in-oil emulsion stabilized by the protein aggregates. At conditions of higher water addition (5, 10 and 25 g water / g protein), the protein aggregates are almost exclusively located at the water-oil interface (Figure 5.3E, F and G). However, no protein aggregates were found inside the enclosed water droplets. When adding 50 g water / g protein, phase inversion takes place, where the added water now forms the continuous phase, and the oil droplets are the dispersed phase (Figure 5.3H). Interestingly, spherical enclosures of water droplets inside the oil droplets can still be observed. Although a few aggregates are now found in the continuous water phase, the majority is still located either at the outer or inner water-oil interface and interestingly, no major oil leakage was observed in any of the samples. This remarkable behaviour shows that the protein aggregates are partially wetted by both phases and capable of stabilizing the oil-water interface, either as an oil-continuous or water-continuous emulsion.

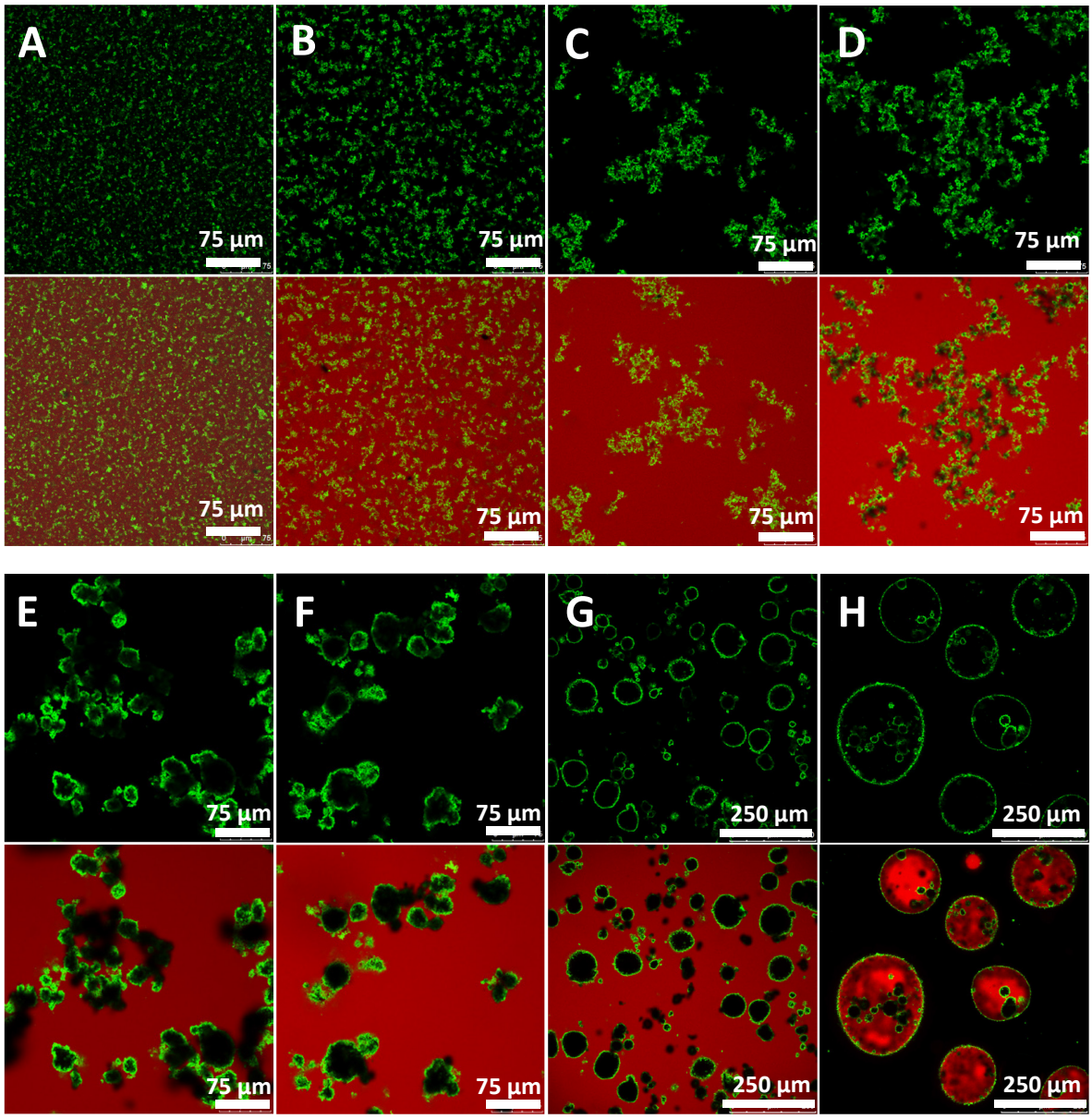

Figure 5.3. CLSM images of 2% whey protein aggregate in oil dispersions with water added in g / g protein: A: 0, B: 0.25, C: 0.50, D: 1.0, E: 5.0, F: 10, G: 25, H: 50. Samples were stained using Nile Blue, where the protein phase appears as green, oil as red and water as black. Upper pictures: protein channel only. Lower pictures: same picture with overlay of protein and oil channel.

Effect of water addition on G'

The effect of water addition on the storage modulus, G', for 2, 4, 6, and 8% protein oleogels is shown in Figure 5.4. As can be seen, at all protein concentrations, the presence of water led to an increase in G' up to a maximum in G' for an addition of 0.5 g water / g protein. At higher water additions, the excess water did not contribute anymore to an increase in G', but G' levels off to a constant value or slightly decreased. These results are consistent with the CLSM images shown in Figure 5.3. As shown for suspensions with 2% protein, free water droplets are observed as the

water addition exceeds 0.5 g / g protein. To check whether also for higher protein content an excess water can be seen, images for higher protein content were also prepared. In the same way, at 6% protein, free water is seen at water levels above 0.5 g / g protein, as visualized in Figure 5.5. Above this maximum hydration level, the formed water droplets did not contribute to a further increase in G' as the water is not incorporated into the protein network. To compare the G' of the different protein networks, the relative increase in gel strength, G'/G'_0 was compared, where G'_0 is the gel strength for gels without added water. The relative increase in G' is up to three orders of magnitude, and depends on the protein concentration as shown by the inset in Figure 5.4. At maximum hydration, the effect on G' was the largest for lower protein concentrations. In the case of 2% protein, G' increased three orders of magnitude, whereas for the highest protein concentration (8%), only an increase of two orders of magnitude can be seen.

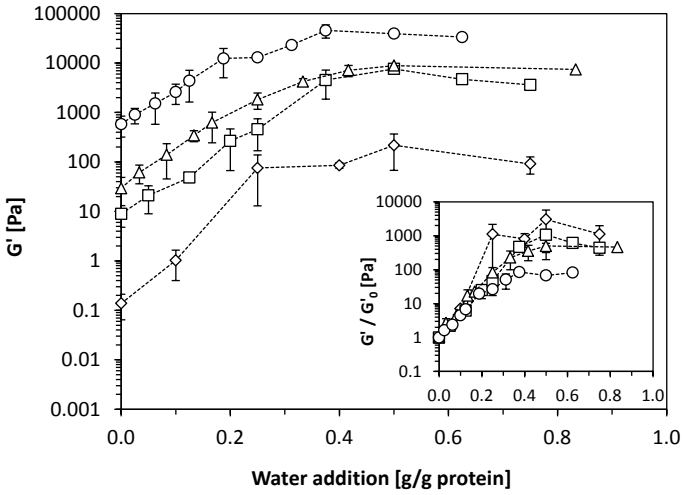

Figure 5.4. G' as a function of water addition for a 2% (◇), 4% protein (□), 6% (△) and 8% (○) protein aggregate suspension in oil. Inset shows the relative increase in G' as a function of water addition.

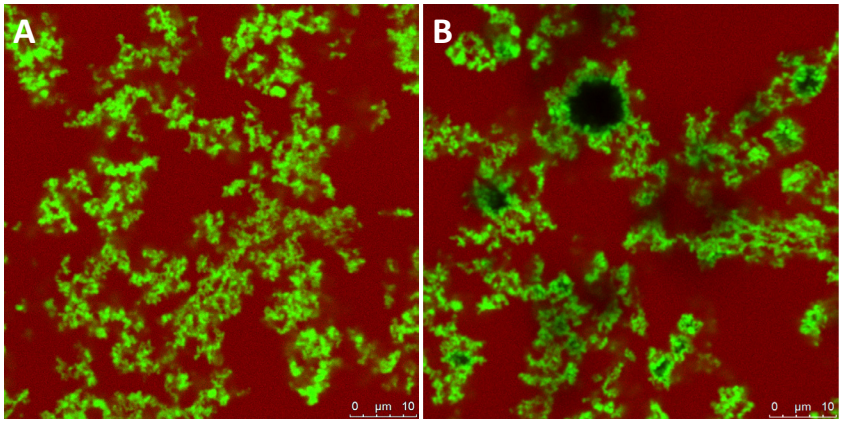

Figure 5.5. CLSM micrograph of a 6% protein oleogel with 0.5 g water / g protein addition (A) and 0.8 g water / g protein addition (B). Used stain is nile blue.

Large deformation rheology

Looking at the CLSM images, it is clear that the protein aggregates could absorb water up to 0.5 g / g protein, without the formation of free water droplets. As a result of the water addition, an increase in gel strength was observed and the hydrated protein aggregates were more densely clustered. Next, the effect of this clustering on large deformation properties for the regime of 0 – 0.5 g water / g protein was determined. The large deformation properties of the oleogels prepared at 4 and 8% protein content are shown in Figure 5.6. Here, G' is displayed for increasing strain amplitude (γ). At low strain, G' is independent on γ, until a critical strain is reached (γ_c) whereupon the material yields. For the oleogels prepared with 4% protein, adding water up to 0.5 g / g protein increased G' by almost 3 orders of magnitude. Besides the increase in G', also γ_c increased as a result of water addition, indicating an increased resistance against structure breakdown. Figure 5.6B and D show the shear stress as a function of the strain. Here, the yield stress can be seen as the point where the relation between the applied strain and the resulting stress deviates from linearity. For a 4% oleogel, the yield stress increased from ~ 0.1 Pa to ~ 500 Pa upon water addition. The same effects are seen at 8% protein, i.e. increase in G', γ_c, and yield stress, where the latter had increased from ~ 50 Pa to ~ 3000 Pa. Water addition therefore not only had an effect on the magnitude of G', but also a pronounced effect on structure breakdown properties.

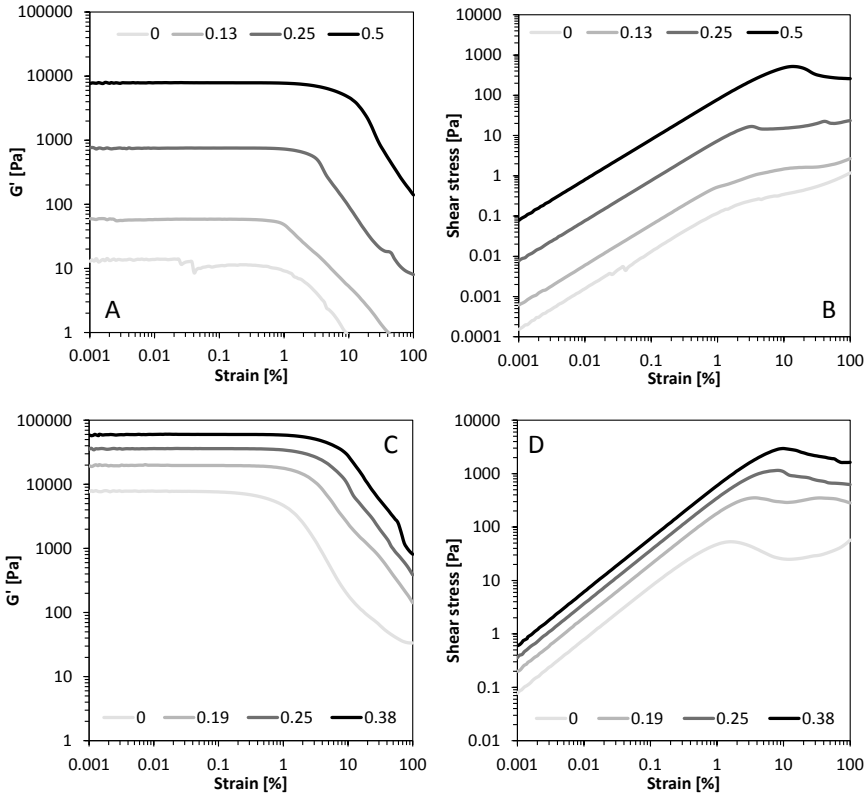

Figure 5.6. G' and shear stress as a function of strain amplitude for a 4% protein oleogels (A and B) and 8% protein oleogels (C and D). Legends shows the amount of water added in g water / g protein.

Effect of heat treatment

Besides the effect of adding water, applying a heat treatment had an effect on the resulting gel structure, as can be seen in Figure 5.7. When adding water, the viscosity and gel strength markedly increased. After heat treatment, a much firmer gel was obtained as shown by the insets in Figure 5.7. When heated in a cylindrical container, the gel retained its shape and formed a firm self-standing and transparent oleogel. As seen from the microstructure in Figure 5.7, the clustering increased as a result of the heat treatment, leading to more pronounced protein-protein interactions. Together with the clustering, slight syneresis was observed, indicating the protein network contracted to some extent, thereby expelling some of the oil.

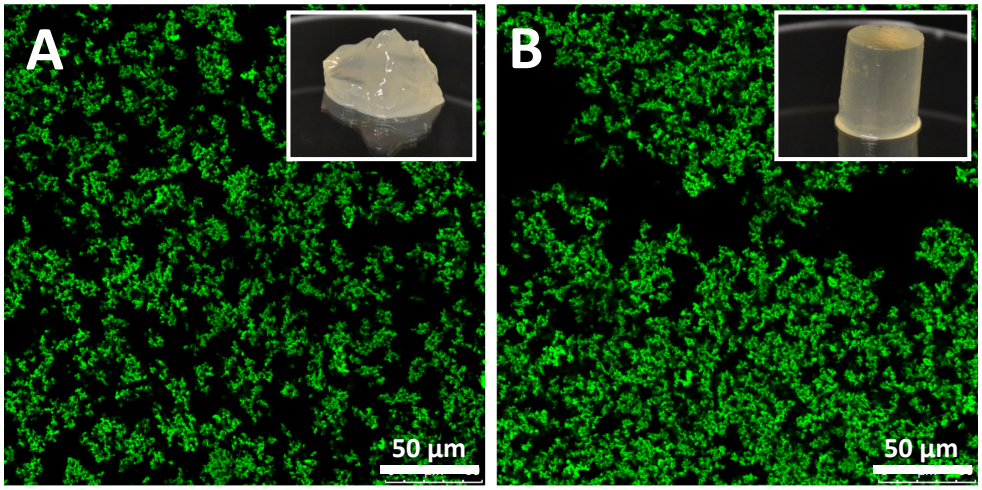

Figure 5.7. CLSM image of a 6% protein oleogel in sunflower oil with 0.5 g / g protein water addition before (A) and after (B) heat treatment at 85 °C. Insets show the appearance of the same sample.

To determine the effect of heat treatment on the resulting gel strength, heating was performed in-situ in the rheometer. Here, the temperature was increased to 85 °C and after a holding time of 15 minutes, the temperature was lowered again to 20 °C. A typical heating and cooling curve for a 5% protein oleogel is shown in Figure 5.8. As can be seen, without added water, G' (circles) did not change and tanδ (G"/G', squares) increased to some extent as a result of the heating and cooling cycle up to 85 °C, indicating that upon heating no additional attractive interaction between the protein aggregates was obtained. When water was added, however, G' (triangles) first decreased as a function of increasing temperature. During the holding phase at 85 °C, G' increased to some extent, and during cooling to 20 °C, G' had increased ~ 5 times compared to that before heating. Throughout the heating and cooling cycle, tanδ (diamonds) remained constant at values much smaller than 1, indicating the system remained a gel, i.e. during heating a network backbone remained.

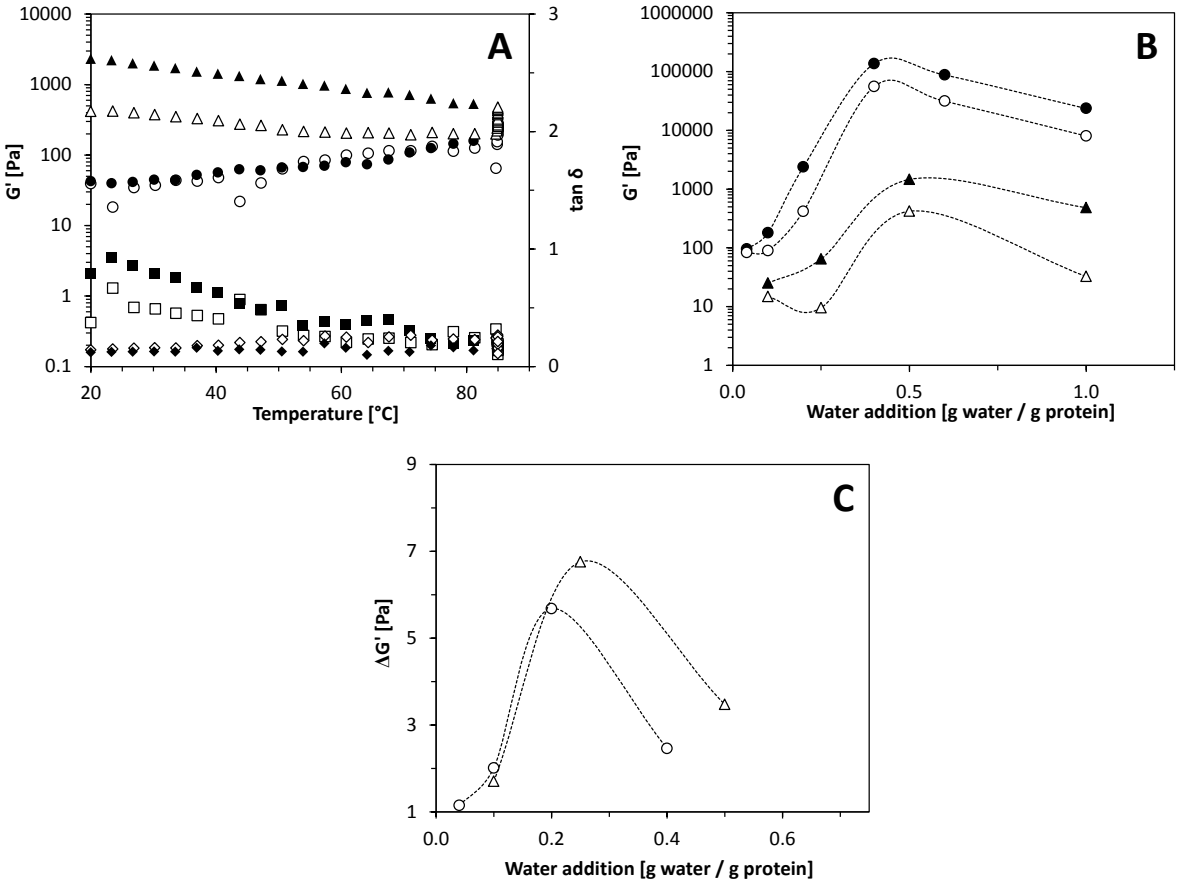

Figure 5.8. A) Development of G' and tan δ during a heating and cooling cycle of a 5% protein oleogel in sunflower oil without (G':○, tanδ:□) and with (G':△, tanδ: ◇) water addition (0.2 g water / g protein). Open symbols: heating cycle, filled symbols: cooling cycle. B) G' before (open symbols) and after (filled symbols) heat treatment for protein oleogels in sunflower oil at 2%(△) and 5%(○) as a function of water addition. C) Difference in G' before and after heat treatment for protein aggregate dispersions in sunflower oil at 2%(△) and 5%(○) as a function of water addition. Dotted lines in B and C were added to guide the eye.

Gel strength before and after heat treatment was determined and compared for oleogels of both 2 and 5% protein as a function of water addition. As can be seen in Figure 5.8B, G' increased for all samples as a result of heat treatment and the maximum G' remained at a hydration of 0.5 g water / g protein. Even when the water addition exceeded maximum hydration, the gel strength increased compared to that before the heat treatment. This increase in gel strength indicates that free water droplets did not lead to instability during heating. Figure 5.8C shows the increase in the gel strength, ΔG', as a function of water addition. As can be seen in the figure, ΔG' appears to have a maximum around 0.2 g water /g protein. Note that this is a water content lower than the maximum water content that can be incorporated in the network (0.5 g water / g protein). As is clear from the CLSM image (Figure 5.7), heat treatment resulted in a densification of the network, and as was discussed, during heat treatment, a network backbone remains. However, parts of the

network, in the form of protein aggregates and their clusters, is able to rearrange due to their higher mobility at higher temperature. Upon subsequent cooling, these parts attach again to the remaining backbone and this rearrangement leads to the densification of the protein network in such a way that the final backbone strength increases.

When performing the same temperature ramp again, G' follows the same path as during the cooling step of the first ramp. This suggests that during the second ramp, no additional rearrangements occur that further strengthen the backbone network. The initial decrease of G' upon increasing temperature during the second ramp must be due to the weakening of the backbone network. This implies that the strength of the interactions within the backbone decreases with increasing temperature. Reversely, the interactions in the backbone increases with decreasing temperature. In order to check if these interactions are of covalent nature, the role of disulphide interaction was investigated next.

The formation of disulphide bonds between protein aggregates was examined by blocking free thiol groups. *N*-ethylmaleimide (NEM) was added at 0.5 and 5 mM to the aqueous aggregate dispersion, similar to the conditions tested by Alting et al. [15]. During the heating and cooling cycle of the oleogels formed at 10% protein and 0.2 g water / g protein, no major differences in elastic response during heat treatment and cooling were observed by NEM addition, as all samples followed the same path as a function of the temperature as shown in Figure 5.9. These results indicate that disulphide bond formation is unlikely to be the main reason leading to the observed increase in G' as a result of heating in the presence of water.

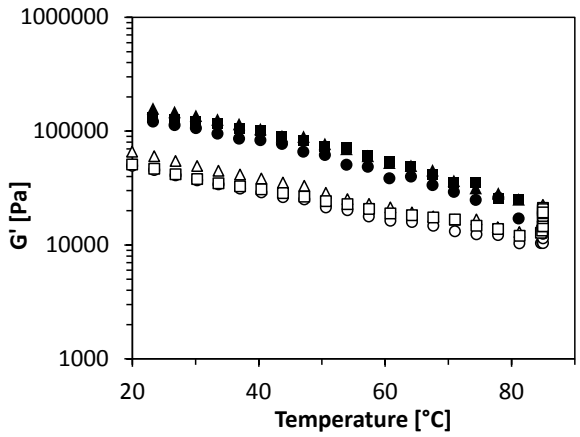

Figure 5.9. Heating and cooling profile of a 10% protein aggregate oleogel with added water at 0.2 g water / g protein for aggregates with unblocked (△) and blocked thiol groups at a NEM concentration of 0.5 (○) and 5 mM (□). Empty symbols: heating ramp, filled symbols: cooling ramp.

General discussion

Particle interactions

Although addition of water to a protein-based oleogel unambiguously had a large impact on the gel strength, yielding properties and response to temperature, the reason for the increased network formation is less obvious.

An explanation for the increased gel strength could be swelling of the protein aggregates as result of water addition. As is well-known, protein gels are capable of binding a large amount of water and swelling is common in whey protein gels when submerged in a good solvent [16]. Whey protein aggregates can show similar swelling behaviour. The degree of swelling is largely dependent on the type of network and the intra-molecular repulsive interactions within the aggregates [17]. As the protein aggregates are relatively dense particles (they were prepared close to the pI of the proteins), swelling is expected to be limited. Indeed, the water binding ability was quite low as the maximum amount of water that could be added without forming free water droplets was 0.5 g / g protein only. Theoretically, at these water concentrations, swelling of the protein aggregates could increase the volume of the aggregates up to 50%. Such an increase in volume fraction would not be sufficient for the formation of a space spanning network as the initial protein concentration was fairly low (< 8%). Moreover, as we observe an increase in G' already at concentrations much lower than 0.5 g water / g protein, swelling could contribute to network formation, but would most likely not be the major factor responsible for the observed rapid increase in G' and yield stress.

It is known that adding a secondary liquid to a particle suspension, immiscible in the primary fluid, can drastically increase the viscosity of the suspension, turning viscous liquids into gel-like pastes. Small amounts (usually < 1%) of such a second liquid leads to the formation of liquid bridges between the particles, creating a large cohesive force, i.e. capillary force, between the particles leading to the formation of a space spanning network [8]. In our suspensions, such capillary forces would arise from water bridges between the protein aggregates when suspended in oil. The ability to form capillary bridges has been shown to depend on the water activity (a_w) of the system. Cavalier et al. described the rheological behaviour of dispersions of calcium carbonate in dioctylphthalate at different a_w levels [18]. Already at an a_w around ~ 0.2, a significant increase in G' and yield stress was observed. In their samples, however, the water activity was argued to be too low to account for capillary bridge formation. For a capillary bridge to form, the minimal required water activity was found to be ~ 0.7 [19, 20]. Instead, the authors attributed the increase

in G' to increased attractive interactions between the particles due to inter-particle hydrogen bonding as a result of the presence of water molecules. In our suspensions, even at the lowest water addition, typical values for a_w are larger than 0.7 (data not shown), which in principle would allow for the formation of a liquid bridge between the particles.

The capillary force (F_c) between two particles upon contact depends on the interfacial tension of the added liquid with the bulk liquid (γ), particle radius (R), and the wetting angle between the secondary solvent with the particle (θ) via $F_c = 2\pi R\gamma \cos\theta$ [8]. Typically, this type of interaction is investigated in suspensions of solid particles such as glass beads or calcium carbonate particles that are impermeable for the added liquid [8]. In this case, all water available is used to create a water 'bridge' between particles, which leads to strong capillary interactions. In recent work, Bossler and Koos showed that when particles in suspension are porous and capable of absorbing the added liquid (i.e. when the wetting angle between the secondary solvent and the particle $\lesssim$ 90°), the liquid is not entirely available for capillary bridge formation [21]. Instead, water is located inside the pores of the particles, and as a result, the increase in gel strength was much lower [21]. In the suspensions used in the current study, confirmed by the change in refractive index as water was added, uptake of water by the protein aggregates is very likely. In this case, the added water would be available for capillary bridge formation between the protein aggregates to a lower extent. However, as pointed out by Bossler and Koos, even when the wetting angle is low and the particle is porous, not all liquid migrates into the particles, but a small amount of liquid remains at the surface of the particle. Upon contact with a second particle, this small amount of liquid is capable of forming small bridges between the particles, even though bridge formation is much lower than for liquids with higher contact angles. The small degree of bridge formation still led to an increase in gel strength. Similarly, in our case, the added water might be partially located at the surface of the aggregates, leading to the formation of liquid bridges between particles upon contact. In turn, this leads to an increase in G'. The measured relative increase in G' in our case, however, is much larger than observed in the work of Bossler and Koos using porous particles. One explanation for this difference is the amount of secondary solvent added, which for their suspensions was only 0.09 g / g particles. In our suspensions this ratio is much higher (up to 5 times), which makes the formation of capillary bridges more likely. Moreover, as the strength of the gel relates to the particle size as ~ R^{-1}, the smaller particle radius in the current study leads to stronger gels than the ones reported in the work of Bossler and Koos. Both the larger amount of added secondary solvent and the smaller particle size could therefore be the reason for the observed large increase in G' for our gels. Likewise, formation of capillary bridges can explain the observed change in the elastic response to temperature. The inter-particle strength of capillary

suspensions is determined by the interfacial tension. For an increase in temperature, the interfacial tension decreases, and weakens the strength of the capillary force between two particles [9]. This results in a decrease in G', which is observed in Figure 5.8A. As the capillary bridge only weakens, the gel network remains and does not lead to a complete gel-sol transition. Reversely, upon lowering the temperature, the interfacial tension increases again leading to the observed increase in gel strength.

If capillary action would play a role, a thin film should be visible between particles. In trying to visualize a thin liquid film between the particles, we examined the CLSM images of a 6% protein oleogel at different water additions more closely. As can be seen in Figure 5.10 from the oil channel (left images), dark spots, indicative of water, appear at the same location in the sample where also protein is observed. Furthermore, these black spots seem to increase with increasing water addition (lower row). However, as can be seen from the overlay images, it is impossible to determine whether the added water resides between the particles or whether this water is located inside the protein aggregates, due to the limitations in the resolution of the CLSM. Although highly probable, we therefore cannot conclude with certainty that capillary bridges are formed as a result of water addition. When capillary bridges would not be present, the increase in G' would be merely a result of hydrogen bond formation between the particles, induced by the presence of water.

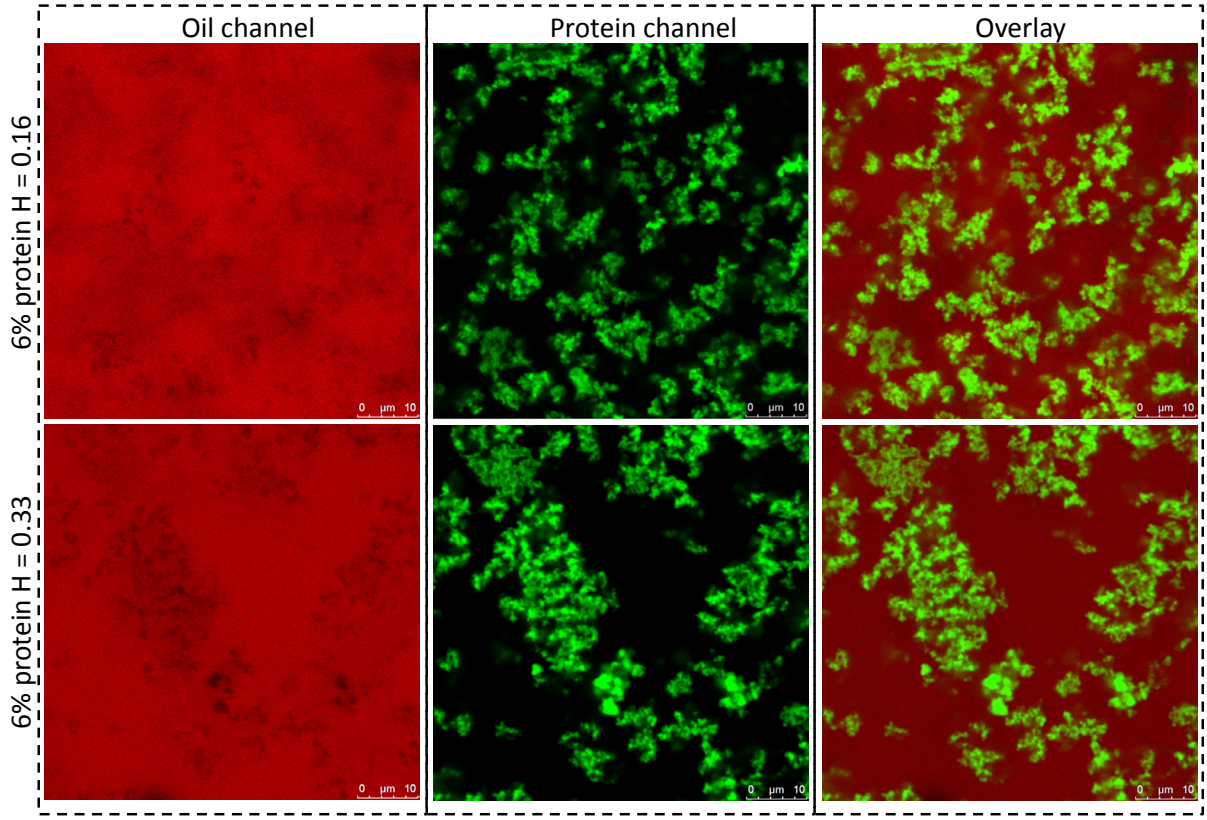

Figure 5.10. CLSM images of 6% protein oleogels at different hydration level (H). Upper row: 0.16 g water / g protein, lower row: 0.33 g water / g protein. Left images are the oil channel, middle images the protein channel and images on the right are the overlay images of both channels. Used stain is nile blue.

Network formation

Considering larger length scales, we investigated the G' dependency on water concentration in more detail. As can be seen in Figure 5.11A, the dependency of G' vs protein concentration (c_p) follows a power-law relation both at high (0.5) and low (0.1) water content addition as $G' \sim c_p^n$. Increasing the hydration level lowered the exponent n from 5.6 to 3.6. This suggests a change in the network structure, as was already observed in the micrographs. Such a change in the exponent was also observed in suspensions of spherical silica particles [22]. In that work, the addition of a secondary solvent induced the formation of strong capillary bridges. This increased the interactions between the silica particles leading to "compact capillary aggregates (primary aggregation) followed by their percolation (secondary aggregation)", leading to a decrease in the exponent. A similar effect was seen in our case, where compact aggregates were formed upon increasing water content (Figure 5.3A-C). According to these results, our system resembles characteristics typically observed in capillary suspensions.

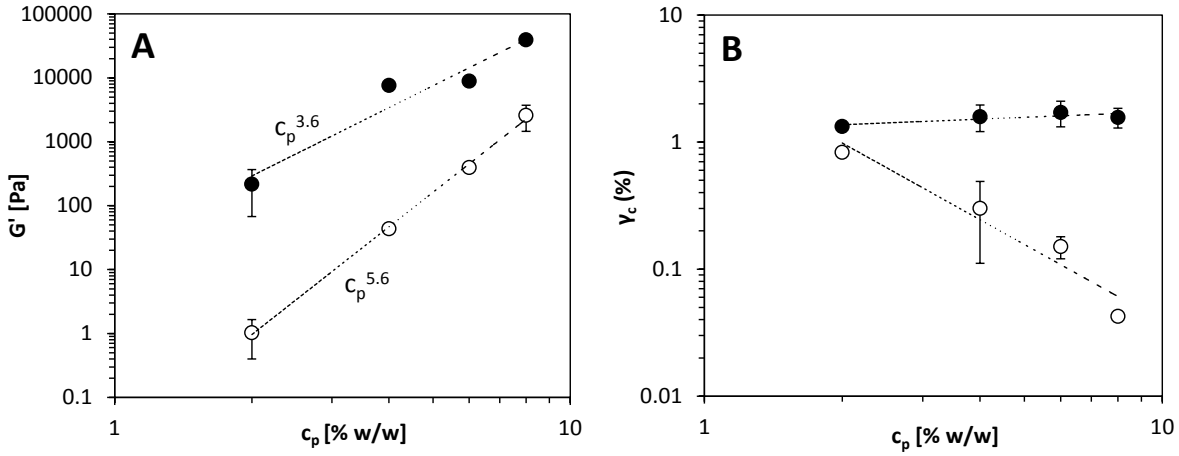

Figure 5.11. A) G' versus protein concentration, B) critical strain versus protein concentration. Open symbols: 0.1 g water / g protein, filled symbols: 0.5 g water / g protein.

Following the power law dependency of G' versus c_p, we can consider our systems as fractal networks [23]. To gain more insight in the network structure, we determined the critical strain (γ_c) and plotted this versus the protein concentration (Figure 5.11B). For low water addition (open symbols), a negative relation is observed as c_p increased. However, a slight increase in γ_c as a function of c_p is measured for high water addition. Within the theoretical framework of fractal gels as laid out by Shih et al. [24], our gels at low amounts of water addition are best described using the strong-link regime, as discussed in Chapter 3. At high water addition, the interactions within the clusters of the network increase, and the gels are then best described using the weak-link regime. Our results mentioned above are very similar to those found for β-lactoglobulin gels, where the interactions between the proteins were altered by the presence of calcium [25]. In this case, the gels without calcium were fine-stranded and followed a power law relation according to $G' \sim c_p^{5.0}$, accompanied by a similar decreasing γ_c for higher protein concentration. In the case of added calcium, the exponent decreased to 3.2 and γ_c increased slightly for increasing protein concentration. The addition of calcium led to an increase in the interactions between the proteins, leading to a different aggregation mechanism. The increased interactions led to the formation of more dense flocs, which was accompanied by an increase in the fractal dimension of the resulting gel network. Such a change in fractal dimension is also observed in our current case. Whether capillary bridges or only hydrogen bonds are responsible for the increased interactions between the protein aggregates, it is clear that attractive interactions between protein aggregates increase upon water addition, leading to smaller and more dense fractal flocs.

In summary, the formed network between the protein aggregates in oil strengthens after water addition and/or applying a heat treatment. Additionally, the network structure remains intact after

subsequent removal of the water. As seen in Figure 5.12B, the appearance of the gel after addition of 0.5 g water / g protein resulted in a transparent paste-like gel and an increase in gel strength due to the formation of additional interactions between the aggregates (as schematically depicted in the lower figures in Figure 5.12). These interactions are most likely due to the formation of capillary bridges between the protein aggregates. Subsequent heat treatment increases the amount of particle-particle interactions further to result in the formation of an even stronger, still transparent, gel. After water removal, the gel structure remains intact and turned back to opaque. This indicates that the interactions and the resulting network remained once the water had been removed. In capillary suspensions, the contact angle between the secondary solvent and the particle has been shown to effect the change in the network upon removal of the secondary solvent. In the case of a high contact angle with the particle (capillary state suspension), removal of the water leads to a weakening of the network and a decrease of the yield stress back to the original values [9]. In our case, the proteins have a high affinity for the water, which gives rise to a low contact angle (pendular state suspension). Therefore, upon water removal, the aggregates are drawn to one another due to strong capillary forces. Upon evaporation of the water, the particles are able to approach each other at short distances and can be captured in a rather deep potential energy well of attractive nature due to short-ranged van der Waals interactions.

The results show that upon addition of water and subsequent heat treatment or water removal, the interactions between the protein aggregates can effectively be tuned and this forms an interesting route to modify rheological behaviour of protein oleogels.

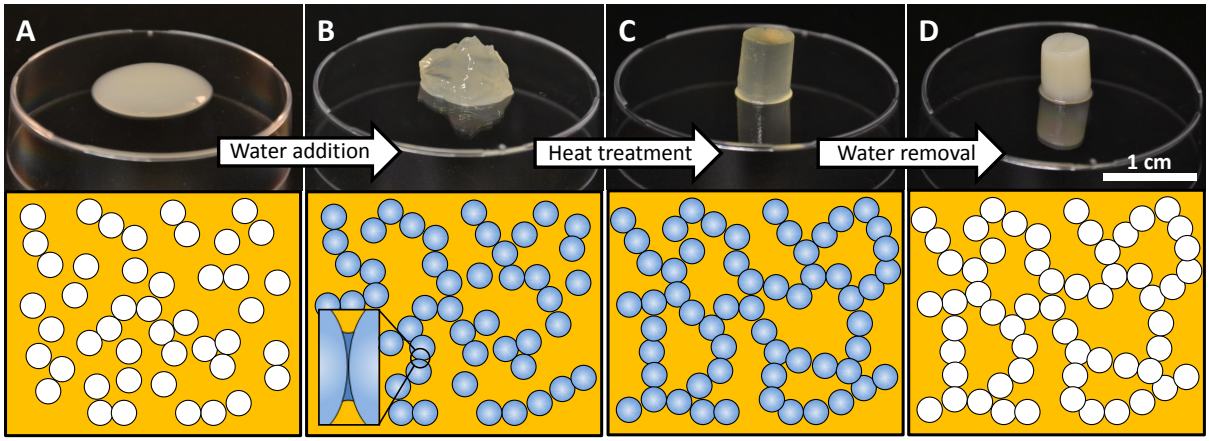

Figure 5.12. Appearances of a 6% protein oleogel after different treatments. A) before water addition, B) after adding 0.5 g water / g protein, C) after heat treatment, C) after removal of the water. Underneath the images, a schematic representation is given for the changes in the protein network.

Conclusions

In this chapter, we investigated the effect of water addition and heat treatment on the network formation of protein aggregates in oil. Addition of small amounts of water resulted in an increase in protein-protein interactions in the formation of protein oleogels. Upon water addition, WPI aggregates rehydrate, and cluster together most likely due to the formation of small films of water between the protein aggregates, providing increased hydrogen bonds or capillary interactions. This increased clustering, resulting from increased protein-protein interactions, dramatically increased gel strength. This increase continued up to a point where the added water forms free droplets, defined as the maximum water binding ability. In the presence of water, heat treatment increased protein-protein interactions even further, resulting in more firm gels by incorporating more protein aggregates in the backbone of the network structure. Even though the water was required to initially increase the gel strength, the formed structure remained intact once the water was removed. This intriguing approach of tuning the interactions by simple methods as adding small fractions of water and heat treatment, provides ample opportunities to alter the network properties, heat resistance, and yielding behaviour. This provides a mechanism for tailor-made design of protein oleogels for different applications.

References

1. Prasad, V., et al., *Rideal Lecture: Universal features of the fluid to solid transition for attractive colloidal particles.* Faraday Discussions, 2003. **123**: p. 1-12.
2. Lin, M.Y., et al., *Universality in colloid aggregation.* Nature, 1989. **339**(6223): p. 360-362.
3. Dickinson, E. and L. Eriksson, *Particle flocculation by adsorbing polymers.* Advances in Colloid and Interface Science, 1991. **34**(C): p. 1-29.
4. Poon, W.C.K., A.D. Pirie, and P.N. Pusey, *Gelation in colloid-polymer mixtures.* Faraday Discussions, 1995. **101**: p. 65-76.
5. Joshi, Y.M., *Dynamics of colloidal glasses and gels.* Annual Review of Chemical and Biomolecular Engineering, 2014. **5**: p. 181-202.
6. Trappe, V. and D.A. Weitz, *Scaling of the Viscoelasticity of Weakly Attractive Particles.* Physical Review Letters, 2000. **85**(2): p. 449-452.
7. Raghavan, S.R., H.J. Walls, and S.A. Khan, *Rheology of silica dispersions in organic liquids: New evidence for solvation forces dictated by hydrogen bonding.* Langmuir, 2000. **16**(21): p. 7920-7930.
8. Koos, E. and N. Willenbacher, *Capillary forces in suspension rheology.* Science, 2011. **331**(6019): p. 897-900.
9. Koos, E., et al., *Tuning suspension rheology using capillary forces.* Soft Matter, 2012. **8**(24): p. 6620-6628.
10. Van Kao, S., L.E. Nielsen, and C.T. Hill, *Rheology of concentrated suspensions of spheres. II. Suspensions agglomerated by an immiscible second liquid.* Journal of Colloid and Interface Science, 1975. **53**(3): p. 367-373.
11. Strauch, S. and S. Herminghaus, *Wet granular matter: a truly complex fluid.* Soft Matter, 2012. **8**(32): p. 8271.
12. Hoffmann, S., E. Koos, and N. Willenbacher, *Using capillary bridges to tune stability and flow behavior of food suspensions.* Food Hydrocolloids, 2014. **40**: p. 44-52.
13. Rickard, D.L., P.B. Duncan, and D. Needham, *Hydration potential of lysozyme: protein dehydration using a single microparticle technique.* Biophys J, 2010. **98**(6): p. 1075-1084.
14. Barer, R. and S. Tkaczyk, *Refractive Index of Concentrated Protein Solutions.* 1954. **173**(4409): p. 821-822.
15. Alting, A.C., et al., *Cold-set globular protein gels: Interactions, structure and rheology as a function of protein concentration.* Journal of Agricultural and Food Chemistry, 2003. **51**(10): p. 3150-3156.
16. Betz, M., et al., *Swelling behaviour, charge and mesh size of thermal protein hydrogels as influenced by pH during gelation.* Soft Matter, 2012. **8**(8): p. 2477-2485.
17. Schmitt, C., et al., *Internal structure and colloidal behaviour of covalent whey protein microgels obtained by heat treatment.* Soft Matter, 2010. **6**(19): p. 4876-4884.
18. Cavalier, K. and F. Larché, *Effects of water on the rheological properties of calcite suspensions in dioctylphthalate.* Colloids and Surfaces A: Physicochemical and Engineering Aspects, 2002. **197**(1-3): p. 173-181.

19. Christenson, H.K., *Adhesion between surfaces in undersaturated vapors-a reexamination of the influence of meniscus curvature and surface forces.* Journal of Colloid And Interface Science, 1988. **121**(1): p. 170-178.
20. Claesson, P.M., et al., *Interactions between hydrophilic mica surfaces in triolein: Triolein surface orientation, solvation forces, and capillary condensation.* Langmuir, 1997. **13**(6): p. 1682-1688.
21. Bossler, F. and E. Koos, *Structure of Particle Networks in Capillary Suspensions with Wetting and Nonwetting Fluids.* Langmuir, 2016. **32**(6): p. 1489-1501.
22. Domenech, T. and S.S. Velankar, *On the rheology of pendular gels and morphological developments in paste-like ternary systems based on capillary attraction.* Soft Matter, 2015. **11**(8): p. 1500-1516.
23. de Vries, A., et al., *Protein oleogels from heat-set whey protein aggregates.* Journal of Colloid and Interface Science, 2017. **486**: p. 75-83.
24. Shih, W.H., et al., *Scaling behavior of the elastic properties of colloidal gels.* Physical Review A, 1990. **42**(8): p. 4772-4779.
25. Hagiwara, T., H. Kumagai, and T. Matsunaga, *Fractal Analysis of the Elasticity of BSA and β-Lactoglobulin Gels.* Journal of Agricultural and Food Chemistry, 1997. **45**(10): p. 3807-3812.

Chapter 6

Controlling agglomeration of protein aggregates for structure formation in liquid oil: a sticky business

This chapter is based on: de Vries, A., Lopez Gomez, Y., Jansen, B., van der Linden, E., Scholten, E., *Controlling agglomeration of protein aggregates for structure formation in liquid oil: a sticky business.* [submitted]

Introduction

It has long been recognized that a diet rich in saturated and *trans* fats is associated with an increase in the amount of LDL cholesterol (Low Density Lipoprotein) at an expense of HDL cholesterol (High Density Lipoprotein) [1], which is related to a higher risk of developing coronary artery disease. On the other hand, a diet rich in *cis*-unsaturated fatty acids decreases these risks [2, 3]. However, food reformulation is not straightforward as the use of saturated and *trans* fats has technological benefits such as providing texture and oxidative stability to food products. One interesting alternative, which has gained much attention over the recent years, is the use of so-called 'oleogels' [4-7]. The purpose of designing edible oleogels is to be able to provide a solid-like structure to liquid oil at room temperature other than by the conventional use of saturated and *trans* fatty acids.

The most common gelling agents of organic liquids, called in a general term 'organogelators', are found within the class of low molecular weight organogelators (LMOGs). Their network formation relies on the complex self-assembly of the components by noncovalent bonds such as dipolar interactions, π-stacking, and intermolecular hydrogen bonds into crystals, tubules or fibrillar structures responsible for the solid-like behaviour [8-10]. These organogels have been studied for different applications, such as oil spills [11, 12], electronics [13], and drug delivery [14-16]. For food purposes, many different edible oil soluble LMOGs have been studied for their gelling properties, such as lecithins [17, 18], monoacylglycerides [19, 20], fatty acids or alcohols [21], sterols [22, 23], or waxes [24-26].

In contrast to the large diversity of low molecular weight compounds, only a limited amount of biopolymers have been studied to structure oil. Due to their predominant hydrophilic nature, these compounds usually do not dissolve in oil. A well-studied exception is the cellulose derivative ethyl cellulose (EC) [27]. EC dissolves in liquid oil at high temperature and upon cooling, the polymer chains interact to form solid structures. The resulting mechanical properties of the gels, depending on polymer-polymer interactions, can be tailored by changing the molecular weight of the polymer chain or by adding surfactants [27, 28]. Another example of a biopolymer studied for its oil structuring ability is the polysaccharide chitin. Modifying crude chitin into "nanocrystals" [29] or hydrophobic "whiskers" [30] was necessary to efficiently provide a structure to liquid oil. To overcome the problem of low dispersibility of biopolymers, other researchers have adopted a foam- or emulsion-template approach. In a first step, hydrophilic polymers like hydroxyl propyl methylcellulose, gelatin and xanthan are used to stabilize an oil-water or air-water interface. Subsequently, the water is removed and by shearing the dried product into the liquid oil, gelled

structures are obtained [31, 32]. However, there is limited control over the network formation as the particle size of the building blocks might be difficult to tune. A better control over the network formation of biopolymers is desirable to tune specific rheological characteristics of such gelled oils.

In Chapters 2-5, a new method was described to create oleogels using whey proteins. Whey proteins are extensively used as ingredients in foods due to their high nutritional value and functional properties, and are therefore an ideal candidate as a structuring agent for liquid oil. First, in Chapter 2, a method was developed in which protein oleogels were prepared in a more direct way. To create oleogels, heat-set whey protein hydrogels were prepared, and a solvent exchange procedure was applied to include the oil in the interstitial areas of the protein network. In this process, the water is first replaced by an oil-miscible solvent, acetone, which is then replaced by liquid oil. To enhance the control over the network formation, in Chapters 3-5, whey protein aggregates of colloidal size were prepared (~ 150 nm) as initial building blocks. In these chapters, it was shown that the solvent exchange procedure was able to prevent agglomeration of pre-formed heat-set aggregates and therefore enabled gel formation due to sufficient protein-protein interactions. Alternatively, when the protein aggregates were freeze-dried to remove the water before they were dispersed in oil, irreversible agglomeration of the initial particles was obtained. This agglomeration led to increased particle size in oil, which was related to an observed poor stability against sedimentation and poor gel formation. However, it is currently not precisely known how the solvent exchange procedure prevents such agglomeration.

The aim of the current chapter is to elucidate on the enhanced stability against agglomeration of whey protein aggregates present in oil after applying a solvent exchange procedure. To this end, we formulate two possible mechanisms:

1) Prevention of stresses such as capillary pressure resulting from drying processes. By keeping the particles ‘solvated’ by the different solvents, starting with water, followed by acetone and finally liquid oil, the wet conditions may avoid strong forces arising from the formation of a solvent-air interface.
2) Conformational changes of the proteins as a function of the properties of the surrounding solvent. Solvents with electronegative atoms, such as oxygen, are able to interfere with intramolecular hydrogen bonding [33, 34], which could lead to the exposure of a larger fraction of hydrophobic groups to the solvent. Potentially, this could result in more favourable protein-solvent interactions and enhanced stability against agglomeration.

To gain insight in the effect of the different solvents on possible agglomeration effects and conformational changes, we have used several solvents of different polarity in the solvent exchange procedure. In addition to acetone, we have included propanol as a solvent with the ability to form hydrogen bonds, and as an alternative for a hydrophobic liquid oil, we have used volatile apolar solvents such as hexane, decane and heptane. To analyse the protein composition and conformation, the protein material was dried from the solvent by evaporation, and agglomeration effects were tested by examining the dispersibility of the dried material in oil. The results were compared to aggregates freeze-dried from water. Understanding the mechanisms involved to prevent irreversible agglomeration could provide insights on how to design a route to obtain a dry protein material that is dispersible in liquid oil and allows for direct network formation without the need for a solvent exchange procedure. This could be beneficial from a product development point of view, since the large amount of solvent needed for a solvent exchange procedure limits practical applicability.

Materials and Methods

Materials

Whey protein isolate (WPI, BiPro) was obtained from Davisco Foods International (Le Sueur, MN, USA). The protein concentration was 93.2% (N x 6.38) and was used as received. Acetone and *n*-hexane were supplied by Actu-All Chemicals (Oss, the Netherlands). Hydrogen chloride, sodium hydroxide, sodium dodecyl sulfate (SDS), and *n*-decane were purchased from Sigma-Aldrich (Steinheim, Germany). 1-propanol and n-heptane were purchased form Merck (Damstadt, Germany). N,N-Dimethyl-6-propionyl-2-naphthylamine (PRODAN) was obtained from Sigma Aldrich. Refined sunflower oil (Vandermoortele NV, Breda, the Netherlands) was bought at a local supermarket and was used without further purification. All chemicals used were of analytical grade. Demineralized water was used throughout the experiments.

Methods

Preparation of WPI aggregates

To prepare a protein stock solution, WPI powder (4% w/w) was dissolved in demineralized water under continuous stirring at room temperature for 2 h. Afterwards, the stock solution was stored overnight at 4 °C to assure complete protein hydration. The next day, the pH of the stock solution was adjusted to 5.7 using a 1 M HCl solution. The resulting solution was heated in 50 mL plastic

tubes with screwcaps at 85 °C for 15 minutes using a temperature-controlled water bath to induce protein denaturation. After cooling in ice water, a weak protein gel was obtained. This weak gel was easily broken into the smaller aggregates by hand shaking and vortexing. The resulting WPI aggregate dispersion was homogenized using a rotor stator homogenizer (Ultra Turrax, T25, IKA Werke, Germany) at 13000 rpm for 3 min. The protein aggregates were then collected as a pellet by centrifugation at 4000 g (Hermle Z383K, Hermle Labortechnik GmbH, Wehingen, Germany) for 20 min at 20 °C. After collection, the pellet was re-dispersed and centrifuged twice with demineralized water to remove remaining soluble protein material. Afterwards, the sample was homogenized using a laboratory scale homogenizer (Labhoscope, Delta Instruments, Drachten, the Netherlands) at 200 bar (3 passes). The final pH of the WPI aggregate suspension was 8.0.

Preparation of the protein oleogels using a solvent exchange procedure

To prepare the protein oleogels, the WPI aggregates were transferred to the oil phase using a solvent exchange procedure, which was based on a method described in Chapter 3. In this procedure, the polarity of the solvent was changed gradually to remove the surrounding water from the WPI aggregates and replace the continuous phase for oil. In short, 15 g of aqueous pellet, containing the WPI aggregates, was re-dispersed in 150 mL acetone, and mixed thoroughly using rotor stator homogenization. Afterwards, the sample was centrifuged at 4000 g for 20 min at 20 °C. Excess acetone was removed by decanting and the pellet, containing the protein aggregates, was collected. The procedure of re-dispersing and centrifugation was repeated once more using acetone to assure water removal. The pellet was then re-dispersed twice in liquid oil. The obtained pellet of WPI aggregates in oil was diluted in a ratio of 1:10 with sunflower oil and left overnight under continuous stirring to allow for evaporation of the remaining acetone. The next day, the suspension was centrifuged at 4000 g for 20 min at 20 °C to increase the concentration of the protein aggregates and induce gel formation.

Preparation of dried WPI aggregates

Evaporation: To determine various properties of the WPI aggregates during the solvent exchange procedure, we dry the aggregates by evaporation from acetone, 1-propanol, hexane, heptane and decane. In order to easily collect the protein material, the protein suspensions were centrifuged at 4000 g for 20 min and the resulting pellet was placed in an aluminium tray (ø = 5 cm) and dried in a fume hood for 16 h at room temperature. After drying, the powder was collected and grinded using a pestle and mortar until no further reduction in particle size was observed. To investigate the effect of the drying conditions, instead of drying from a concentrated pellet, a 1% w/w protein

aggregate suspension was dried from water, acetone or hexane by evaporation. The solvent was evaporated in the same way as described before for the drying method using the concentrated pellets.

Freeze drying: After the aqueous suspension was washed twice with demineralized water, the resulting suspension was homogenized using a lab scale homogenizer (Labhoscope) at 200 bar (3 passes) followed by centrifugation. The pellet was frozen at -20 °C in a freezer for 16 h. Thereafter, the sample was freeze dried (Christ alpha 2-4 LD plus, Martin Christ Gefriertrocknungsanlagen GmbH, Osterode am Harz, Germany) for 48 h to remove all water. In another experiment, the liquid suspension of WPI aggregates (1% w/w) was added dropwise into liquid nitrogen (-195 °C) to rapidly freeze the material. Thereafter, the frozen sample was freeze-dried as described above.

Composition

Protein content: The nitrogen content was determined using Dumas (Dumas Flash EA 1112 Series, N Analyser, Thermo Scientific). After weighing, the samples were dried overnight in an oven at 60 °C before analysis. To calculate the protein content, a nitrogen conversion factor of 6.38 was used.
Water content: The water content in the oleogel was determined by dry matter determination. Aluminium cups (ø = 5 cm) were first heated to 105 °C in an oven (Venticell, BMT Medical Technology, Brno, Czech Republic) to remove any water contamination. Afterwards, approximately 1 g of oleogel sample was added to the cup, and its weight was recorded before and after drying for 4 h at 105 °C. Water content in the dried powders was determined by Karl Fisher titration. Measurements were performed in duplicate.

Chemical stability

In order to assess the internal bonds involved in the stabilizing mechanism of the WPI aggregates, several denaturants were added to a 1 wt% of WPI aggregate dispersion. The denaturants used were 10 M Urea to examine disruption of hydrogen bonds, 140 mM Sodium Dodecyl Sulfate (SDS) for hydrophobic interactions and 50 mM dithiothreitol (DTT) for disulphide interactions [35]. Several combinations of these denaturing agents were tested and whenever DTT was used, heat treatment was applied at 70 °C for 15 min.

Sodium dodecylsulfate polyacrylamide gel electrophoresis (SDS-PAGE)

The protein composition of the freeze-dried aggregates, the acetone-dried aggregates, the hexane-dried aggregates, as well as the protein composition in the supernatant after centrifugation was analysed under reducing conditions by SDS-PAGE using the Novex NuPAGE gel system (Invitrogen, Thermo Fischer Scientific). Samples were prepared by the addition of NuPAGE LDS sample buffer (4x) and NuPAGE Reducing agent (10x) to a final protein concentration of 2 mg/ml. Thereafter, samples were vortexed and heated at 75 °C for 10 min in a water bath. After cooling, samples were loaded into the wells of a NuPage 4-12% Bis-Tris gel. As a running buffer, NuPAGE MES SDS (20x) was used, with antioxidant in the cathode chamber. Electrophoresis was performed by applying a constant voltage of 200 V for 40 min. Afterwards, gels were stained using coomassie blue (SimplyBlue™). The apparent molecular weight of the proteins present in each sample was determined by comparing the position of the bands to a reference sample with proteins of various molecular weights (Mark12™ unstained standard, Invitrogen). The gels were scanned in a densitometer (Gelscanner GS-900, Bio-Rad, Hercules, CA, USA) with Image Lab software, which allows for the identification of the proteins present in each sample.

Surface hydrophobicity

The surface hydrophobicity of the aggregates obtained through the solvent exchange method and freeze-drying was measured against the native WPI by means of the fluorescent probe method, with N,N-Dimethyl-6-propionyl-2-naphthylamine (PRODAN) as the binding probe. The procedure to determine the surface hydrophobicity was similar as reported by Haskard et al. [36]. Five different concentrations of protein were prepared ranging from 0.04 to 0.2 mg/ml and analysed in duplicate. PRODAN was dissolved in acetone at a concentration of 0.0041 M and stored in a freezer (-20 °C) protected from light and evaporation. Ten µL of PRODAN solution was added to each 4 mL sample and vortexed well. The relative fluorescence intensity (RFI) was measured using a fluorimeter (Perkin Elmer luminescence spectrometer LS50B) after 15 min of reaction of the PRODAN with the proteins in the dark at room temperature, using disposable acrylic cuvettes (Sarstedt, Nümbrecht-Rommelsdorf, Germany). The measurement settings were set to an excitation wavelength of 365 nm, emission and excitation slit widths of 5 nm, emission scan from 300 to 600 nm, and a scan speed of 200 nm/min. The net RFI values of each sample (protein with PRODAN) was obtained by subtraction of the blank (protein without PRODAN).

Attenuated Total Reflectance Fourier Transform Infrared Resonance (ATR-FTIR)

To directly analyse protein conformation of the dried protein aggregates, samples were analysed using infrared spectroscopy. Dried protein material was placed directly on the crystal using an ATR-FTIR spectrometer (Platinum Tensor, Bruker Optics, Coventry, UK). The IR spectrum was recorded from 4000-600 cm^{-1} and for each sample, 64 scans with a resolution of 4 cm^{-1} were averaged. After averaging the scans, the spectrum was cut to obtain the amide I and II region at 1400 – 1750 cm^{-1}, baseline corrected, and vector normalized using the OPUS software to analyse the Amide I, II and III region. In order to assess the protein conformation, the second derivative of the amide I region (1600 – 1700 cm^{-1}) was taken and smoothened using the OPUS software. All samples were measured in duplicate.

Particle Size Analysis

The particle size distribution of WPI aggregates was determined by static light scattering (Mastersizer 2000, Malvern Instruments, Worcestershire, UK) with either sunflower oil or demineralized water as the continuous phase. The refractive index of water was set to 1.33 and for sunflower oil to 1.469. The refractive index of the protein aggregates was set to 1.45 for aqueous protein samples and 1.54 for protein samples in sunflower oil to correct for the change in refractive index upon dehydration. The particle size distribution was determined as an average of three measurements.

Scanning Electron Microscopy (SEM)

A Scanning Electron Microscope (Phenom G2 Pro, Phenom-World BV, Eindhoven, and The Netherlands) was used to visualize the structure of the different protein powders and used to analyse any structural differences between the different samples. To this end, a small sample was taken and fixated using carbon tabs on aluminium stubs (SPI Supplies/Structure Probe Inc., West Chester, USA). Conveniently, due to the low voltage used (5kV), sample pre-treatment was not necessary and the appearance of the powders could be visualized directly.

Rheology

Oscillatory rheology was performed on the oleogel made with WPI aggregates obtained via either the solvent exchange procedure or via freeze drying. Both samples were standardized to 10 wt% protein and 1.2 wt% water to allow for comparison between the samples. Before the measurement, the samples were homogenized using rotor-stator homogenization (135000 rpm) for 180 s. Afterwards, samples were degassed using a vacuum pump for 30 min and loaded into a

stress-controlled rheometer (AP 502, Anton Paar GmbH, Graz, Austria) between sandblasted parallel plates (ø = 49.978 mm) to prevent slip phenomena. The temperature was controlled for all measurements at 20°C. Before any measurements were performed, the samples were allowed to equilibrate for 60 min at a frequency of 1 Hz and a strain (γ) of 0.01% (which was within the linear viscoelastic region). Frequency sweeps were performed by increasing the frequency logarithmically from 0.01 to 50 Hz at γ = 0.01%. Amplitude sweeps were performed by increasing the strain logarithmically from 0.001 to 100% at 1 Hz. All measurements were performed in triplicate.

Results and Discussion

Characteristics of whey protein aggregates

To understand possible changes in the protein aggregates during the solvent exchange procedure, we first examined the characteristics of the protein aggregates prepared in aqueous conditions. Figure 6.1A shows the particle size distribution of the whey protein isolate (WPI) aggregates after heat treatment. The major fraction of the WPI aggregates had a particle size around 150 nm, which is of comparable size to what has been reported in other studies [37]. Upon heating a protein solution above the protein denaturation temperature, heat-set aggregates are formed that are stabilized through physical and chemical interactions. The strength of these interactions determine the stability of the protein aggregates against external forces such as those resulting from shear and drying processes.

To assess which interactions are involved that lead to the stability of the protein aggregates, several denaturants were added to an aqueous 1% WPI aggregate suspension. After adding SDS, urea or a combination of both, we noticed that the suspensions remained turbid, suggesting that hydrogen bonds and hydrophobic interactions were not the only interactions responsible for the stabilization. However, when DTT was added, the suspension turned completely transparent as a result of disintegration of the aggregates. This suggests that the structure of the WPI aggregates is partially stabilized by internal covalent disulphide bonds and is in agreement with other studies using heat-set WPI aggregates prepared at similar conditions [38].

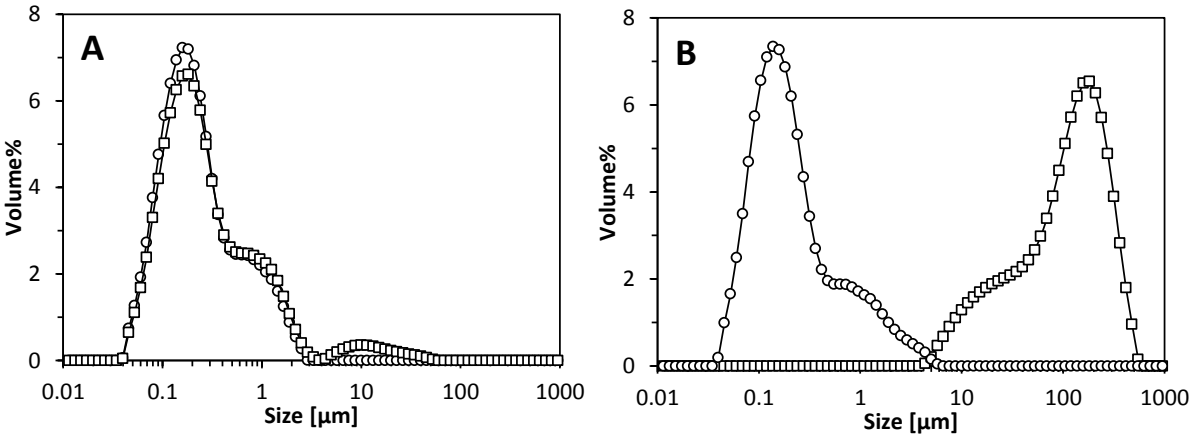

Figure 6.1. Particle size distribution of dispersions of WPI aggregates. A) Particle size in water measured either directly after homogenization (○) or re-dispersed after freeze-drying (□). B) Particle size of aggregates in sunflower oil using freeze-drying (□) or a solvent exchange procedure (○).

After freeze-drying the WPI aggregates, the resulting powder was re-dispersed in demineralized water. The resulting particle size distribution was comparable before freeze drying, as is presented in Figure 6.1A. As already discussed in Chapter 3, the freeze-dried aggregates do not readily disperse in oil and particles of more than 100 microns were obtained, as is depicted in Figure 6.1B. Alternatively, when a solvent exchange procedure was used to disperse the aggregates in the oil, a particle size of 150 nm was found (open circles in Figure 6.1B). Although these results show that the solvent exchange procedure prevents agglomeration of the protein aggregates, the underlying mechanism is not yet understood. To gain more insight in the effect of the solvents during the solvent exchange process, hexane was used as an alternative nonpolar solvent in the following sections to easily isolate the aggregates during the solvent exchange process by evaporation. Hereafter, we studied the properties of the dried aggregates in terms of composition, conformation, and dispersibility in liquid oil.

Protein composition

Since WPI is a mixture of several proteins, the composition of the proteins present in the aggregates might be different as a result of exposure to different solvents. To exclude these differences, the freeze-dried, acetone-dried and hexane-dried WPI aggregate samples were analysed using SDS-PAGE. After the heating step in aqueous conditions, only 80% of the protein material was found to be included in the WPI aggregates (i.e. in the pellet), and 20% was still present in the supernatant. For this reason, also the supernatant was analysed for its composition. Native WPI was analysed for comparison. The SDS-PAGE electrophoretograms are shown in Figure 6.2. Lane 1 shows the electrophoretogram of native WPI and the major whey protein fractions can easily be recognized. Major bands found around 66, 18 and 14 kDa correspond to Bovine Serum Albumin (BSA), β-lactoglobulin (β-lac), and α-lactalbumin (α-lac), respectively. The major protein fraction, as indicated by the higher band intensity, is β-lac. Comparable to the native sample, the freeze-dried WPI aggregates (lane 2) showed bands at all major protein fractions. However, the intensity of the band corresponding to α-lac (14 kDa) seems to be lower, as will be discussed in more detail below. The acetone- and hexane-dried WPI aggregates (lane 3 and 4) showed a high similarity with the freeze-dried sample. The protein composition of the supernatant, i.e. soluble protein material after heat treatment and centrifugation, showed a distinctly different electrophoretogram (lane 5). The band corresponding to BSA is not detected, the band intensity of β-lac is less intensive and the band intensity of α-lac has increased compared to the samples containing the aggregates.

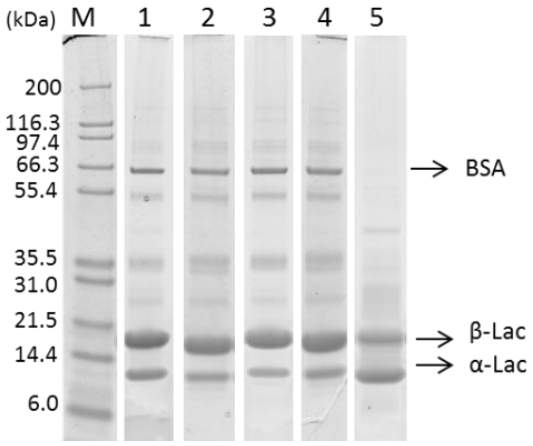

Figure 6.2. Scans of SDS-PAGE electrophoretograms of native whey protein isolate (1), freeze-dried WPI aggregates (2), acetone-dried WPI aggregates (3), hexane-dried aggregates (4), supernatant after centrifuging the whey protein aggregates (5). M: molecular weight markers.

To estimate the relative content of β-lac and α-lac in each sample, we have taken the band intensity of β-lac as an internal standard per electrophoretogram, and determined the ratio α-lac/β-lac for the different samples (Figure 6.3). The α-lac/β-lac ratio of the aggregates was found to be lower compared to the native WPI, whereas for the supernatant, this ratio was much higher. Our result suggest that the disulphide crosslinked aggregates contain a higher amount of BSA and β-lac compared to its native protein composition, and that α-lac is to a lesser extent incorporated into the aggregates. Taking the gelation mechanism of the different proteins into account, the results can be explained since both BSA and β-lac have a higher gelation rate and have a free thiol group available to from disulphide bonds [39, 40].

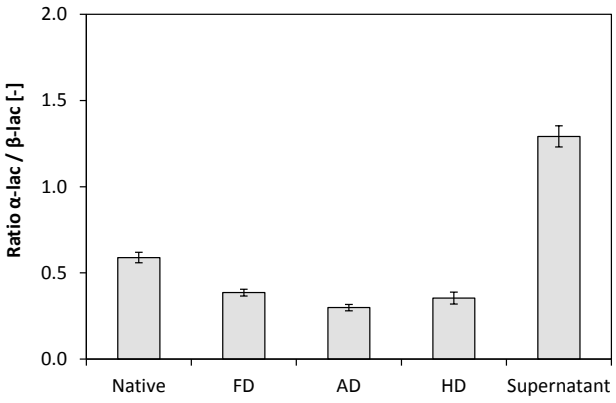

Figure 6.3. Ratio α-lactalbumin/β-lactoglobulin in the different protein samples. FD, AD and HD represent freeze-dried, acetone-dried and hexane-dried aggregates respectively. Supernatant was taken after centrifuging the whey protein aggregates.

From these results, we can conclude that changing the aqueous solvent to acetone or hexane had no apparent influence on the internal protein composition of the aggregates. This indicates that the protein aggregates were stable during the solvent exchange procedure, regardless of the drying method or solvents used. Therefore, changes in oil dipsersibility as a result of the solvent exchange, is not caused by a change in protein composition of the aggregates.

Particle Morphology

The obtained powders, dried by either freeze drying from water or evaporation from organic solvents, were analysed by Scanning Electron Microscopy (SEM) to determine the particle morphology. As can be seen in Figure 6.4A, the freeze-dried powder contained large particles (~ 50 – 100 μm), but have an open, porous structure. The morphology of the particles when evaporated from acetone (Figure 6.4B) had a similar appearance as the freeze-dried sample, i.e. large particles with similar porosity. In contrast, the hexane-dried protein powder is absent of any large particles, and the powder consists of small, porous particles (10 – 20 μm).

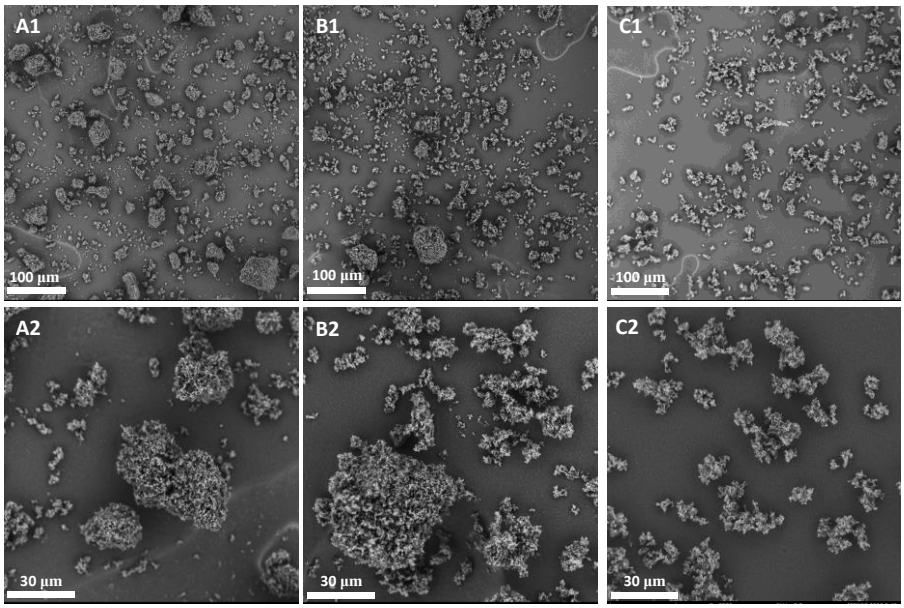

Figure 6.4. SEM micrographs of dried WPI aggregates: (A) freeze-dried from water, (B) evaporated from acetone, (C) evaporated from hexane. Numbers 1 and 2 refer to a different magnification of the same sample.

It shows that the nature of the solvent had a large influence on the powder morphology. The packing density of the powders was estimated by weighing 1 mL of dried material in a graded cylinder. The packing densities were found to be approximately 0.26 g/cm^3 for the freeze-dried powder, 0.14 g/cm^3 for the acetone-evaporated powder, and 0.07 g/cm^3 for the hexane-evaporated

powder. Clearly, when WPI aggregates are dried from solvents with low polarity, the powder morphology changed from large agglomerated particles to loosely packed particles.

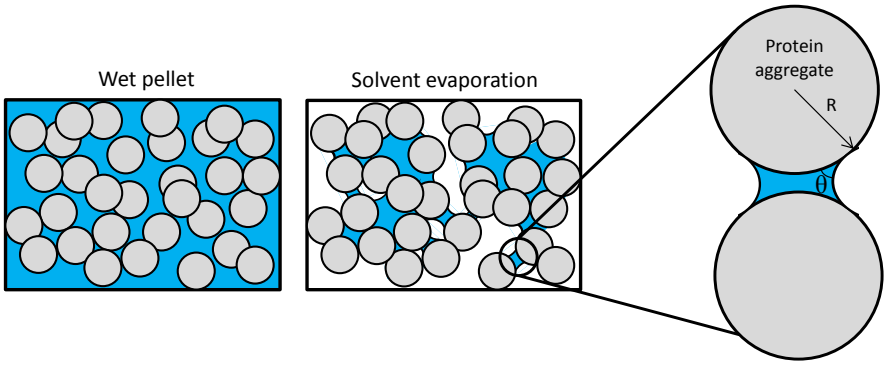

Figure 6.5. Schematic drawing of a liquid bridge between two spherical particles during evaporation of the solvent.

The effects of different drying conditions are dependent on the hydrophobicity of the solvent, which seem to change the interactions between the protein aggregates. By removal of the solvent by evaporation, initially the solvent evaporates from the bulk, but will eventually form a liquid bridge between two particles, as schematically depicted in Figure 6.5. This causes a capillary force (F_c) across two particles as a result of a curved interface governed by the interfacial tension, γ. When the distance between two particles approaches zero, F_c becomes [41]:

$$F_c = 2\pi R\gamma \cos\theta \qquad (6.1)$$

where R is the particle radius and θ is the contact angle between the liquid and the solid, which in our case is the protein aggregate (Figure 6.5). When the capillary force is sufficiently high, this may result in large attractive forces between the particles. Therefore, in the production of nanometre sized ZrO_2, Al_2O_3, or TiO_2 particles, solvents with a low surface tension were used during drying to reduce their agglomeration and increase their specific surface area [42, 43]. Similarly, in the case of aerogels, it has been shown that large capillary forces leads to a collapse of the initial microstructure. In order to prevent this undesired effect, often alternative solvents and/or supercritical drying methods are used to change the wetting angle and interfacial tension [44, 45]. In our case, the solvent evaporates from the interstitial spaces between and from the surface of the aggregates, which may lead to increased capillary forces between the aggregates. When the solvent has a high surface tension and a small contact angle, capillary pressure facilitates particle agglomeration. The contact angle is related to the difference in polarity between the particle and the solvent [46]. In the case of water, with a high surface tension of 73 mN/m and an estimated low contact angle ($\theta < 90°$), the resulting high capillary force would lead to a large

degree of agglomeration. However, in the case of hexane, the lower interfacial tension (19 mN/m) and a higher contact angle (given the low polarity of hexane) leads to much lower values of the capillary force and therefore a low degree of agglomeration, in accordance with our experiments. In the case when $\theta > 90°$, the resulting force could even lead to and effective repulsion between two protein aggregates.

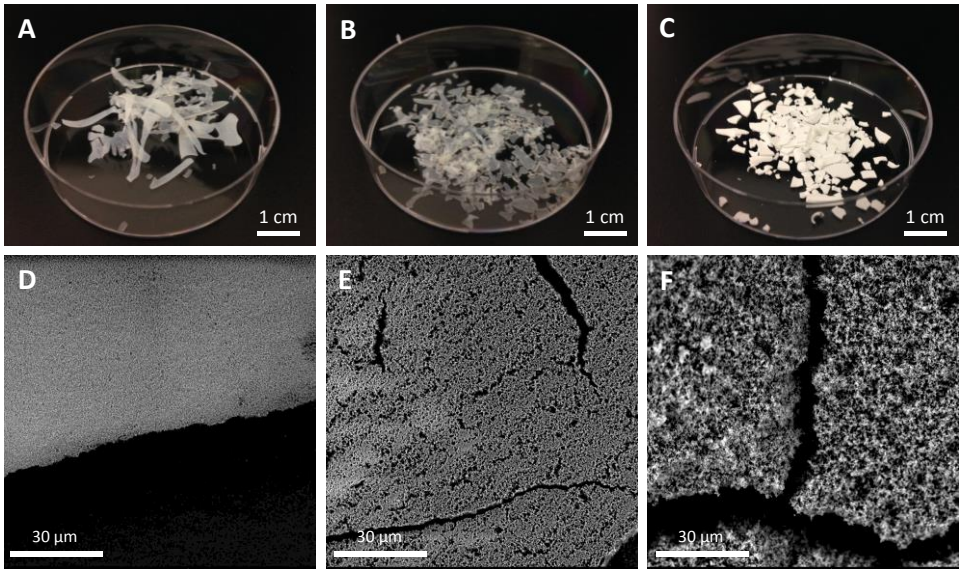

Figure 6.6. Appearance of dried protein suspensions from water (A), acetone (B), or hexane (C) at ambient conditions and corresponding SEM micrographs (D-F).

To visualize the effect of the drying conditions more clearly, we dried a liquid suspension of WPI aggregates from the solvents water, acetone, or hexane and observed the appearance and microstructure of the film formed. Figure 6.6 shows the difference in the appearance of the dried protein material as well as the microstructure of the films at a smaller length scale. When the drying medium was water, the resulting film was hard and almost translucent. The SEM micrograph shows a tight packing of the protein aggregates. Drying from acetone (Figure 6.6B) resulted in a more brittle film, which was more difficult to handle than the water-dried protein film. The microstructure shows more cracks or gaps between the protein aggregates. When the protein aggregate suspension was dried from hexane, film formation was inhibited and the sample was very brittle, resulting from limited interactions between the protein aggregates. In addition, the resulting material was opaque (Figure 6.6C). The limited interactions can be seen more clearly in Figure 6.6F, where a very porous structure can be observed with larger distances between the individual aggregates. This is consistent with the observed powder morphology in Figure 6.4, where drying from hexane prevents agglomeration. Prevention of strong capillary forces during drying thus seems to reduce agglomeration between the particles.

Dispersibility of dried whey protein aggregates in liquid oil

The dried protein aggregates obtained from different drying methods were tested for their dispersibility in liquid oil. To this end, a 1% w/w dispersion was prepared by adding the dried powders to sunflower oil, and the resulting particle size was measured after homogenization. As can be seen in Figure 6.7A, the acetone-dried sample showed poor dispersibility. A large increase in particle sizes (10 – 300 μm) compared to the sizes observed in the original aqueous dispersion is indicative of irreversible particle agglomeration during drying. Even though during drying the surface tension and wettability of acetone is lower than that of water, apparently the capillary forces are not yet decreased to such extent that agglomeration is prevented. In contrast, good dispersibility was obtained when the drying medium was hexane (Figure 6.7B), since a large amount of small (< 1 μm) particles was obtained. Although agglomeration was not fully prevented as shown by the presence of a smaller peak at 10 – 100 μm, the major fraction of the protein aggregates retained their small initial size, shown by the large peak at ~150 nm. Since the difference in particle agglomeration was observed by SEM, it seems that drying-induced agglomeration was largely irreversible. Mixing the agglomerated powders into the oil by shear hardly seems to break any formed agglomerates and leads to poor dispersibility in oil.

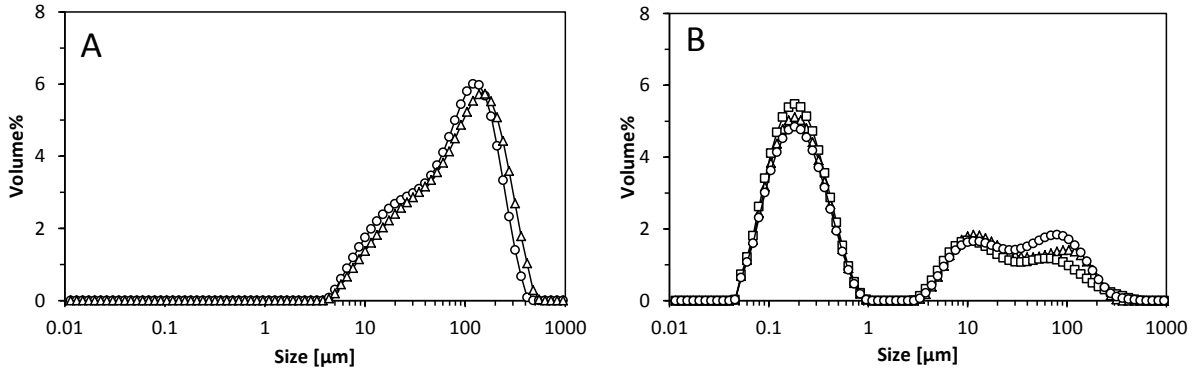

Figure 6.7. Particle size distribution of dispersed WPI aggregates in liquid oil. A) size distribution of aggregates dried from 1-propanol (○) and acetone (△). B) Particle size distribution of aggregates dried from hexane (△), heptane (□) or decane (○).

To test which physical properties of the solvent have an effect on particle agglomeration and resulting dispersibility in oil, 1-propanol, heptane and decane were also used as the suspending solvents during drying. These solvents differ in surface tension and dielectric constant as can be seen in Table 6.1. Here, we use the dielectric permittivity as a measure for the polarity. As can be seen in Figure 6.7, drying from 1-propanol led to a similar size distribution as acetone, whereas decane and heptane led to a similar particle size distribution as hexane. Interestingly, although the

surface tension of decane and 1-propanol is similar, the resulting dried aggregates showed a very different size distribution when dispersed in oil. A low surface tension does not seem to be the most important prerequisite to prevent irreversible agglomeration. Particle agglomeration seems to be better related to the dielectric permittivity i.e. the polarity of the solvent. The low polarity causes a low wettability with the mainly hydrophilic proteins and subsequently a large contact angle. In turn, this results in a lower capillary pressure across two protein aggregates during solvent evaporation, which leads to less irreversible agglomeration and better dispersibility of the aggregates into oil.

Table 6.1. Properties of the solvents used for drying WPI aggregates.

	Dielectric permittivity, ε (298K)	Surface tension mN/m (293K)
Water	80.1	72.8
Acetone	21.4	25.2
1-Propanol	19.4	23.7
n-Hexane	1.8	18.4
n-Heptane	1.8	20.1
n-Decane	1.8	23.8

Protein conformation

The previous results show that prevention of agglomeration by choosing a solvent with a low polarity is an important factor for the increased dispersibility of protein aggregates. However, changes within the proteins aggregates may also add to this effect. Since proteins are subjective to structural reorientation as solvent conditions are changed, it is possible that the protein conformation is altered upon contact with solvents like acetone or hexane. Possibly, this contributes to increased protein-solvent interactions by structural reorientations. To determine if the protein conformation differed amongst WPI aggregates as a result of the type of solvent it was dried from, we analysed the different powders by Attenuated Total Reflectance Fourier Transform Infrared Resonance (ATR-FTIR). This technique is capable to determine the protein conformation (i.e. secondary structure) as well as the hydration level [47]. The amide I region (1600 – 1680 cm^{-1}) is mostly due to C=O stretching and is closely related to changes in protein conformation. The amide II region (1480 – 1560 cm^{-1}), caused by NH bending and CN stretching is closely related to protein hydration and less sensitive to conformational changes [48]. Conveniently, we can probe the conformation as well as the hydration level of the obtained dried samples directly. Figure 6.8A shows the amide I and II region of different WPI aggregate samples as well as the native WPI sample. We display the results for aggregates dried from hexane (HD) and acetone (AD), as these

solvents gave a large difference in morphology and particle size, and compared these samples to aggregates dried via freeze-drying (FD).

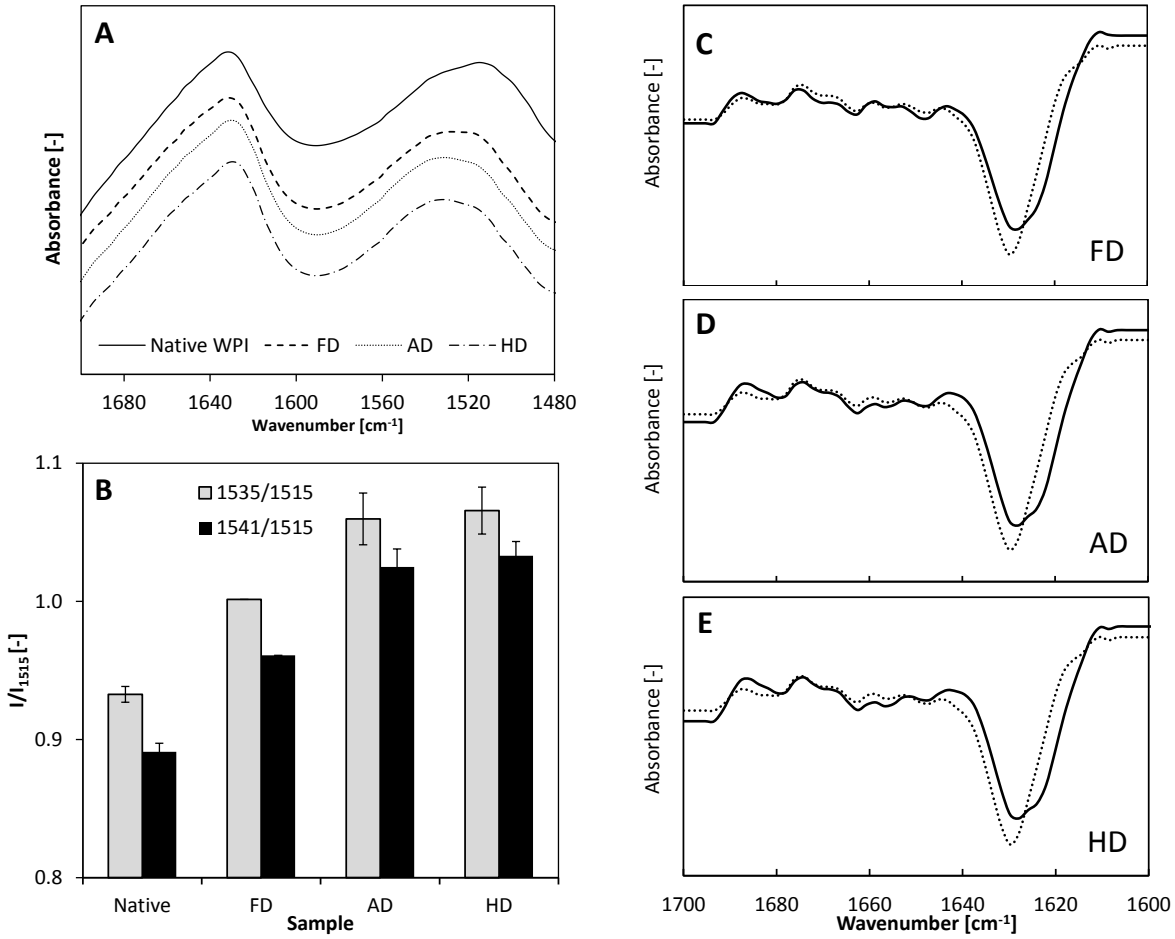

Figure 6.8. FTIR results for native WPI powder, freeze-dried aggregates (FD), acetone-dried aggregates (AD) and hexane-dried aggregates (HD). A) Amide I and II IR-spectra, B) Band intensity ratio of selected band/1515 cm^{-1} (I/I1515). White bars: 1535 cm^{-1} black bars: 1541 cm^{-1}. C-E) Second derivative of Amide I band of dried whey protein aggregates (solid lines). In each figure, native WPI powder was added as a reference (dotted line).

Looking at the amide I region, a slight shift in peak position towards higher wavenumbers can be observed for all WPI aggregate samples compared to native WPI. However, no obvious changes are visible amongst the different WPI aggregate samples. Changes in the shape of the amide II region are more extensive between the samples than changes of the amide I region. This indicates a change in hydration level of the proteins, which can be probed by comparing the intensity ratio of the peak at 1535 cm^{-1} and 1541 cm^{-1} to the peak at 1515 cm^{-1}. The vibration at 1515 cm^{-1} is related to tryptophan and is insensitive to hydration [49], which makes this a valuable internal standard. These intensity ratios were used by other researchers to assess the hydration level during

film drying of β-lactoglobulin films [50]. Figure 6.8B shows that the I_{1535}/I_{1515} and I_{1541}/I_{1515} ratios are higher for all dried aggregates compared to the native WPI powder. Aggregates obtained from freeze drying showed lower hydration levels than the aggregates dried from both acetone and hexane, but no differences were seen between acetone or hexane dried aggregates. The lower hydration levels were confirmed by Karl Fisher titration, where the measured water content was 6.3% (± 0.1) for native WPI, 7.0% (± 0.1) for the freeze-dried aggregates, 7.9% (± 0.1) for acetone-dried aggregates and 7.9% (± 0.3) for hexane-dried aggregates. Most likely, the amount of water present in the solvent-dried samples (either acetone or hexane) was slightly higher because of the hygroscopic nature of the protein powder, attracting moisture from the air. This effect can be enhanced for powders with low density and large contact area. However, the increased dispersibility and the small particle size of the hexane-dried aggregates compared to acetone-dried protein aggregates in oil is not related to these differences in water content.

To determine the protein conformation, the second derivative of the amide I region was obtained for native WPI and the WPI aggregates and displayed in Figure 6.8C-E. Since the solvent exchange did not affect protein composition of the sample, this allows for direct comparison between the aggregates. In all graphs, the second derivative of native WPI was added as a reference (dotted line). Compared to the signal from the native WPI, the aggregates did not show major differences. Only a broadening of the major band is noticeable at 1630 cm^{-1}, assigned to an increase of intermolecular β-sheet formation, and is indicative of aggregation [51, 52]. Between the WPI aggregates, however, regardless of the drying method, no obvious differences were seen. The only noticeable difference is the slight increase in the intensity around 1640 cm^{-1} for the samples dried from acetone and hexane compared to the freeze-dried sample, which might be related to the small difference in hydration. Although small changes are observed between the aggregates dried from the different solvents, we suspect that these differences are not large enough to account for significant changes in the structure of the proteins. Note that also the spectra of the second derivative of WPI aggregates dried from 1-propanol, heptane, and decane did not differ from those shown in Figure 6.8. Moreover, we observed no changes in the second derivative of the amide I region when WPI aggregates were suspended in oil using a solvent exchange procedure (data not shown). The increased dispersibility of the aggregates as a result of the solvent exchange procedure thus seems to be unrelated to any changes in protein conformation since the results from the FTIR measurements for these samples show a high level of similarity.

Surface hydrophobicity

Though FTIR was unable to detect differences in conformation, we checked the surface hydrophobicity of the freeze-dried and the hexane-dried WPI aggregates. Using PRODAN, a fluorescent probe, the relative fluorescence intensity (RFI) was measured as a function of protein concentration and the results are displayed in Figure 6.9. The slope of RFI versus protein concentration, is used as a measure of hydrophobicity. We have added the results of native WPI as a comparison. As can be seen, the affinity for PRODAN increased as a result of applying a heat treatment, as a higher slope was measured for the aggregates than for the native proteins. This increase in hydrophobicity is expected as the heating process leads to exposure of hydrophobic groups normally buried within the native folded structure of proteins [53]. Between the two WPI aggregate samples, however, there was no clear difference between the freeze-dried and hexane-dried sample, as the slope shows a high similarity. From this, we conclude that the hydrophobicity does not change resulting from drying from different solvents, consistent with the results discussed before. However, these results have to be taken with care, since these measurements were performed in aqueous environments and therefore only irreversible changes as affected by the different drying methods can be measured.

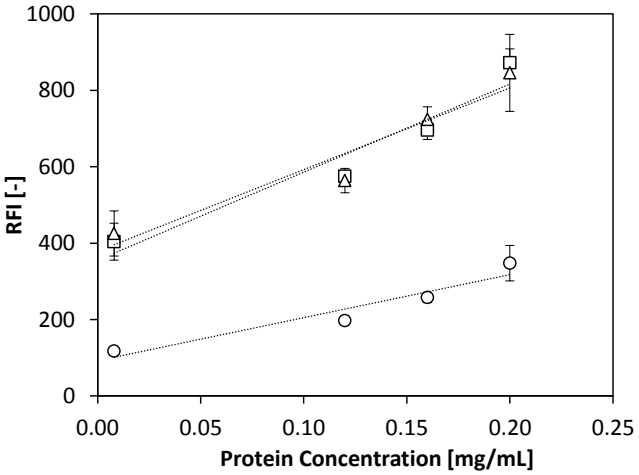

Figure 6.9. Relative fluorescence intensity (RFI) as a function of protein concentration for native WPI (○), freeze-dried WPI aggregates (□), and hexane-dried WPI aggregates (△).

In summary, from the results obtained by SDS-PAGE, FTIR and hydrophobicity measurements, we can conclude that no differences in protein composition, conformation or hydrophobicity occurred as affected by the presence of different types of solvents. This shows that structural changes on a molecular level are therefore most likely not responsible for the enhanced dispersibility of WPI aggregates in oil. A slight difference in water content was found as result of the different drying methods, but this does not seem to explain the difference in dispersibility between the acetone-

and hexane-dried aggregates. Instead, other factors than water content or conformational changes seem to dominate the dispersibility. We propose that prevention of capillary forces between the aggregates during drying is most likely the cause for the increased dispersibility of the aggregates in oil. It suggests that an optimized drying process to avoid particle agglomeration could be an alternative for the solvent exchange procedure. Since a solvent exchange requires a large amount of solvent, an alternative method would provide many advantages from a practical point of view. Therefore, we examined the process of freeze-drying more closely by considering different rates of freezing.

Effect of freeze drying conditions

During the process of freeze-drying, water is removed from the sample by sublimation of ice at low pressure. Although freeze-drying is considered a mild drying technique, freezing effects can play a significant role in the agglomeration of particles. Ice formation in a colloidal suspension, such as our suspension of aggregates, typically expels the particles from the frozen areas, effectively increasing the particle concentration locally. The formed ice crystals pack the particles close to one another with high forces that can overcome repulsive forces and thus induce (irreversible) particle agglomeration. When conditions are carefully chosen, in a process called 'freeze casting', directional ice formation can even occur, leading to the formation of a layered pattern [54]. When the freezing rate is increased, however, the formed ice crystals are small, and tight packing of the particles is prevented to some extent and instead, the particles remain more evenly distributed [55].

Therefore, as an alternative to the slow freezing at -20 °C, we investigated the effect of a higher freezing rate by dripping a 1 wt% aqueous WPI aggregate suspension directly into liquid nitrogen. The temperature difference, and subsequently the freezing rate, was thus roughly increased by a factor 5. After the material was freeze-dried, the dried powder was dispersed directly into oil by homogenization. The resulting particle size distribution was measured and as can be seen in Figure 6.10, the sample contains two main size populations as is noticeable by the appearance of two distinct peaks. One population having a size of approximately 150 nm, the other a broad range of larger particle sizes (~ 10 – 500 μm). The resulting size distribution was different from the sample frozen at -20 °C (Figure 6.1B), where only large agglomerates were observed. The peak at 150 nm shows that irreversible agglomeration of the aggregates was prevented to some extent by the process of fast freezing and subsequent freeze-drying. Even though the average particle size was reduced, we found that agglomeration into larger agglomerates was still unavoidable. These larger aggregates (>100 μm) were removed by centrifugation at low speeds (500 g). The particle size

distribution of the supernatant (Figure 6.10, open squares) shows that the peak at smaller particle sizes became more prominent. Even though a bimodal distribution can be seen, the major fraction of the particles was now below 1 μm. Comparing the size as a surface weighted diameter, $d_{3,2}$, we found an average of 140 nm for the aggregates obtained with the solvent exchange procedure, and 220 nm for the WPI aggregates in the supernatant obtained with the freeze-drying method using rapid freezing. This shows that a high freezing rate can prevent particle size agglomeration to a large extent.

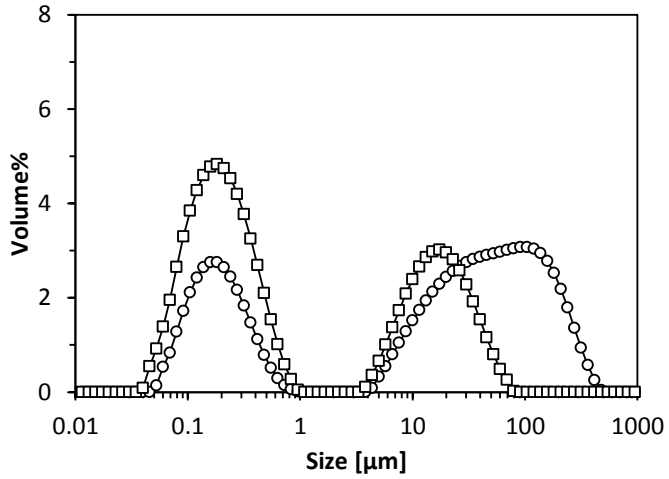

Figure 6.10. Particle size distribution of freeze-dried aggregates in sunflower oil using a high freezing rate (○), and the supernatant of the same sample after centrifugation at 500 g (□).

Rheology of WPI oleogels prepared via solvent exchange and freeze drying

From a practical point of view, freeze-drying as an alternative for a solvent exchange is desirable since much less solvent is needed to transfer the protein aggregates to the oil phase and the dried protein powder can be added to the oil directly. To assess the capability of the freeze-dried WPI aggregates to form a network in liquid oil, the supernatant was centrifuged at higher speeds (4000 g, 40 min) to collect the protein aggregates as a dense pellet. The rheological properties of the protein oleogel prepared from freeze-dried aggregates were compared to those of the oleogel prepared using the solvent exchange procedure. To allow for comparison between the different oleogels, the composition of the samples was standardized for protein (10 wt%) and water content (1.2 wt%) as determined by Dumas and dry matter analysis, respectively. Both samples were paste-like gels and the results of the frequency dependence can be seen in Figure 6.11A. Both oleogels show a high degree of similarity as G' was roughly an order of magnitude higher than G" for both samples, indicating an elastic network had formed. Since G' was only slightly dependent on frequency and the complex viscosity decreased linearly with the applied frequency, it shows

that for both gels, the viscoelastic response was not significantly affected by the rate of deformation.

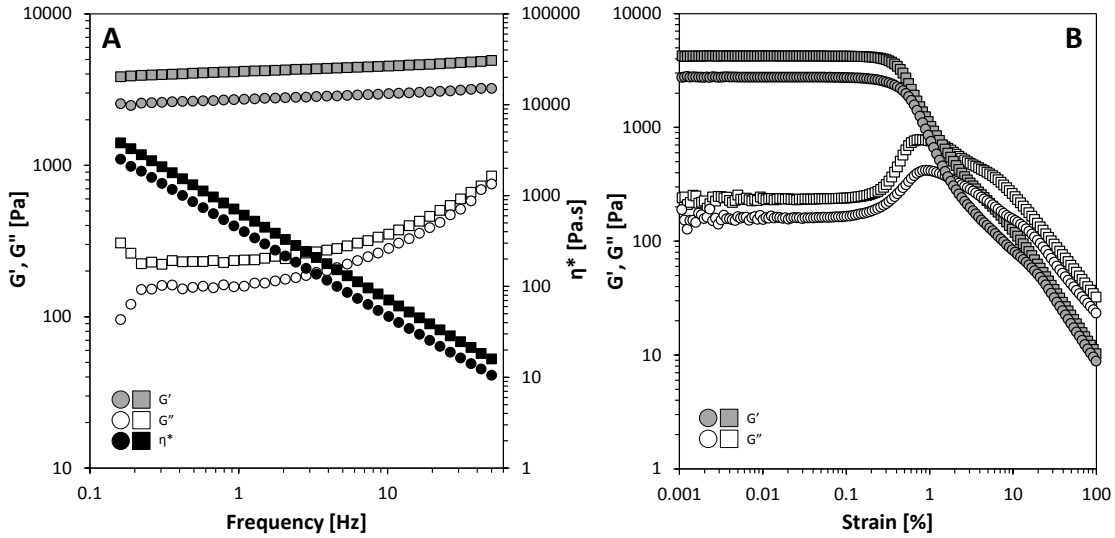

Figure 6.11. Frequency sweeps (A) and strain sweeps (B) of 10% w/w protein oleogels prepared by solvent exchange (□) or by freeze-drying (○). A) frequency sweep, B) strain sweep. Error bars of triplicate measurements were typically not larger than the symbols and were left out for clarity.

Figure 6.11B displays for both oleogels the rheological response to an increased strain amplitude of deformation. It can be seen that both samples had a similar linear viscoelastic region, as the G' deviated from linearity at roughly the same strain value. Furthermore, the overshoot in G" can be noticed in both samples, which indicated fast rearrangements in the network structure during deformation [56]. Even though the rheological response is highly similar, the magnitude of G' was somewhat lower for the sample with freeze-dried WPI aggregates. This small difference can be explained by the larger particles present in the freeze-dried sample, which were not observed by applying a solvent exchange procedure. Since larger particles are less effective in creating a network structure, given the lower surface area available, this leads to a less efficient network formation and lower values for the moduli. Nonetheless, by preventing severe particle agglomeration due to the high freezing rate, the increased surface area available for protein-protein interactions resulted in effective gel formation. Given that the results are similar for both type of oleogels, we can conclude that the solvent exchange and the freeze-drying method both lead to effective network formation of the protein aggregates in liquid oil. Therefore, tuning the conditions during drying, such as a fast freezing process, could be an effective strategy to produce a protein powder which is well dispersible in oil and directly capable of forming a gelled structure.

Conclusions

The aim of the current paper was to elucidate on the enhanced stability against agglomeration of whey protein isolate (WPI) aggregates in oil after applying a solvent exchange procedure. To this end, heat-set WPI aggregates were transferred from water to several solvents differing in polarity. We have shown that drying protein aggregates by evaporation from solvents with a low polarity (eg. hexane) resulted in a low density powder, which showed good dispersibility of the aggregates into liquid oil. When the aggregates were dried from more hydrophilic solvents, such as acetone, 1-propanol or water, the drying process resulted in agglomeration of the protein aggregates, and poor dispersibility in oil. No change in protein composition, protein conformation, or surface hydrophobicity was observed as a result of the solvent exchange procedure. Therefore, we concluded that reduced agglomeration is dominated by a reduction of attractive capillary forces between the protein aggregates during drying. Nonpolar solvents such as hexane, having a low surface tension and low wettability, prevent agglomeration by avoiding a capillary pressure build up during drying. This result suggests that the drying conditions can be tuned to minimize the degree of irreversible agglomeration of the protein aggregates. Indeed, we were able to show that by increasing the freezing rate prior to freeze-drying the water, irreversible agglomeration was prevented to a large extent. The resulting particle size distribution of the freeze-dried WPI aggregates after fast freezing showed to be close to that of the solvent exchange sample. For both methods, the small aggregates were effective in forming a gel network where G' > G". This research has shown that by carefully designing a drying process, irreversible agglomeration of WPI aggregates can be prevented to obtain a dried protein material that can be used directly for structure formation in liquid oil.

References

1. Mensink, R.P. and M.B. Katan, *Effect of dietary trans fatty acids on high-density and low-density lipoprotein cholesterol levels in healthy subjects.* New England Journal of Medicine, 1990. **323**(7): p. 439-445.
2. Mensink, R.P., et al., *Effects of dietary fatty acids and carbohydrates on the ratio of serum total to HDL cholesterol and on serum lipids and apolipoproteins: A meta-analysis of 60 controlled trials.* American Journal of Clinical Nutrition, 2003. **77**(5): p. 1146-1155.
3. Hu, F.B. and W.C. Willett, *Optimal diets for prevention of coronary heart disease.* Journal of the American Medical Association, 2002. **288**(20): p. 2569-2578.
4. Patel, A.R. and K. Dewettinck, *Edible oil structuring: an overview and recent updates.* Food & Function, 2016. **7**(1): p. 20-29.
5. Rogers, M.A., *Novel structuring strategies for unsaturated fats – Meeting the zero-trans, zero-saturated fat challenge: A review.* Food Research International, 2009. **42**(7): p. 747-753.
6. Rogers, M.A., A.J. Wright, and A.G. Marangoni, *Oil organogels: the fat of the future?* Soft Matter, 2009. **5**(8): p. 1594-1596.
7. Marangoni, A., *Organogels: An Alternative Edible Oil-Structuring Method.* Journal of the American Oil Chemists' Society, 2012. **89**(5): p. 749-780.
8. Terech, P. and R.G. Weiss, *Low molecular mass gelators of organic liquids and the properties of their gels.* Chemical Reviews, 1997. **97**(8): p. 3133-3159.
9. Van Esch, J.H. and B.L. Feringa, *New functional materials based on self-assembling organogels: From serendipity towards design.* Angewandte Chemie - International Edition, 2000. **39**(13): p. 2263-2266.
10. Abdallah, D.J. and R.G. Weiss, *Organogels and low molecular mass organic gelators.* Advanced Materials, 2000. **12**(17): p. 1237-1247.
11. Basak, S., J. Nanda, and A. Banerjee, *A new aromatic amino acid based organogel for oil spill recovery.* Journal of Materials Chemistry, 2012. **22**(23): p. 11658-11664.
12. Vibhute, A.M., V. Muvvala, and K.M. Sureshan, *A Sugar-Based Gelator for Marine Oil-Spill Recovery.* Angewandte Chemie International Edition, 2016. **55**(27): p. 7782-7785.
13. Wicklein, A., et al., *Self-assembly of semiconductor organogelator nanowires for photoinduced charge separation.* ACS Nano, 2009. **3**(5): p. 1107-1114.
14. Sagiri, S.S., et al., *Organogels as Matrices for Controlled Drug Delivery: A Review on the Current State.* Soft Materials, 2013. **12**(1): p. 47-72.
15. Singh, V.K., et al., *Development and Characterization of Sorbitan Monostearate and Sesame Oil-Based Organogels for Topical Delivery of Antimicrobials.* AAPS PharmSciTech, 2015. **16**(2): p. 293-305.
16. Vintiloiu, A. and J.C. Leroux, *Organogels and their use in drug delivery - A review.* Journal of controlled release, 2008. **125**(3): p. 179-192.

17. Nikiforidis, C.V. and E. Scholten, *Self-assemblies of lecithin and α-tocopherol as gelators of lipid material.* RSC Advances, 2014. **4**(5): p. 2466-2473.
18. Pernetti, M., et al., *Structuring edible oil with lecithin and sorbitan tri-stearate.* Food Hydrocolloids, 2007. **21**(5-6): p. 855-861.
19. Da Pieve, S., et al., *Shear Nanostructuring of Monoglyceride Organogels.* Food Biophysics, 2010. **5**(3): p. 211-217.
20. Ojijo, N.K.O., et al., *Effects of monoglyceride content, cooling rate and shear on the rheological properties of olive oil/monoglyceride gel networks.* Journal of the Science of Food and Agriculture, 2004. **84**(12): p. 1585-1593.
21. Schaink, H.M., et al., *Crystal network for edible oil organogels: Possibilities and limitations of the fatty acid and fatty alcohol systems.* Food Research International, 2007. **40**(9): p. 1185-1193.
22. Bot, A. and W.G.M. Agterof, *Structuring of edible oils by mixtures of γ-oryzanol with β-sitosterol or related phytosterols.* Journal of the American Oil Chemists' Society, 2006. **83**(6): p. 513-521.
23. Sawalha, H., et al., *The influence of the type of oil phase on the self-assembly process of γ-oryzanol + β-sitosterol tubules in organogel systems.* European Journal of Lipid Science and Technology, 2013. **115**(3): p. 295-300.
24. Blake, A.I., E.D. Co, and A.G. Marangoni, *Structure and physical properties of plant wax crystal networks and their relationship to oil binding capacity.* JAOCS, Journal of the American Oil Chemists' Society, 2014. **91**(6): p. 885-903.
25. Hwang, H.S., et al., *Organogel formation of soybean oil with waxes.* Journal of the American Oil Chemists' Society, 2012. **89**(4): p. 639-647.
26. Toro-Vazquez, J.F., et al., *Thermal and Textural Properties of Organogels Developed by Candelilla Wax in Safflower Oil.* Journal of the American Oil Chemists' Society, 2007. **84**(11): p. 989-1000.
27. Davidovich-Pinhas, M., S. Barbut, and A.G. Marangoni, *The gelation of oil using ethyl cellulose.* Carbohydrate Polymers, 2015. **117**: p. 869-878.
28. Davidovich-Pinhas, M., S. Barbut, and A.G. Marangoni, *The role of surfactants on ethylcellulose oleogel structure and mechanical properties.* Carbohydrate Polymers, 2015. **127**: p. 355-362.
29. Nikiforidis, C.V. and E. Scholten, *Polymer organogelation with chitin and chitin nanocrystals.* RSC Advances, 2015. **5**(47): p. 37789-37799.
30. Huang, Y., et al., *Hydrophobic modification of chitin whisker and its potential application in structuring oil.* Langmuir, 2015. **31**(5): p. 1641-1648.
31. Patel, A.R., et al., *Biopolymer-based structuring of liquid oil into soft solids and oleogels using water-continuous emulsions as templates.* Langmuir, 2015. **31**(7): p. 2065-2073.
32. Patel, A.R., et al., *A foam-templated approach for fabricating organogels using a water-soluble polymer.* RSC Advances, 2013. **3**(45): p. 22900-22903.
33. Barteri, M., et al., *New stable folding of β-lactoglobulin induced by 2-propanol.* Biochimica et Biophysica Acta - Protein Structure and Molecular Enzymology, 1998. **1383**(2): p. 317-326.

34. Yoshida, K., et al., *A study of alcohol-induced gelation of β-lactoglobulin with small-angle neutron scattering, neutron spin echo, and dynamic light scattering measurements.* Physical Chemistry Chemical Physics, 2010. **12**(13): p. 3260-3269.
35. Havea, P., A.J. Carr, and L.K. Creamer, *The roles of disulphide and non-covalent bonding in the functional properties of heat-induced whey protein gels.* Journal of Dairy Research, 2004. **71**(3): p. 330-339.
36. Haskard, C.A. and E.C.Y. Li-Chan, *Hydrophobicity of Bovine Serum Albumin and Ovalbumin Determined Using Uncharged (PRODAN) and Anionic (ANS-) Fluorescent Probes.* Journal of Agricultural and Food Chemistry, 1998. **46**(7): p. 2671-2677.
37. Schmitt, C., et al., *Multiscale Characterization of Individualized beta-Lactoglobulin Microgels Formed upon Heat Treatment under Narrow pH Range Conditions.* Langmuir, 2009. **25**(14): p. 7899-7909.
38. Schmitt, C., et al., *Internal structure and colloidal behaviour of covalent whey protein microgels obtained by heat treatment.* Soft Matter, 2010. **6**(19): p. 4876-4884.
39. Hines, M.E. and E.A. Foegeding, *Interactions of alpha-lactalbumin and bovine serum-albumin with beta-lactoglobulin in thermally induced gelation.* Journal of Agricultural and Food Chemistry, 1993. **41**(3): p. 341-346.
40. Edwards, P.B., et al., *Chapter 6 - Structure and stability of whey proteins A2 - Thompson, Abby*, in *Milk Proteins*. 2008, Academic Press: San Diego. p. 163-203.
41. Strauch, S. and S. Herminghaus, *Wet granular matter: a truly complex fluid.* Soft Matter, 2012. **8**(32): p. 8271.
42. Shan, H. and Z. Zhang, *Preparation of nanometre-sized ZrO2/Al2O3 powders by heterogeneous azeotropic distillation.* Journal of the European Ceramic Society, 1997. **17**(5): p. 713-717.
43. Hu, Z.S., J.X. Dong, and G.X. Chen, *Replacing solvent drying technique for nanometer particle preparation.* Journal of Colloid and Interface Science, 1998. **208**(2): p. 367-372.
44. Kraiwattanawong, K., H. Tamon, and P. Praserthdam, *Influence of solvent species used in solvent exchange for preparation of mesoporous carbon xerogels from resorcinol and formaldehyde via subcritical drying.* Microporous and Mesoporous Materials, 2011. **138**(1-3): p. 8-16.
45. Betz, M., et al., *Preparation of novel whey protein-based aerogels as drug carriers for life science applications.* Journal of Supercritical Fluids, 2012. **72**: p. 111-119.
46. Giovambattista, N., P.G. Debenedetti, and P.J. Rossky, *Effect of surface polarity on water contact angle and interfacial hydration structure.* Journal of Physical Chemistry B, 2007. **111**(32): p. 9581-9587.
47. Barth, A., *Infrared spectroscopy of proteins.* Biochimica Et Biophysica Acta-Bioenergetics, 2007. **1767**(9): p. 1073-1101.
48. Wellner, N., P.S. Belton, and A.S. Tatham, *Fourier transform IR spectroscopic study of hydration-induced structure changes in the solid state of ω-gliadins.* Biochemical Journal, 1996. **319**(3): p. 741-747.

49. Almutawah, A., S.A. Barker, and P.S. Belton, *Hydration of gluten: A dielectric, calorimetric, and fourier transform infrared study.* Biomacromolecules, 2007. **8**(5): p. 1601-1606.
50. Bouman, J., et al., *Coating Formation During Drying of beta-Lactoglobulin: Gradual and Sudden Changes.* Biomacromolecules, 2015. **16**(1): p. 76-86.
51. O'Loughlin, I.B., et al., *Concentrated whey protein ingredients: A Fourier transformed infrared spectroscopy investigation of thermally induced denaturation.* International Journal of Dairy Technology, 2015. **68**(3): p. 349-356.
52. Shivu, B., et al., *Distinct beta-Sheet Structure in Protein Aggregates Determined by ATR-FTIR Spectroscopy.* Biochemistry, 2013. **52**(31): p. 5176-5183.
53. Stănciuc, N., et al., *Fluorescence spectroscopy and molecular modeling investigations on the thermally induced structural changes of bovine β-lactoglobulin.* Innovative Food Science & Emerging Technologies, 2012. **15**: p. 50-56.
54. Deville, S., et al., *Freezing as a path to build complex composites.* Science, 2006. **311**(5760): p. 515-518.
55. Lee, J. and Y. Cheng, *Critical freezing rate in freeze drying nanocrystal dispersions.* Journal of Controlled Release, 2006. **111**(1-2): p. 185-192.
56. Hyun, K., et al., *Large amplitude oscillatory shear as a way to classify the complex fluids.* Journal of Non-Newtonian Fluid Mechanics, 2002. **107**(1-3): p. 51-65.

Chapter 7

General discussion

Introduction

In many food applications, proteins are used for their high nutritional value, for functional properties such as their ability to modify viscosity, gelling ability, and their ability to stabilize oil-water or air-water interfaces. This thesis is concerned with extending this protein functionality towards being an effective structuring agent for a continuous oil phase, leading to a so-called oleogel. The aim of this thesis was to design effective routes to structure oil using protein building blocks and understand the mechanical aspects of the resulting oleogels. The main findings of this thesis are discussed below and are summarized in a schematic representation in Figure 7.1.

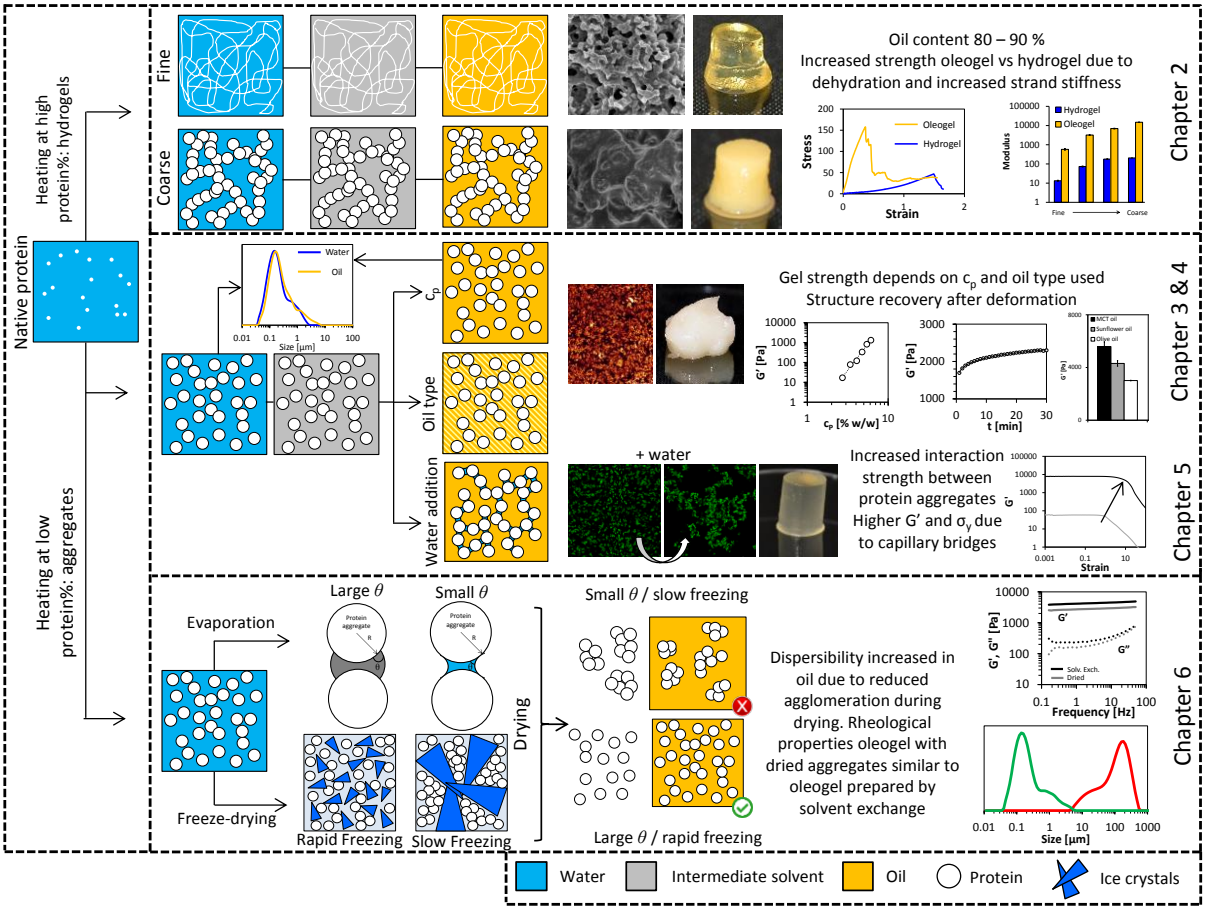

Figure 7.1. Overview of the main results of this thesis.

In Chapter 2, a novel method was presented to create protein-based oleogels by incorporating liquid oil into a heat-set Whey Protein Isolate (WPI) gel matrix by a solvent exchange procedure. After being transferred to the oil phase, the pre-set gel matrix was capable of incorporating a large amount of liquid oil (80 – 90%). In Chapter 3, protein oleogels were prepared using a similar solvent exchange procedure from small, submicron protein aggregates. This route was explored to enhance the control over network formation. The protein aggregates, at sufficiently high concentration, formed an elastic network with fractal characteristics. In Chapter 4, the interactions

between the protein aggregates (described in Chapter 3) were altered by using different types of oil. Indeed, the gel strength was affected by the type of oil used in the preparation of the oleogels. The gel strength was shown to reduce upon increasing oil polarity. Furthermore, it was shown that the elastic network was prone to yielding at low deformations, but the protein aggregates rapidly reformed a network once the deformation was reduced. Next, in Chapter 5, water was added in order to further tailor the gel properties and explore the function of water in protein based oleogels. It was shown that G' and the yield stress of the gels can be greatly increased by adding small quantities of water. This increase was mainly attributed to the formation of capillary bridges between the protein aggregates. Upon heat treatment, the network was strengthened even further. Lastly, in Chapter 6, the underlying mechanism for the degree of dispersibility of protein aggregates in oil was studied to examine an alternative for the solvent exchange procedure for dispersing protein aggregates in oil. The degree of agglomeration in protein powders was the determining factor for oil dispersibility, and this was shown to be related to the nature of the solvent it was dried from. When the solvent had a high wetting angle (apolar solvents) and low surface tension, agglomeration was largely reduced, making the protein powder well dispersible in liquid oil. Agglomeration was also reduced by increasing the freezing rate of the sample, preceding the step of sublimation of the water by freeze-drying. The resulting dried protein aggregates resulted in oleogels with similar rheological properties as the protein oleogels obtained via the solvent exchange method. As such, two routes to produce protein aggregates that are dispersible in oil have been identified: a solvent exchange procedure and a rapid-freezing route.

The route from protein hydrogels to protein oleogels

Protein isolates are widely available in a native, powdered form. Obtained usually by spray drying, such protein powders are prone to a large degree of agglomeration and sedimentation and do not readily dissolve in liquid oil, as is the case for WPI. To be able to gelate oil using proteins, an alternative route has to be used. To use predominantly hydrophilic biopolymers such as proteins for the formation of a network in liquid oil, a carefully designed process is necessary in which water is removed and substituted for liquid oil. In current available literature, emulsion or foam-templated approaches have been described to be able to use hydrophilic polymers as oil gelators [1, 2]. In this approach, the hydrophilic polymers are absorbed at the oil-water or water-air interface to form a space spanning network. Upon subsequent removal of the water by freeze-drying, the obtained dehydrated emulsion or dry foam is subsequently sheared to create oleogels. Although highly interesting, this process has the inherent limitation of poor control over the size of the building blocks and the subsequent gel strength of the resulting network. In this thesis, alternative processes were explored.

Using solvent exchange to create protein oleogels

In the current thesis, the initial route to transform aqueous protein gels or aqueous suspensions of protein aggregates to protein oleogels was based on a solvent exchange procedure. In Chapter 2, we have shown that a simple solvent exchange is an effective way to remove the water from a protein hydrogel and replace the water for liquid oil. This procedure involves the use of an intermediate solvent that is oil miscible. We chose acetone or tetrahydrofuran (THF) for this intermediate solvent. These solvents are fully miscible with both water and oil, and could therefore be used to create a full range of solvent mixtures with different polarity. Although this simple procedure was found to be highly effective to be able to create protein-based oleogels, solvents such as acetone or THF are not common in food preparation. Even though the remaining acetone concentration in the oleogel is low (~ 2 ppm), as discussed in Chapter 3, and the toxicity levels of acetone are generally considered to be low, the use of large quantities of these solvents for applying a solvent exchange procedure hampers the practical applicability of this method nonetheless. Designing an alternative process would therefore be required to use protein-based oleogels on a large scale. Based on the results of this thesis, some possible alternatives will be given, which will be discussed later.

Designing stable protein building blocks

Since proteins do not dissolve readily in oil, let alone assemble into a network, an alternative is to first prepare protein building blocks in the aqueous phase. These building blocks can be prepared by heating an aqueous WPI solution to induce network formation. Increasing the temperature changes the structure of proteins in such a manner that hydrophobic groups become exposed to the solvent. Moreover, sulfhydryl and cysteine groups become chemically reactive. As a result, monomeric proteins start to polymerize through the formation of both physical and chemical bonds [3]. The resulting protein aggregates, stabilized by hydrophobic interactions and intermolecular disulphide bonds, were used as starting material either linked together as macroscopic gels (Chapter 2), or as dispersed submicron protein aggregates (Chapter 3-6). For both the hydrogels and submicron aggregates, the heating process does not lead to incorporation of all protein material into the gel. As shown in Chapter 6, after preparing the aggregates a considerable amount (~ 20%) of protein was still present in the liquid phase, and the composition of the soluble proteins was different from that incorporated into the aggregates. A higher fraction of α-lactalbumin was found in the soluble fraction, as it lacks a free thiol-group for the formation of disulphide bridges [4, 5]. The interactions that are involved in protein aggregation should therefore be taken into account to evaluate the suitability of proteins to form aggregates able to act as building blocks to gelate oil.

Although the results described in the previous chapters were limited to WPI as the protein source (Figure 7.2A), other proteins were examined for their ability to form protein oleogels as well. When egg-ovalbumin was used to create heat-set gels, the resulting network structure was also able to incorporate a considerable amount of oil (Figure 7.2B). However, when gelatin was used, the material collapsed, as can be seen in Figure 7.2C. The reason for this behaviour can likely be found in the type of interactions that are involved in the gelling mechanism. For the globular proteins whey and ovalbumin, the applied heat treatment causes irreversible aggregation by the formation of intermolecular disulphide bonds [6]. Instead, gelatin gels are created by reversible aggregation. More specifically, gelatin in water forms gels by helix formation through hydrogen bonding. In this case, the addition of acetone led to a large degree of swelling of the gelatin gels and a loss of their gel-like character. As the solvent quality for the protein is reduced further, i.e. when oil is subsequently added to the solution, the gelatin molecules collapsed onto each other, without incorporating any oil. A similar collapse of gelatin gels in water – acetone mixtures has been reported before [7].

These results show that the type of interactions involved in creating the aqueous protein gels is important for their stability throughout the solvent exchange procedure and their stability in oil. Therefore, in choosing a protein source to design building blocks suitable for structure formation in oil, the ability to form disulphide bonds is important as it leads to the formation of rigid and chemically stable building blocks whose interaction, once formed, does not strictly depend on the nature of the solvent. Indeed, disulphide interactions are reported to give resistance to structural rearrangements and gel coarsening [8]. It is likely, like in the case of gelatin, that protein gels stabilized only through physical bonds like hydrophobic interaction, or hydrogen bonds are less suitable for structure formation in oil when a solvent exchange procedure is applied, since the introduction of a solvent of another polarity will induce structural rearrangements when possible. In particular, aggregates stabilized through hydrophobic interactions only are prone to disintegration when present in oil, due to increased hydrophobic protein-solvent interactions. A similar observation was made by Betz et al. [9], where heat-set WPI gels were used as precursors for supercritical drying. The authors observed that gels prepared at acidic pH disintegrated when following a solvent exchange using ethanol. This could be due to the lack of sufficient disulphide bond formation as lowering the pH inhibits their formation [10].

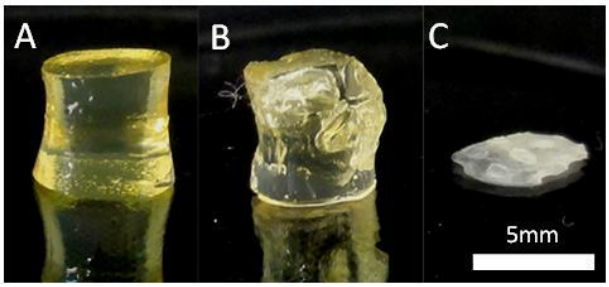

Figure 7.2. Appearance of a protein gel matrix after applying a solvent exchange from water to sunflower oil, using acetone as an intermediate solvent. A: whey protein isolate, B: egg-ovalbumin, C: bovine gelatin.

Instead of starting with a macroscopic gel, it would be beneficial to control the network formation by using smaller protein building blocks. In preliminary experiments, it was observed that the size of the building blocks is important; protein building blocks (aggregates) should be large enough to be harvested by centrifugation, and small enough to provide enough surface area for contact between the aggregates to form a network. Moreover, like in the case of macroscopic protein gels, the aggregates should be stable to prevent disintegration during the solvent exchange. When heat-set aggregates were prepared under controlled conditions, aggregates of 150 – 200 nm were obtained, as described in Chapter 3. These aggregates did not disintegrate due to internal covalent disulphide bonds, as shown in Chapter 6. After centrifugation of the aggregates oil dispersion, the sediment could be readily dispersed in oil using conventional shearing techniques without affecting the initial particle size. This allowed for efficient network formation using these submicron protein aggregates into oleogels, as shown in Chapters 3-6.

Protein aggregate interactions in oil versus in water

To be able to control the network formation and the resulting rheological behaviour of the protein oleogels, the interactions between the protein aggregates in oil should be understood. Interactions between proteins and protein aggregates in water are well studied. The number of studies on interactions between proteins in an oil phase are practically nil. In the following section, the different contributions to interactions between proteins in liquid oil will be discussed and compared to the interactions occurring between proteins in water.

Electrostatic interactions

Electrostatic interactions between proteins or between protein aggregates in an aqueous environment are rather well-described. Due to ionisable groups on the protein surface, counter ions separate from the protein surface leading to the formation of a so-called electric double layer. In a nonpolar solvent however, the formation of charged species is energetically disfavoured since

ions do not dissolve in the nonpolar oil. In solvents with a low dielectric permittivity (ε_r ~ 2), interactions based on charges have a much longer range than in solvents with a high dielectric constant. This is quantified by the Bjerrum length (λ_B), which is defined as the distance between two charged species at which the Coulombic energy matches the thermal energy and is given by:

$$\lambda_B = \frac{e^2}{4\pi\varepsilon_o\varepsilon_r k_B T} \quad (7.1)$$

where e is the elementary charge, ε_0 is the permittivity of free space, k_B is the Boltzmann constant, and T the absolute temperature. In water (ε_r ~ 80), the Bjerrum length, λ_B, is 0.71, while in oil (ε_r ~ 3) λ_B ~ 19 nm, which makes the formation of charges in oil an energetically unfavourable process. Electrostatic interactions in oil are therefore minimal, as dissociation of surface charges from the surface of the protein aggregates is unlikely to occur. The stabilization of charges in non-polar media is possible by the addition of surfactants [11, 12]. Surfactants are able to act as charge carriers in non-polar systems, and can induce electrostatic stabilization. Since charge control agents were not used in the systems described in this thesis, electrostatic effects between the protein aggregates in oil are assumed to be negligible.

Van der Waals interaction

The van der Waals forces contribute to the attractive forces between the protein aggregates in the oil. The van der Waals force between two spherical particles with a radius *R* can be calculated using [13]:

$$F_{vdW} = \frac{A_H R}{12D^2} \quad (7.2)$$

where *D* is the distance between the two particles and A_H is the Hamaker constant. For two identical phases (1) acting across a medium (2), using their dielectric permittivity, ε_1 and ε_2, and their refractive index, n_1 and n_2, A_H can be calculated according to [13]:

$$A_H = \frac{3}{4}k_B T\left(\frac{\varepsilon_1-\varepsilon_2}{\varepsilon_1+\varepsilon_2}\right)^2 + \frac{3h\nu_e}{16\sqrt{2}}\frac{\left(n_1^2-n_2^2\right)^2}{\left(n_1^2+n_2^2\right)^{3/2}} \quad (7.3)$$

where *h* denotes Plank's constant, and ν_e denotes the electronic absorption frequency for the dielectric permittivity (3 x 10^{15} s^{-1}). Taking the values for the dielectric permittivity and refractive index as given in Table 7.1, and a particle radius of 75 nm at contact (where *D* ~ 0.2 nm), we find

F_{vdW} equals ~ 0.4 nN for protein aggregates in sunflower oil and ~ 0.9 nN for protein aggregates in water. As discussed in Chapter 4, different oil types affected the protein – protein interactions and therefore the resulting gel strength. In Chapter 4, we only took into account the hydrophobic interactions and hydrogen bonds. We did not take into account the van der Waals interactions. However, as the refractive index and dielectric constant for these oils are different, the van der Waals force between two protein aggregates in the oils will also be different. Indeed, with increasing polarity of the oil, the refractive index increases as MCT oil has n ~ 1.45 (low polarity) and for extra virgin olive oil n ~ 1.47 (high polarity). Based on these values, the van der Waals force between two protein aggregates (assuming ε to be ~ 3 for both oils) increases with a factor 1.4 from 0.33 nN in extra virgin olive oil to 0.45 nN in MCT oil. Given that we see an increase in the according gel strength (G') with a factor 1.8 of MCT compared to olive oil, the increased van der Waals force might have a contribution to this effect. However, the fact that the highest gel strength was observed for transparent oleogel samples, as described in Chapter 5, indicates that the van der Waals interactions cannot be solely responsible for this effect. If the sample is transparent, this indicates that the refractive index of the protein aggregates matches that of the solvent and consequently, that F_{vdW} ~ 0. Hence, attractive interactions other than van der Waals interactions have to be responsible for the network formation. Indeed, in Chapter 5, it was shown that upon water addition the gel strength increases considerably, which shows the importance of hydrogen bonds and capillary forces as attractive force contributions.

Table 7.1: Dielectric permittivity and refractive index for the different media.

	Dielectric permittivity, ε (298 K)	Refractive index, n (298 K)
Water	80	1.33
Sunflower oil	3[a]	1.46
Protein, hydrated	10[b]	1.45
Protein, dehydrated	10[b]	1.54

[a] *Obtained from ref. [14]*

[b] *Obtained from ref. [15]*

Hydrogen bonds

In aqueous environments, hydrogen bonds are formed between a hydrophilic particle surface and water molecules, which causes hydration of the surface, giving rise to a repulsive hydrophilic force, also known as the hydration- or solvation force (Figure 7.3A) [16]. In non-polar media, due to its composition, limited hydrogen bond formation is possible between the particle and the solvent. Instead, hydrogen bonds can be formed between two dispersed particles, leading to an attractive force between them. Exposed polar side groups on the particles, containing hydroxyl

groups, have unfavourable interactions with the surrounding oil, but favourable interactions with polar side groups on other particles, giving rise to attractive inter-particle hydrogen bonds (Figure 7.3B). Hydrogen bonds form at a distance of ~ 0.24 nm and are much stronger than the van der Waals forces [13]. Therefore, hydrogen bonds between particles are considered to contribute to a large extent to the gelation of nonpolar solvents [17, 18]. In Chapter 5, it was indeed noted that the gel strength already increased at low water additions, which shows the importance of hydrogen bond formation. As discussed in Chapter 4, the different oil types have an effect on the interactions between the particles. Oils have a different polarity, as shown by the difference in interfacial tension. It is likely that more polar, unrefined oils such as extra virgin olive oil, contain a larger amount of polar substances that have favourable interactions with exposed polar groups on the surface of the protein aggregate, thereby limiting the available attractive particle-particle interactions. Oils with the ability to form hydrogen bonds through hydroxyl group, such as castor oil, are even able to limit particle-particle interactions to such extent that gel formation is inhibited. However, a further study is needed to quantify the contributions of the different interactions. Of importance would be to separate the forces arising from van der Waals forces and hydrogen bond formation, either by carefully changing the solvent composition, or by modifying the surface of the protein aggregates.

Hydrophobic interaction

In water, during heat-induced gelation of globular proteins, hydrophobic interactions are perhaps the most dominant physical interaction between two denatured proteins. Besides intermolecular disulphide bridging, hydrophobic interactions are important for the formation of aggregates and hydrogels. This interaction arises from the lower entropy state of water molecules at the surface of an exposed hydrophobic patch on the particle, effectively pulling the two hydrophobic parts together as they approach, thereby increasing the entropy of the water molecules by their release into the region far away from the surface. This results in an attractive force, whose magnitude and range is much larger (D ~ 10 – 20 nm) than the van der Waals force [16], as shown in Figure 7.3A. In liquid oil, however, exposed hydrophobic patches on the protein aggregates have a favourable interaction with the nonpolar solvent. This interaction can therefore be seen as a solvation force of a repulsive nature, as indicated in Figure 7.3B.

Capillary forces

As was shown in Chapter 5, adding water to a suspension of protein aggregates in oil greatly increased the gel strength. It was found that upon water addition, protein aggregates cluster more

densely together in the space spanning network. The added water was found to migrate into the protein aggregates, as observed by a change in the refractive index. Water could be added up to 0.5 g / g protein before free water droplets were observed. As a result of water residing at the surface of the aggregates, a liquid bridge can be formed between two aggregates. This liquid bridge is known as a capillary bridge, resulting in very strong attractive interactions. The attractive force between two particles upon contact as a result of such a liquid bridge, can be given as:

$$F_c = 2\pi R\gamma \cos\theta \qquad (7.4)$$

where R is the particle radius, γ is the surface tension of the liquid with the surrounding environment and θ is the contact angle of the liquid and the solid particle. Assuming the interfacial tension to be 30 x 10^{-3} Nm^{-1} and taking R as 75 nm, the resulting capillary force is 14 nN in the case the wetting angle is zero, so $\cos\theta = 1$. This is much larger than the calculated van der Waals force in oil. It is therefore easy to see that when attractive capillary forces are present, this effect dominates. The possibility for formation of these bridges is highly related to the water activity (a_w) of the system. It was shown previously that for capillary bridges to form, a_w should be > 0.7 [19, 20]. Another important consideration is when the particles are porous and capable of absorbing the added secondary liquid, the formation of capillary bridges is greatly reduced [21]. As mentioned in Chapter 5, the combined contribution of the small size of the protein aggregates, the relative large amounts of water added, and the large a_w of the oil suspension (a_w > 0.7), the observed rapid increase in G' is likely to be related to the formation of a capillary suspension. The introduction of strong capillary interactions provides a promising way to effectively alter the mechanical properties of the resulting oleogels.

In literature, two types of capillary suspensions are distinguished. One state, the so-called 'capillary state' is formed when the contact angle between the particle and the added secondary liquid is > 90°. Alternatively, a 'pendular state' suspension is formed when the contact angle is < 90° (see Figure 7.1). Since water is expected to have a low contact angle with the protein aggregates in oil, the protein aggregate suspension will likely be in the pendular state. Interestingly, when this water is removed, as shown in Chapter 5, the gel structure remained (Figure 7.4C), indicating strong interactions without the presence of the water bridges. In the case the suspension is in the pendular state, the aggregates are drawn to each other as the water evaporates, as a result of the strong capillary action. This is not the case for capillary state suspensions (i.e. large θ), where the suspension returns to its original state upon removal of the secondary liquid [22]. Both effects have been observed in the protein aggregate suspensions, as discussed in Chapter 6. As shown,

the conditions during drying of a suspension of protein aggregates determine to a large extent the interactions between the aggregates. When the protein aggregate suspension was dried from a solvent with a high polarity (low contact angle), the capillary bridges formed between the particles induced a strong attractive force during drying. This resulted in a highly agglomerated powder, incapable of being dispersed well in oil, indicating a large degree of attraction between the protein aggregates. In contrast, when the protein suspension was dried from solvents with a high contact angle, such as hexane, agglomeration reduced noticeably due to the lower capillary forces involved in this case, as also predicted by equation 7.4 and schematically depicted in Figure 7.1. The results show that capillary forces are important in controlling both favourable as well as unfavourable agglomeration between protein aggregates.

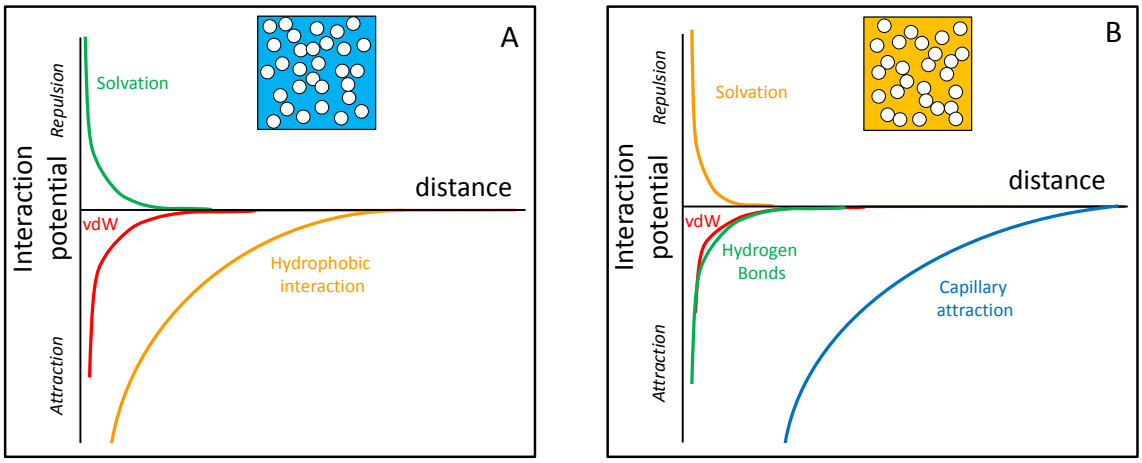

Figure 7.3. Schematic representation of the interactions involved between protein aggregates in water (A) and in liquid oil (B). In both figures, repulsive forces as a result of electrostatic interaction are not taken into consideration.

Protein gelation in water versus gelation in oil

The results as laid out in the current thesis, allow to speculate on a comparison between the 'conventional' protein gelation in water, and protein gelation in oil. Figure 7.3 gives a schematic overview of the nature of the repulsive and attractive interactions in water and oil. In Figure 7.4, the interactions are specified for the different oleogels studied. Here, we will compare protein hydrogels and protein oleogels based on two examples. The first example relates to the results in Chapter 2, where a protein oleogel was created based on a pre-set protein hydrogel. The second example that will be discussed is that of creating gels from pre-formed heat-set protein aggregates. In aqueous systems, gelation can be achieved by removing the electrostatic repulsive barrier by acidification or by adding salt. In this case, the protein aggregates interconnect into so-called 'cold-set' gels.

In Chapter 2, we compared the large deformation properties of protein oleogels to their preceding hydrogels. In these gel matrices, the water was effectively exchanged for oil as the measured remaining water content in the oleogels was very low (~1%). Compared to the preceding hydrogels, the resulting gel strength had increased substantially for the oleogels, as the gel stiffness (Young's modulus) and fracture stress had increased roughly two orders of magnitude. In the case of exchanging the solvent inside a pre-set protein gel matrix, the proteins in the existing network are already in close contact, stabilized by covalent disulphide bonds. In such a network, exposed hydrophilic side groups have favourable interactions with water as the solvent, but when the solvent quality is reduced in the case of oil, particle-solvent interactions decrease. Since the proteins are trapped in a network, the possibilities for free particle rearrangements is limited. In this case, the network maximizes protein – protein interactions within the protein strands, minimizing contact with the solvent and hence shrinkage was observed. Moreover, water is not only removed from the interstitial areas in the protein network, but also within the protein strands that make up the network. It is likely that oil is to a lesser extent able to migrate within these close-packed protein strands on a molecular level, causing a contraction and consequent stiffening of the strands.

When proteins are dispersed in oil as submicron aggregates, their interactions lead to the formation of paste-like gels (Figure 7.4B). The measured storage modulus, G', as a measure of gel strength, arises from protein-protein interactions that build a network of protein aggregates of fractal nature. The measured gel strength, however, is lower compared to cold-set whey protein hydrogels at comparable concentrations [23-25]. Indeed, in preliminary experiments, the measured gel strength of the aggregates in water was found to be higher than in the case the same aggregates were dispersed in oil. This is somewhat counterintuitive when predicting gel strength solely based on the concept of lowering the solvent quality, as discussed previously for the pre-set gel matrices. In fact, we need to consider both attractive and repulsive forces between proteins in the two solvents, as schematically depicted in Figure 7.3. In this case, in both water and oil, electrostatic interactions are negligible, which seems justified as in the case of cold-set protein hydrogels, the electrostatic double layer is reduced significantly.

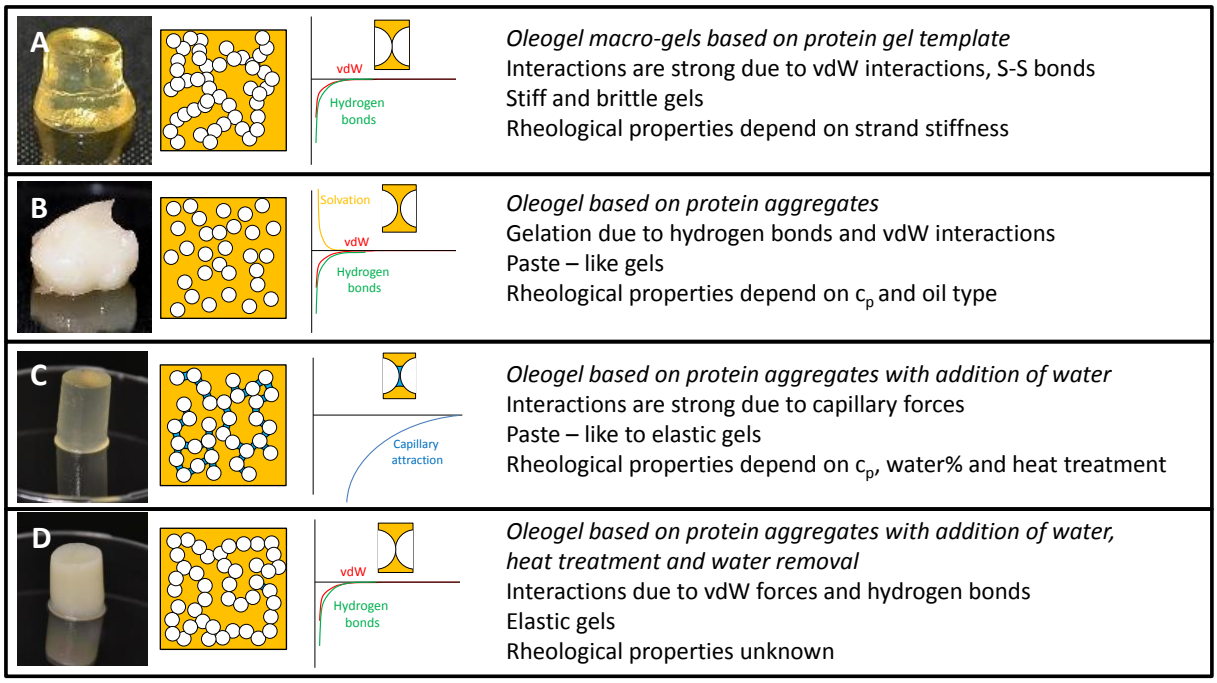

Figure 7.4. Different interactions for oleogel formation using proteins A) based on protein gel template, B) based on protein aggregates, C) based on protein aggregates and resulting from the formation of capillary bridges by adding water, D) based on protein aggregates and resulting from formation and subsequent removal of capillary bridges.

In the case of cold-set gelation of pre-heated protein aggregates in water, due to the removal of the electrostatic repulsion, exposed hydrophobic groups on the surface of the aggregates cause an attractive interaction between heat-denatured aggregates. This is counteracted by solvation forces, arising from favourable interactions through hydrogen bonding between the protein aggregates and the surrounding water. As in this case the hydrophobic interactions are much stronger than the solvation forces, aggregation of the proteins occurs and results in the formation of firm gels. In case the protein aggregates are dispersed in oil, aggregation is induced via polar interactions. In this case, exposed polar groups result in particle – particle interactions, counteracted by a repulsive force, arising from solvation forces of hydrophobic nature as shown in Figure 7.4B. It seems that the attractive hydrophobic forces between protein aggregates in water are larger than the attractive forces through polar interactions (hydrogen bonds) between proteins in oil.

To form hydrogen bonds between the aggregates in oil, the aggregates have to be able to approach each other at close distance. However, the large triglyceride molecules of the oil are likely to give rise to an oscillatory attractive-repulsive force at small distances, of orders of magnitude larger than the van der Waals force at these distances. This effect is analogous to the effects described for a range of hydrophobic solvents [26]. The repulsive contribution was attributed to the packing of the hydrophobic molecules between the surfaces; as the distance becomes smaller by forcing the surfaces together, oil molecules need to be 'squeezed out' at

certain regular distance intervals between the surfaces. The regular distance intervals correlate with the molecular size of the triglycerides. In order to have aggregates in oil come together spontaneously, an attractive force would be required to overcome this repulsive force. Van der Waals forces are not strong enough to accomplish this, and additional attractive forces are required. Such an additional attractive force could be provided by capillary bridges, as was shown for mica surfaces in triolein [19]. As shown in Chapter 5, once water is added, strong attractive interactions are obtained, presumably according to hydrogen binding and/or due to the formation of capillary bridges (as schematically depicted in Figure 7.4C). During removal of the water, the hydrogen bonding and strong capillary interactions drive the protein aggregates together (Figure 7.4D). At the resulting close distance, the van der Waals interaction is now strong enough to keep the particles together, even in the absence of the capillary bridges.

Towards feasible protein oleogel preparation

As was shown in Chapter 3, the solvent exchange procedure leads to high dispersibility of the protein aggregates with a low degree of agglomeration, thereby retaining the small size of the protein aggregates when dispersed in oil. In contrast, freeze drying a suspension of protein aggregates led to agglomeration and low dispersibility. This agglomeration was found to be reversible in water, but irreversible in oil as shown in Chapters 3 and 6. This irreversible agglomeration is highly unfavourable, as it reduces the amount of available surface area for effective protein-protein interactions in oil. Even though the solvent exchange procedure is able to retain a similar size distribution of protein aggregates, the process itself is highly unfavourable as it has inherent practical limitations due to the large amount of solvent required. Therefore an alternative process for the solvent exchange procedure is required when used on an industrial scale.

The results in Chapter 6 show that the high dispersibility of the protein aggregates is not related to changes in the protein conformation. Unlike native protein, whose conformation can change distinctly upon introducing solvents like ethanol [27] acetonitrile [28], DMSO [29], or hexane [30], heat denatured proteins showed no change in the protein conformation or its protein composition as a result of applying a solvent exchange procedure. Structural changes, therefore, are not necessary for enhanced dispersibility and the only requirement in designing an alternative process to the solvent exchange procedure is preventing particle agglomeration.

One alternative approach to the solvent exchange procedure would be to design a process to produce a protein powder that is free of large agglomerates. As such, a dried protein powder of

protein aggregates could be obtained that is directly dispersible in liquid oil. As described in Chapter 6, drying processes can lead to large compressive forces between the aggregates, leading to irreversible agglomeration. Such forces may arise from capillary action [31, 32] or through the formation of large ice crystals, expelling the protein aggregates from the frozen areas and forcing them to cluster together [33, 34]. Agglomeration during drying can be prevented by:

1) Prevention of strong capillary forces, and/or
2) Prevention of freeze-concentration

Capillary forces can be prevented to a large extent by using solvents with a low surface tension and high wetting angle during evaporation. As shown in Chapter 6, solvents such as hexane are able to prevent agglomeration during evaporation and freeze-concentration can be limited by applying high freezing rates prior to freeze-drying. Although the process of rapid freezing or using solvents as hexane are still of limited practical applicability, the results show that dried protein aggregates can be easily dispersed into oil when the drying process is carefully designed. The drying process could be optimized by identifying suitable hydrophobic solvents during drying, or by altering the freezing rate and the concentration of the protein aggregate suspension.

To further increase practical applications, other alternative processes may be considered, such as supercritical liquid CO_2 drying. The advantage of liquid CO_2 drying is that the formation of an interface and subsequent interfacial tension, leading to capillary forces, is avoided [35, 36]. As liquid CO_2 has a limited solubility in water, this process would still require the protein material to be transferred to another, more suitable solvents like alcohols. Nevertheless, given the fact that CO_2 drying is commercially available, it could be a suitable alternative. Next to air- or freeze-drying, pervaporation could be an interesting alternative to the solvent exchange method. During pervaporation, a liquid mixture is fed over a membrane where a vacuum is created at the permeate side, whilst the feed side of the membrane remains at atmospheric or elevated pressure. This pressure difference creates a driving force for selective permeation through the membrane, where the permeant evaporates at the membrane surface due to the low pressure [37, 38]. It was shown that pervaporation can be used to efficiently and economically remove water from isopropanol-water mixtures [39]. A similar process could be applied to remove water from a protein suspension in a water-alcohol mixture, leaving a dehydrated alcohol retentate, containing the protein aggregates. Further processing by adding oil and subsequent distillation would be technically feasible.

Besides changes in the process, also changes in the composition could form the basis of an alternative approach. Emulsifiers could be used to enhance the dispersibility of protein aggregates

in the oil. In the patent literature, a method is described in which proteins fibrils are covered with a large amount of surfactant, prior to drying [40]. The surfactants prevent the agglomeration during drying due to steric repulsion between the particles. After mixing the protein-surfactant complexes into oil, gels can be obtained. Alternatively, polymers like gelatin can also be added to a water-in-oil emulsion. Here, the gelatin dissolves in the water phases, leading to gelation of the sample [41, 42]. In both cases, a large amount of surfactant is needed to increase the dispersibility of the proteins in the oil phase. However, the surfactants may limit inter-particle interactions due to steric repulsion. Nevertheless, since there are several potential ways of transferring proteins to the oil phase, future research will be necessary to determine their individual potential.

Towards feasible protein oleogel applications in food systems

Although the rheological properties of protein oleogels can be tuned to some extent, their use as a solid fat alternative in 'real' food applications is yet to be determined. As a first attempt, to assess whether protein oleogels are capable of replacing solid fat, shortbread cookies and frankfurter style sausages were prepared. The protein oleogel replaced margarine (30 wt%) in the shortbread cookie recipe and pork fat (25 wt%) in the sausage recipe. As a control, sunflower was also used as replacement for either margarine or pork fat.

For the preparation of food grade oleogels, significant changes needed to be made. Instead of demineralized water, regular tap water was used to dissolve WPI, and the pH was adjusted by adding acetic acid instead of HCl. To perform the solvent exchange procedure, food-grade ethanol was used instead of acetone. Although ethanol dissolved to a lesser extent in the sunflower oil, a similar paste-like oleogel was obtained after evaporation of the ethanol, with no noticeable differences compared to when acetone was used. However, no additional testing of particle size or gel strength was done.

Shortbread cookies

For the preparation of the cookies, after mixing all the ingredients together, the batter was cut into disks of 0.5 cm thick and with a diameter of 5 cm. To enhance the flavour of the oleogel and sunflower oil cookie, a few drops of butter aroma was added to the batter. Thereafter, the samples were baked in an oven for 15 min at 170 °C. It was noticed that the added sugar did not dissolve properly and was therefore partially replaced for glucose syrup.

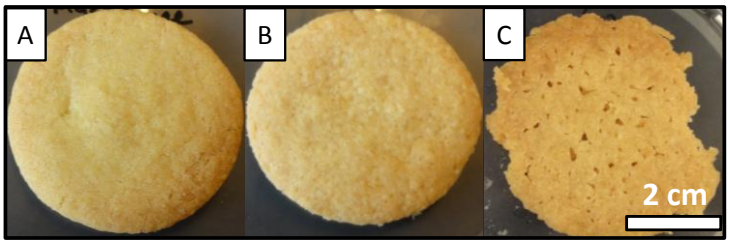

Figure 7.5. Appearance of shortbread cookies prepared with (A) margarine, (B) protein oleogel and (C) sunflower oil.

The appearance of the baked cookies can be seen Figure 7.5. The standard recipe with margarine resulted in a typical solid cookie, as seen in Figure 7.5A. As expected, the replacement of margarine by sunflower oil resulted in an inferior product, as the oil leaked out heavily (Figure 7.5C). The resulting product was very brittle, with little cohesion. Therefore, no further testing was done with this sample. The oleogel cookie (Figure 7.5B) on the other hand, showed a much better appearance. The cookie showed some spreading during baking, and after cooling a firm product was obtained. As seen from the cross-section, a decent crumb structure had formed (Figure 7.6). It shows that, at least as a first attempt, replacement of margarine with a protein oleogel resulted in an acceptable appearance.

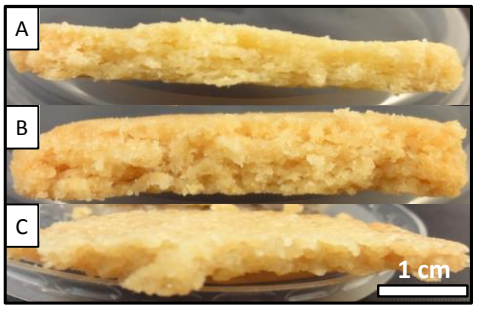

Figure 7.6. Cross section of shortbread cookies prepared with (A) margarine, (B) protein oleogel and (C) sunflower oil.

Frankfurter-style sausages

To prepare the meat batter, lean pork meat batter was kindly provided by Darling Ingredients, to which either pork fat, protein oleogel, or sunflower oil was added together with 25% ice water, salt, and spices. Sausages were prepared in plastic casings and were heated at 78 °C for 15 min. After cooling, samples were stored at 4 °C overnight, before removing the casing and further testing. The appearance of the sausages can be seen in Figure 7.7. A difference was noted for the sunflower oil samples, where oil leakage was observed after heating and overnight storage, which was not observed for sausages with either pork fat or oleogel.

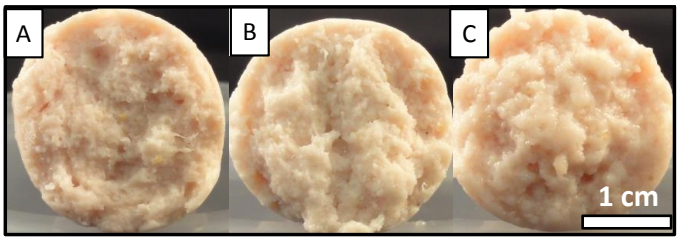

Figure 7.7. Appearance of cross section of frankfurter sausages prepared with (A) pork fat, (B) protein oleogel, (C) sunflower oil.

Textural properties

In order to assess whether a simple 1 to 1 replacement of the margarine in the cookie or pork fat in the sausages with oleogel or sunflower oil would result in an acceptable product, the texture of the food products were tested using a texture analyser (TA.TX plus, Stable Micro Systems Ltd., Godalming, UK). For the cookies, a 3-point bending test was performed. By applying a constant deformation speed, the force was measured to break the sample. For the sausages, cylindrical shaped samples were deformed at a constant deformation speed until 60% deformation. The resulting force – distance curves are shown for the cookies in Figure 7.8A, and for the sausages in Figure 7.8B. For the cookies, a clear fracture point can be identified by the peak force measured to break the sample. As can be seen, the standard cookie was much firmer compared to the oleogel cookie, indicated by a higher fracture force. The deformation at fracture was similar for both samples. For the sausages, no large differences are observed. The sample prepared with sunflower oil was slightly less firm, and the oleogel sausage was slightly more firm compared to the standard product.

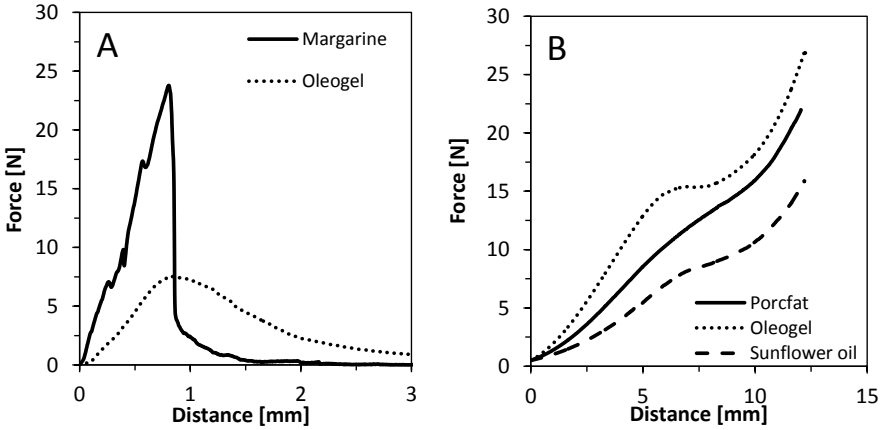

Figure 7.8. (A) Force-distance curves of a 3-point bending test of shortbread cookies prepared with margarine or protein oleogel. (B) Force-distance curves for frankfurter-style sausages prepared with pork fat, protein oleogel or sunflower oil.

Sensory perception

Next, the two products were tested for sensory evaluation by an untrained panel (n = 10). Panellist were asked to rate several attributes on a line scale from low – high. For the cookies, the attributes of interest were 'crunchy', 'fatty', 'mouth coating', and 'overall liking'. Panellists found the margarine cookie more crunchy ($p < 0.01$), as was expected from the results of the three-point-bending tests. Interestingly, the attributes 'fatty' and 'mouth coating' were rated higher ($p < 0.01$) for the cookie prepared with the oleogel. It is however unclear whether this is related to the structure of the cookie, the difference in recipe, or due to the presence of the oleogel. The overall liking, however, was higher ($p < 0.01$) for the standard cookie. Qualitatively though, it was noted that some panellists liked the oleogel cookie better, due to the more crumbly texture. The results of the sensory evaluation of the different sausages did not lead to significant differences among the attributes tested, except the attribute 'firmness'. The sausage prepared with sunflower oil was perceived as less firm, compared to the other two sausages. Although the sensory tests can only be seen as a first trial, and many factors that might contribute to the sensory perception were poorly controlled, the results are promising and further evaluation of the potential of the oleogels as a fat replacer would be highly interesting.

Outlook and recommendations

Development of non-TAG structure formation in lipid phases has increased during the last years, and is likely to continue in the near future as finding a versatile replacement for saturated and *trans* fat is still of high interest. This thesis gives, as a first attempt, an idea on how such a structure in oil can be created using proteins. This thesis showed that proteins have interesting properties as an alternative structuring agent for oil.

Using proteins as a structuring agent for lipid phases, a wide diversity of structures can be obtained. Interactions between the proteins can, to some extent, be controlled and the rheological properties of the resulting protein oleogels can be tuned. Although the versatility in the structure design has in principle a great potential, a practical production method for protein oleogels is still lacking. Therefore, an alternative for the solvent exchange procedure would be highly desired. Of importance is to prevent particle agglomeration and some aspects to control this are identified in this thesis. Of particular interest is the development of alternative water removal processes.

In the current work, only two protein sources were tested for their suitability to form oleogels, and only one was used to examine the oleogels in more detail. Of particular interest would be to investigate the use of proteins from vegetable sources, as this provides an additional advantage from a sustainability point of view. Given the fact that a number of protein sources are commercially available, and that the protein aggregation behaviour can be controlled to a large degree, gives ample opportunities to alter the properties of the building blocks for oleogel formation. Besides the type of oil used for oleogel formation to control network formation and the resulting rheological properties, parameters like the particle size, shape, hydrophobicity and porosity, to name a few, can also be investigated to determine its effect on the oleogel characteristics.

One of the most striking effects as described in this thesis, in terms of affecting network properties, was the addition of water as a second solvent. It is encouraging to see that by altering interactions with simple changes in the system, such as water addition or a heat treatment, the rheological properties can be tuned effectively and substantially. It is therefore worth investigating the exact mechanism behind this phenomenon, as it seems to be of high importance to tune interactions between proteins in oil.

Conclusions

This thesis was aimed to design effective routes to create protein based oleogels and subsequently, understand the mechanistic aspects of these routes. Through the process of a solvent exchange route, it was found to be possible to use proteins for gel formation in oil, and study protein interactions in different environments. Even though this work can be seen as a first attempt to relate protein interactions on a molecular scale to properties like gel strength of the networks formed on a macroscopic scale, it shows that the interactions between proteins in oil can be tuned to a large extent. The resulting protein oleogels range from stiff and brittle gels, to soft and spreadable gels. The possibility to alter the mechanical properties of the gels formed by altering the solvent type or the addition of water in combination with applying a heat treatment, gives opportunities to design a large diversity of protein-based oleogels with widespread rheological properties suitable for different applications. Moreover, as it turns out that the main requirement to be able to gelate oil phases with proteins is merely the ability to control protein aggregation and prevent agglomeration during the transfer from the water to the oil phase, other routes than a solvent exchange were proven possible.

The general concept of protein-based oil gelation fits well into the growing general interest to reduce solid fats from food products along with the industries need in flexibility in terms of their choice of ingredients. Further research in this field will be necessary to extend the knowledge on both the processing as well as the gelation properties to allow for further development of this new class of oleogels.

References

1. Patel, A.R., et al., *Biopolymer-based structuring of liquid oil into soft solids and oleogels using water-continuous emulsions as templates.* Langmuir, 2015. **31**(7): p. 2065-2073.
2. Patel, A.R., et al., *A foam-templated approach for fabricating organogels using a water-soluble polymer.* RSC Advances, 2013. **3**(45): p. 22900-22903.
3. Roefs, S. and K.G. Dekruif, *A model for the denaturation and aggregation of beta-lactoglobulin.* European Journal of Biochemistry, 1994. **226**(3): p. 883-889.
4. Hines, M.E. and E.A. Foegeding, *Interactions of alpha-lactalbumin and bovine serum-albumin with beta-lactoglobulin in thermally induced gelation.* Journal of Agricultural and Food Chemistry, 1993. **41**(3): p. 341-346.
5. Edwards, P.B., et al., *Chapter 6 - Structure and stability of whey proteins A2 - Thompson, Abby*, in *Milk Proteins*. 2008, Academic Press: San Diego. p. 163-203.
6. Broersen, K., et al., *Do sulfhydryl groups affect aggregation and gelation properties of ovalbumin?* Journal of Agricultural and Food Chemistry, 2006. **54**(14): p. 5166-5174.
7. Liu, W.G., et al., *Intrinsic fluorescence investigation on the change in conformation of cross-linked gelatin gel during volume phase transition.* Polymer, 2000. **41**(20): p. 7589-7592.
8. Alting, A.C., et al., *Acid-induced cold gelation of globular proteins: Effects of protein aggregate characteristics and disulfide bonding on rheological properties.* Journal of Agricultural and Food Chemistry, 2004. **52**(3): p. 623-631.
9. Betz, M., et al., *Preparation of novel whey protein-based aerogels as drug carriers for life science applications.* Journal of Supercritical Fluids, 2012. **72**: p. 111-119.
10. Visschers, R.W. and H.H. de Jongh, *Disulphide bond formation in food protein aggregation and gelation.* Biotechnol Adv, 2005. **23**(1): p. 75-80.
11. Smith, G.N. and J. Eastoe, *Controlling colloid charge in nonpolar liquids with surfactants.* Physical Chemistry Chemical Physics, 2013. **15**(2): p. 424-439.
12. Espinosa, C.E., et al., *Particle Charging and Charge Screening in Nonpolar Dispersions with Nonionic Surfactants.* Langmuir, 2010. **26**(22): p. 16941-16948.
13. Israelachvili, J., *Intermolecular & Surface Forces*. Second edition ed. 1991, London: Academic Press.
14. Hu, L.Z., K. Toyoda, and I. Ihara, *Dielectric properties of edible oils and fatty acids as a function of frequency, temperature, moisture and composition.* Journal of Food Engineering, 2008. **88**(2): p. 151-158.
15. Li, L., et al., *On the 'Dielectric "Constant" of Proteins: Smooth Dielectric Function for Macromolecular Modeling and Its Implementation in DelPhi.* Journal of Chemical Theory and Computation, 2013. **9**(4): p. 2126-2136.
16. Donaldson, S.H., Jr., et al., *Developing a general interaction potential for hydrophobic and hydrophilic interactions.* Langmuir, 2015. **31**(7): p. 2051-2064.
17. Raghavan, S.R., H.J. Walls, and S.A. Khan, *Rheology of silica dispersions in organic liquids: New evidence for solvation forces dictated by hydrogen bonding.* Langmuir, 2000. **16**(21): p. 7920-7930.

18. Burns, N.A., et al., *Nanodiamond gels in nonpolar media: Colloidal and rheological properties.* Journal of Rheology, 2014. **58**(5): p. 1599-1614.
19. Claesson, P.M., et al., *Interactions between hydrophilic mica surfaces in triolein: Triolein surface orientation, solvation forces, and capillary condensation.* Langmuir, 1997. **13**(6): p. 1682-1688.
20. Christenson, H.K., *Adhesion between surfaces in undersaturated vapors-a reexamination of the influence of meniscus curvature and surface forces.* Journal of Colloid And Interface Science, 1988. **121**(1): p. 170-178.
21. Bossler, F. and E. Koos, *Structure of Particle Networks in Capillary Suspensions with Wetting and Nonwetting Fluids.* Langmuir, 2016. **32**(6): p. 1489-1501.
22. Koos, E., et al., *Tuning suspension rheology using capillary forces.* Soft Matter, 2012. **8**(24): p. 6620-6628.
23. Alting, A.C., et al., *Cold-set globular protein gels: Interactions, structure and rheology as a function of protein concentration.* Journal of Agricultural and Food Chemistry, 2003. **51**(10): p. 3150-3156.
24. Ikeda, S., E.A. Foegeding, and T. Hagiwara, *Rheological study on the fractal nature of the protein gel structure.* Langmuir, 1999. **15**(25): p. 8584-8589.
25. McClements, D.J. and M.K. Keogh, *Physical-properties of cold-setting gels formed from heat-denatured whey-protein isolate.* Journal of the Science of Food and Agriculture, 1995. **69**(1): p. 7-14.
26. Liang, Y., et al., *Interaction forces between colloidal particles in liquid: theory and experiment.* Advances in Colloid and Interface Science, 2007. **134-135**: p. 151-166.
27. Renard, D., et al., *Gelation by phase separation in a whey protein system: in-situ kinetics of aggregation.* Journal of Biotechnology, 2000. **79**(3): p. 231-244.
28. Griebenow, K. and A.M. Klibanov, *On protein denaturation in aqueous-organic mixtures but not in pure organic solvents.* Journal of the American Chemical Society, 1996. **118**(47): p. 11695-11700.
29. Voets, I.K., et al., *DMSO-Induced Denaturation of Hen Egg White Lysozyme.* Journal of Physical Chemistry B, 2010. **114**(36): p. 11875-11883.
30. Dong, A.C., et al., *Effect of secondary structure on the activity of enzymes suspended in organic solvents.* Archives of Biochemistry and Biophysics, 1996. **334**(2): p. 406-414.
31. Wang, B.H., et al., *Progress in drying technology for nanomaterials.* Drying Technology, 2005. **23**(1-2): p. 7-32.
32. Dittmann, J., E. Koos, and N. Willenbacher, *Ceramic Capillary Suspensions: Novel Processing Route for Macroporous Ceramic Materials.* Journal of the American Ceramic Society, 2013. **96**(2): p. 391-397.
33. Lee, J. and Y. Cheng, *Critical freezing rate in freeze drying nanocrystal dispersions.* Journal of Controlled Release, 2006. **111**(1-2): p. 185-192.
34. Deville, S., et al., *Freezing as a path to build complex composites.* Science, 2006. **311**(5760): p. 515-518.

35. Cai, J., et al., *Cellulose aerogels from aqueous alkali hydroxide-urea solution.* ChemSusChem, 2008. **1**(1-2): p. 149-154.

36. Tewari, P.H., A.J. Hunt, and K.D. Lofftus, *Ambient-temperature supercritical drying of transparent silica aerogels.* Materials Letters, 1985. **3**(9): p. 363-367.

37. Ong, Y.K., et al., *Recent membrane development for pervaporation processes.* Progress in Polymer Science, 2016. **57**: p. 1-31.

38. Huang, R.Y.M. and V.J.C. Lin, *Separation of liquid mixtures by using polymer membranes. I. Permeation of binary organic liquid mixtures through polyethylene.* Journal of Applied Polymer Science, 1968. **12**(12): p. 2615-2631.

39. Van Hoof, V., et al., *Economic comparison between azeotropic distillation and different hybrid systems combining distillation with pervaporation for the dehydration of isopropanol.* Separation and Purification Technology, 2004. **37**(1): p. 33-49.

40. Savin, G., et al., *Oil gel*, Nestec S.A., Switzerland, 2011, European Patent EP 2347658A1.

41. Atkinson, P.J., et al., *Structure of microemulsion-based organo-gels.* Journal of the Chemical Society-Chemical Communications, 1989(23): p. 1807-1809.

42. Atkinson, P.J., et al., *Structure and stability of microemulsion-based organo-gels.* Journal of the Chemical Society-Faraday Transactions, 1991. **87**(20): p. 3389-3397.

Summary

Acknowledgements

Author information

List of publications

Completed training activities

Summary

This thesis describes an alternative to crystalline triacylglycerides (TAGs) to structure lipid phases for food products. These TAGs contain mainly saturated and *trans* fatty acids capable of forming a space-spanning crystal network entrapping the liquid oil into a solid structure. Although solid fat has many advantages when it comes to providing the desired texture and stability to food products, consuming saturated and *trans* fatty acids has been related to adverse effects on human health, with the prevalence of cardiovascular diseases (CVD) in particular. On the other hand, consuming unsaturated fatty acids, as found in liquid oils, decreases these risks. For this reason, food researchers are looking for alternatives to transform a liquid oil into a semi-solid structure with similar properties as solid fat, but without using saturated or *trans* fatty acids.

The structuring of liquid oil into so-called "oleogels" is a relatively new, but promising field of research, not only because it allows to design food products that would fit better in a healthy diet, but also to increase flexibility in the choice of structuring agents. Although several alternative structuring agents have been identified, there is still a need to identify food grade and versatile oil structuring agents. This thesis is concerned with using proteins as an alternative ingredient to solidify liquid oils. As a novel structuring agent, proteins are highly promising as they have many advantages, such as their high nutritional value, their food grade nature, and because they are already widely used as a common food ingredient. Since proteins do not readily dissolve in liquid oil, a new route had to be developed to transfer proteins from the aqueous phase to the oil phase. The aim of this thesis was to design effective routes to structure oil using protein building blocks and understand the mechanical aspects of the resulting oleogels.

In Chapter 2, a novel route was investigated to transform whey protein isolate (WPI) heat-set hydrogels into protein oleogels. In a first step, protein hydrogels were prepared varying in microstructure and network density. It was shown that by applying a stepwise solvent exchange procedure using an intermediate solvent, being either acetone or tetrahydrofuran (THF), the protein matrix was capable of incorporating a considerable amount (80 – 90 %) of oil. It was found that the oil was homogeneously distributed within the pre-set protein matrix without damaging the network structure. The oil holding capacity depended on the microstructure of the gel, the polarity of the intermediate solvent and the kinetics of the solvent exchange. From uni-axial compression

tests, it was found that the resulting protein oleogels increased considerably in stiffness, brittleness, and fracture stress compared to the preceding hydrogels.

To allow for better control of network formation, Chapter 3 describes how heat-set WPI aggregates (diameter ~ 200 nm) can be used as building blocks for oleogel formation in liquid oil. When the formed aggregates were freeze-dried to remove the water, the resulting agglomerated dried particles did not disperse fully in oil. Alternatively, when the particles remained in a 'wet state' by applying a solvent exchange procedure to remove the water and replace it for an oil phase, agglomeration was avoided and the aggregates were found to have a similar size in both water and oil. Given their small size, the protein building blocks assembled into a space-spanning network, forming a paste-like oleogel. Rheological measurements indicated that the aggregates are highly effective in forming a space-spanning network. It was found that at a protein concentration of ~ 3%, G' > G" and G' scales with protein concentration as $G' \sim c_p^{5.3}$. When applying a fractal gel network theory to the data, the results showed that the gels can be described using the strong link regime with a fractal dimension of 2.2. This alternative solvent exchange route provided a novel and promising way to directly create oleogels with tunable rheological properties using pre-set protein aggregates. The relevant interactions between the protein aggregates were examined further in the following chapters.

The formation of a network structure is related to both particle-particle and particle-solvent interactions. These interactions can be altered by changing the oil type. In Chapter 4, oleogels were prepared using protein aggregates in different oils that varied in polarity. The results showed that gel strength of the network was affected by the polarity of the oil, resulting in weaker gels in more polar oils as a result of larger particle-solvent interactions. Besides the polarity of the oil, also the chemical composition of the oil was shown to play a large role. When the oil contained polar hydroxyl groups, gel formation was prevented due to strong particle-solvent interactions. Large deformation oscillatory rheology shows that protein oleogels exhibit a yielding behaviour under large deformation, but regenerate its elasticity quickly after deformation is reduced.

To alter the interactions between protein aggregates in oil and tune the rheological properties of the resulting oleogels, the effect of water and heat treatment was investigated in Chapter 5. Addition of water showed to induce intensive clustering of the protein aggregates up to 0.5 g water / g protein. Exceeding this value resulted in the formation of free water droplets. The intensive clustering of the aggregates upon water addition was found to increase G' dramatically, i.e. up to three orders of magnitude. Moreover, an increase in critical strain and yield stress was

observed, which indicates that the resulting oleogels were much stronger. The gels became even stronger as G' increased even further, after an additional heat treatment due to enhanced particle-particle interactions. The changes in gel strength can most likely be attributed to the formation of capillary bridges between the protein aggregates. The addition of water and heat treatment provided an effective way to tune the rheological properties of protein oleogels.

As was shown in Chapter 3, preventing irreversible agglomeration of the protein aggregates during water removal was a prerequisite to allow for efficient gel formation in oil. In Chapter 6, the underlying mechanism of reduced agglomeration during the solvent exchange was studied. In one approach, the pre-set protein aggregates were transferred from water to several organic solvents that differed in polarity. It was shown that drying the aggregates using solvents with a low polarity (eg. hexane) resulted in a protein powder that had a good dispersibility of the aggregates in liquid oil. Aggregates dried from solvents with a high polarity lead to irreversible agglomeration and low dispersibility. This difference in dispersibility was found to be unrelated to changes in protein composition or conformation, but instead could be related to the formation of liquid capillary bridges between the protein aggregates during drying. Apolar solvents prevented the formation of strong attractive capillary forces due to a low wetting angle. Agglomeration could also be prevented by using high freezing rates prior to a freeze-drying process. Oleogels prepared with such freeze-dried protein aggregates were shown to have similar gel strength compared to oleogels prepared using a solvent exchange procedure.

In Chapter 7, an overview is given on how interactions between protein aggregates in oil can be controlled to tune the gel network properties, based on the results of the different chapters. For different oleogels, the most important forces acting between the protein aggregates were identified and discussed. Protein agglomeration by liquid bridges was proven to be of paramount importance both with respect to the suitability of the solvent exchange procedure, and to control the network properties of the final oleogel. Based on the results of this thesis, alternative routes for oleogel preparation using proteins is discussed as well. Additionally, the potential of the protein oleogels as a solid fat replacement was shown in two different types of food. Future challenges are discussed to identify new research routes to sustain momentum on developing this highly promising novel structuring agent for liquid oils.

Acknowledgements

Many people contributed in one way or another to the completion of this thesis. A few of them I would like to thank in particular. First, I would like to thank my both supervisors, Elke and Erik. I truly enjoyed working with you on this difficult topic, which was certainly challenging in more than one way. I found myself very comfortable in your guidance, confidence, and patience, wrapped in a good sense of humour. Moreover, the 'open-door policy', which extends throughout the whole group, is something I valued greatly.

For this, and many other things, I thank all my colleagues at FPH, including 'my' BSc and MSc students. I enjoyed the good atmosphere during work hours and lunch breaks, and the willingness to help each other in any way possible. Not only during work-time but also during the USA & Canada PhD-trip, the PhD-weekends, and several conferences, I always enjoyed 'hanging-out' with 'youse' guys! ;)

I am very grateful for the never-ending support of family and the never-ending sarcasm of my friends. Finally, I thank in particular my girl Floor, for making my life more colourful.

Author information

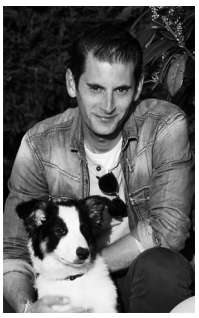

Auke de Vries was born in the far east of the Netherlands during the summer of 1984. After completing his BSc degree in Food Technology from the University of Applied Sciences in Leeuwarden, he started working for a large potato processing firm. After three years, he continued his studies by applying for the MSc program Food Science at Wageningen University. He performed his MSc thesis at the chair group Physics and Physical Chemistry of Foods and a final internship at the Nestlé Research Centre in Lausanne, Switzerland. After he obtained his MSc degree in 2012, he started working as a PhD candidate at Wageningen University within the same chair group. His work was part of the project 'Dispersed fat systems', financed by the Top Institute Food and Nutrition. He can be contacted via auke.devries@gmx.com.

List of publications

Peer reviewed publications

de Vries, A., Nikiforidis, C.V., Scholten, E., *Natural amphiphilic proteins as tri-block Janus particles: Self-sorting into thermo-responsive gels.* Europhysics Letters, 2014. 107(5), 58003.

de Vries, A., Hendriks, J., van der Linden, E., Scholten, E., *Protein oleogels from protein hydrogels via a stepwise solvent exchange route.* Langmuir, 2015. 31(51): p. 13850-13859.

de Vries, A., et al., *Protein oleogels from heat-set whey protein aggregates.* Journal of Colloid and Interface Science, 2017. 486: p. 75-83.

de Vries, A., Lopez Gomez, Y., Jansen, B., van der Linden, E., Scholten, E., *Controlling agglomeration of protein aggregates for structure formation in liquid oil: a sticky business.* [Submitted]

de Vries, A., Jansen, D., van der Linden, E., Scholten, E., *Tuning the rheological properties of protein-based oleogels by water addition and heat treatment.* [Submitted]

de Vries, A., Lopez Gomez, Y., van der Linden, E., Scholten, E., *The effect of oil type on network formation by protein aggregates into oleogels.* [Submitted]

Patents

Scholten, E., de Vries, A., Protein stabilized oleogels, (2016), International Publication Number: WO2016/062685

Completed training activities

Discipline specific activities

TIFN Annual conference, 2013, Amsterdam, the Netherlands

TIFN Annual conference, 2014, Utrecht, the Netherlands

From molecules to functionality symposium, 2014, Amsterdam, the Netherlands*

Food colloids conference, 2014, Karlsruhe, Germany

Delivery of Functionality in complex food systems, 2015, Paris, France*

Food structure and functionality conference, 2016, Singapore*

Food colloids conference, 2016, Wageningen, the Netherlands*

Winter school of physical chemistry, 2016, Han-sur-lesse, Belguim

General courses

Vlag PhD week, 2013, Baarlo, the Netherlands

Basic Intellectual Property course (TIFN), 2013, Wageningen, the Netherlands

Data management in research (TIFN), 2013, Wageningen, the Netherlands

Writing a world-class paper, symposium, 2013, Wageningen, the Netherlands

Techniques for writing and presenting a scientific paper, 2014, Wageningen, the Netherlands

Voice matters presentation training, 2014, Wageningen, the Netherlands

Scientific writing, 2014, Wageningen, the Netherlands

Optional courses and activities

Preparation of research proposal, 2012

Organized and participated in the PhD trip, 2014, USA – Canada*

Project meetings TIFN FS002, "Dispersed fat systems" Vendome, France,* Lausanne, Switzerland,* Son, the Netherlands,* Wageningen, the Netherlands.*

Weekly group meetings Physics and Physical Chemistry of Foods

* Oral presentation

The research described in this thesis was performed within the framework of Top Institute Food & Nutrition.

Financial support from Wageningen University and the Top Institute Food & Nutrition is gratefully acknowledged.

Cover design: Giovanni van Heydoorn
Printed by Gildeprint B.V.